VYSOKÉ UČENÍ TECHNICKÉ V BRNĚ

BRNO UNIVERSITY OF TECHNOLOGY

FAKULTA STROJNÍHO INŽENÝRSTVÍ

FACULTY OF MECHANICAL ENGINEERING

ÚSTAV AUTOMOBILNÍHO A DOPRAVNÍHO INŽENÝRSTVÍ

INSTITUTE OF AUTOMOTIVE ENGINEERING

REKUPERACE ENERGIE Z VÝFUKOVÝCH PLYNŮ V ELEKTROMOTOREM ASISTOVANÉM TURBODMYCHADLE PRO HYBRIDNÍ VOZIDLA

ENERGY RECOVERY FROM EXHAUST GASES IN AN ELECTRIC-ASSISTED TURBOCHARGER FOR HYBRID VEHICLES

DIPLOMOVÁ PRÁCE
MASTER'S THESIS

AUTOR PRÁCE   Bc. Daniel Calábek
AUTHOR

VEDOUCÍ PRÁCE   doc. Ing. Pavel Novotný, Ph.D.
SUPERVISOR

BRNO 2021

Assignment Master's Thesis

Institut:	Institute of Automotive Engineering
Student:	**Bc. Daniel Calábek**
Degree programm:	Mechanical Engineering
Branch:	Automotive and Material Handling Engineering
Supervisor:	**doc. Ing. Pavel Novotný, Ph.D.**
Academic year:	2020/21

As provided for by the Act No. 111/98 Coll. on higher education institutions and the BUT Study and Examination Regulations, the director of the Institute hereby assigns the following topic of Master's Thesis:

Energy Recovery from Exhaust Gases in an Electric–assisted Turbocharger for Hybrid Vehicles

Brief Description:

This thesis deals with the possibilities of using exhaust gas energy recovery in hybrid vehicles including electric motor assisted turbochargers. It is assumed to analyze different types of hybrid vehicles and evaluate the suitability of using energy recuperation. The work includes an analysis of the energy flows for different variants of the arrangement of each subsystem and for different operating conditions.

Master's Thesis goals:

Analyse the suitability of exhaust gas energy recuperation in an electric motor assisted turbocharger for propulsion of selected types of hybrid vehicles.
Compile an evaluation of selected types of hybrid vehicles with respect to the possibilities of energy recoperation.

Recommended bibliography:

MI, Chris a M. Abul MASRUR. Hybrid Electric Vehicles: Principles and Applications with Practical Perspectives. 2nd Edition. Hoboken, N.J.: Wiley, 2017. ISBN ISBN978-0-470-74773-5.

PISTOIA, Gianfranco. Electric and Hybrid Vehicles: Power Sources, Models, Sustainability, Infrastructure and the Market. Boston: Elsevier, 2010. ISBN 978-0-444-53565-8.

Deadline for submission Master's Thesis is given by the Schedule of the Academic year 2020/21

In Brno,

L. S.

....
prof. Ing. Josef Štětina, Ph.D.
Director of the Institute

....
doc. Ing. Jaroslav Katolický, Ph.D.
FME dean

ABSTRAKT

Obsahem této diplomové práce byla vhodnost využití turbodmychadla s přidruženým motor-generátorem pro vybrané typy hybridních vozidel a následná analýza energetických toků pro danou motorovou aplikaci. Přístup prezentovaný v práci zahrnuje termodynamický model motoru v programu GT-SUITE ve kterém jsou zkoumány možnosti energetických toků při změně velikost turbínového a kompresorového kola turbodmychadla. Přístup je aplikován na turbodmychadlo s variabní geometrií lopatek s přidruženým motor generátorem pro donáškové vozidlo, kde je možné při různých zatíženích motoru rekuperovat energii z turbodmychadla. Zároveň byli zjištěny možnosti snížení spotřeby paliva v určitých provozních bodech motoru.

KLÍČOVÁ SLOVA

E-Turbo, motor-generátor, rekuperace, turbodmychadlo, E-VNT, EGR, VNT, Iveco Daily

ABSTRACT

The content of this diploma thesis was the suitability of using a turbocharger with an associated motor-generator for selected types of hybrid vehicles and the subsequent analysis of energy flows for a given engine application. The approach presented in the work includes a thermodynamic model of the engine in the GT-SUITE program in which the possibilities of energy flows when changing the size of the turbine and compressor wheel of a turbocharger are investigated. The approach is applied to a turbocharger with a variable geometry which is associated with motor-generator for a delivery vehicle, where it is possible to recover energy from the turbocharger at different engine loads. At the same time, the possibilities of reducing fuel consumption at certain operating points of the engine were identified.

KEYWORDS

E-Turbo, motor-generator, recuperation, turbocharger, E-VNT, EGR, VNT, Iveco Daily

BIBLIOGRAPHIC CITATION

Calábek, Daniel. *Energy Recovery from Exhaust Gases in an Electric-assisted Turbocharger for Hybrid Vehicles*. Brno, 2021. Master´s Thesis. Brno University of Technology, Faculty of Mechanical Engineering, Institute of Automotive Engineering. 95 s. Supervisor doc. Ing. Pavel Novotný, Ph.D.

DECLARATION

I declare that this master´s thesis to be my own work, I have elaborated this thesis independently under the supervision of doc. Ing. Pavel Novotný Ph.D. with the use of listed sources.

In Brno, May 21st, 2020　　　　　　……………………………………………………..

　　　　　　　　　　　　　　　　　　　　　　　　　Bc. Daniel Calábek

ACKNOWLEDGMENT

TABLE OF CONTENTS

INTRODUCTION

We are witnessing deteriorating climatic conditions in all parts of the world. One of the factors in these deteriorating conditions is the production of greenhouse gases, especially CO_2, where European Union for example seeks to regulate these greenhouse gases through emission regulations in all sectors of industry, most often in the automotive industry. These regulations, and the possible fines for violating these regulations, force the vehicle manufacturer to switch to other alternative powertraines, most often to hybrid powertrains and purely eletric powertrains in the future.

Hybrid powertrain unit is consisted of an internal combustion engine and an electric motor, where these engines are able to operate simultaneously and also separately in specific configurations. Hybrid powertrains will form a transition between internal combustion engines and purely electric engines.

Due to the limited size of the batteries that provide electricity for the electric motor in the hybrid unit, the energy in the batteries can be quickly consumed while the vehicle is driving purely electric. However, the hybrid powertrain system allows part of the vehicle´s kinetic energy to be recovered during braking (Regenerative braking system) and transfer it to the batteries.

Another way to obtain energy is by using a turbocharger and utilizing the energy of the exhaust gases. A substantial part of the energy from the exhaust gases is used to drive the turbine part of the turbocharger and thus the compressor which leads to an increase in the performance characteristics of the engine. However, depending on the turbine-compressor connection, there may also be a lack of energy to drive the compressor or and excess of energy when part of this energy is not utilized. By adding a motor-generator to the turbocharger, this excess energy can be utilized and converted into electrical energy. This recovered electrical energy can be transferred to other electrical components of the vehicle. In case of a hybrid powertrain unit, the recovered energy can be supplied to the battery and the range of the purely electric drive or hybrid drive can be extended. The use of purely electric powertrain for example in urban traffic, can lead to reduced the emissions in urban areas where is greater production of greenhouse gases due to the increased incidence of car traffic or e.g. factories.

1 PROBLEM DEFINITION

The use of an internal combustion engine using liquid transportation fuel will presumably continue to hold a major role over the next few decades [3]. However, there are still significant challenges for improving fuel efficiency and especially emissions reducing, considering the rapid growth of environmental concerns.

From the research report [44] transportation is the second largest source of carbon dioxide (CO_2) emission in the United States. Out of this transportation sector, passanger cars and light-duty trucks are responsible for almost 60% of CO_2 production. This indicates that the improvement of the fuel economy and CO_2 emission reduction in road vehicles have a significant impact on the conversation of the global environment.

The regulatory authorities around the world have established certain fuel economy, greenhouse and specifically CO_2 emission standards. The global emission legislation is different for almost every part of world region and it is shown in Figure 1.
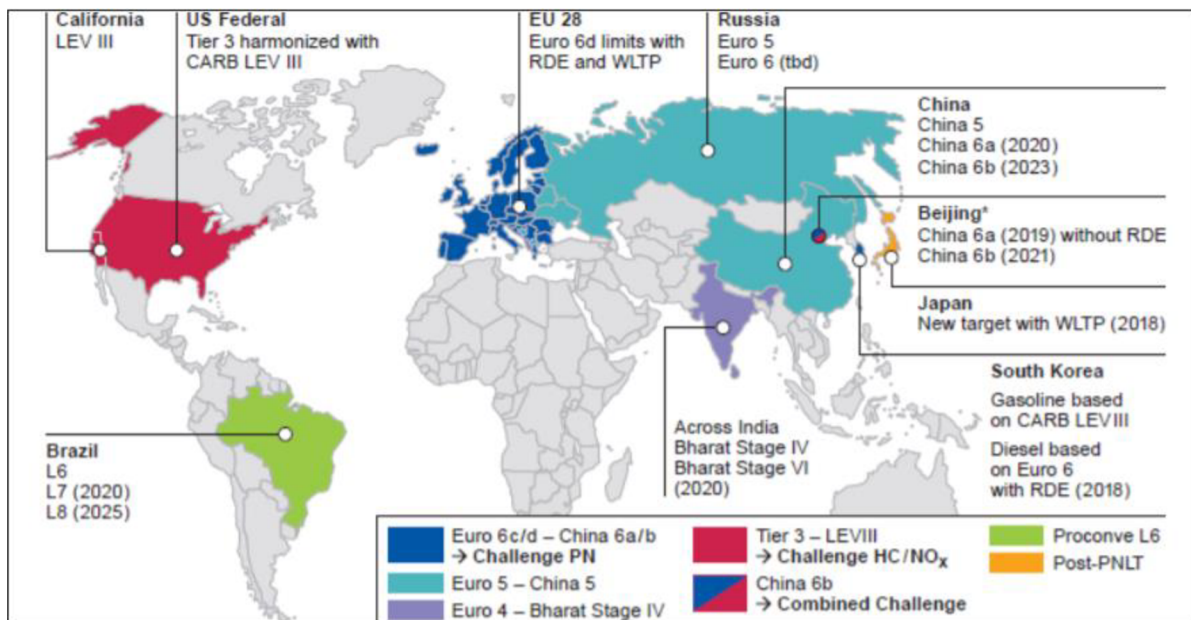
Figure 1 Global emission legislation by world region [4]

Due to these restrictions, automotive brands have to pay huge amounts for violating these standards. World regions have also different targets for CO_2 emission restrictions for passanger cars, see Figure 2. The amount of CO_2 emission was normalized for NEDC driving cycle in Figure 2 but nowdays these numbers of CO_2 can be dissimilar due to the replacement of NEDC driving cycle to WLTP driving cycle in 2017 which can provides more accurate view on fuel consumption and greenhouse emissions including CO_2.

Figure 2 CO_2 emission history and targets for specific world regions [4]

Over the past few years, automotive industry has introduced a number of new technologies to meet these new fuel and emission regulations such as integration of light weight material, energy regenerative braking systems, downsizing with a turbocharger or electrified turbocharger and hybrid or battery electric vehicles [44]. Electric vehicle has the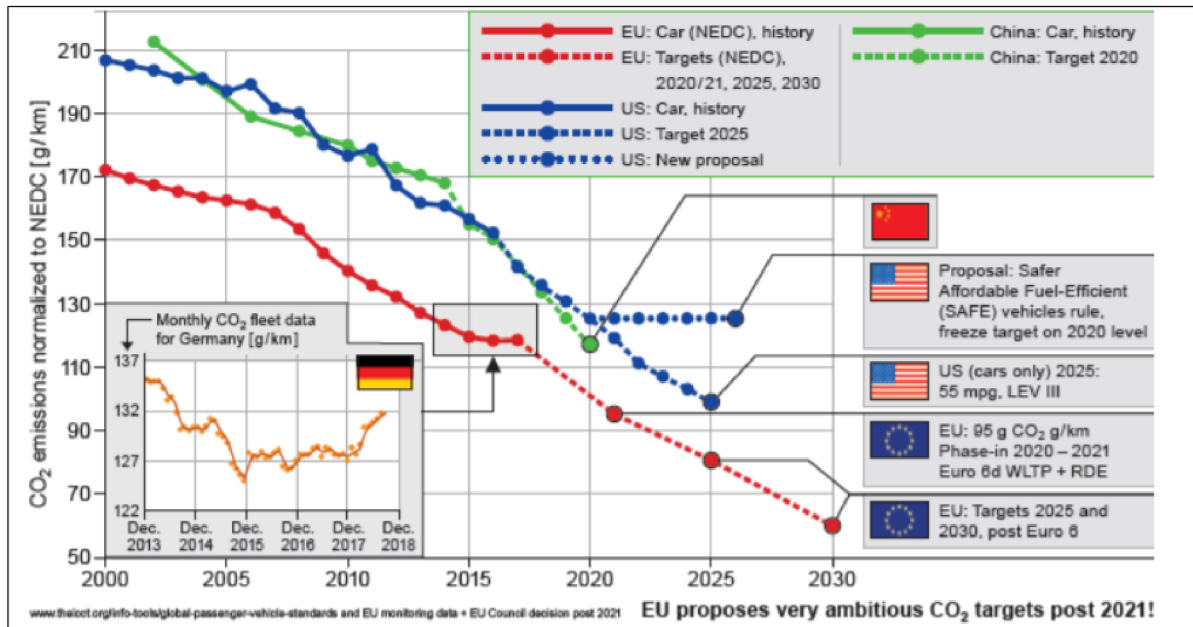 best impact on environment because of none greenhouse production while driving but battery costs are so high that there is still significant margin to evolve the internal combustion engine based hybrids to higher efficiencies and lower CO_2 emissions than fully eletric vehicles [41].

Another option to meet these stringent regulations, engine manufacturers have paid attention towards engine downsizing as one of the most suitable technology to meet these requirements. Engine downsizing with forced induction system such as a turbocharger or and electrically assisted turbocharger (EAT) is gaining popularity as viable solution. Compared to a conventional non-electric turbocharger, the newly introduced electrically assisted turbocharger has several benefits including improved transient response (reduced turbo lag), energy regenerative capability, engine downsizing, improved engine output power etc.

By connection hybrid vehicle with electrically assisted turbocharger it is possible to gain many benefits of these technologies but one of the most important is energy recovery. Hybrid vehicle system batteries provide limited amount of energy for hybrid driving (utilizing internal combustion engine and electric engine at the same time) or purely electric driving which is preffered especially in urban areas. There are two options which could lead to recover energy, store it into batteries and thus extend the range of purely electric drive or hybrid drive.

First option is energy recovery braking system used in hybrid vehicles where kinetic energy from braking is converted into the electric energy and stored in batteries. This process is possible due to the electric motor which can switch into generator mode and converts a portion of kinectic energy into electrical energy. This regenerative braking system will be more specifically detailed in chapter 4.

Second option of energy recovery is electrically assisted turbocharger also turbocharger with motor-generator. By recovering waste exhaust energy, the electrical power generated can be used to feed hybrid system batteries and leading to the to beneficial reductions in specific fuel consumption, NO_x and CO_2 emissions [49]. Harvesting electrical energy throught motor-generator is possible in specific parts of engine loads where turbine side of turbocharger provides sufficient amout of energy to power the compressor and the excess of the kinetic energy can be converted into electrical energy.

Correct compressor-turbine sizing is critical for turbocharger function. Especially turbine has influence on turbocharger performance and thus possible energy recovery. Various turbine sizes or turbine wheels allow different energy harvesting at specific speed and load conditions due to the different pre-turbine pressure and temperature, deeper expression is covered in chapter 3. Influence of different turbines on energy recovery is presented in [45] study. In chapter 6 will be shown influence of different turbine wheels or compressor wheel on energy recovery for specific engine model.

2 TURBOCHARGER CHARACTERISTICS

For energy recovery turbocharger it is essential to know the characteristics of conventional turbocharger e.g. methods of turbocharging, parts of the turbocharger influencing the performance or resulting characteristics of these parts.

Originally was the turbocharger invented primarily for aircraft engines. Nowadays turbochargers are on a different development level with various ways of enhancements which assure accomplishment of demanding requirements. Due to the use of turbochargers in many branches of industry, companies must provide a wide range of different sizes, types or other requirements.

The principle of the turbocharger system is to use turbine to expand the high pressure and hight temperature exhaust gases that are expelled from the engine cylinder after combustion. The power extracted from the exhaust gases by the turbine wheel is used to drive compressor wheel which is connected to the same shaft as the turbine wheel. The compressor wheel will compress the incoming air above ambient pressure and thus the air density increases. During the compression phase the air temperature is also increased and it has to be cooled in an intercooler, further increasing the density before inducing it into the cylinder. With a larger charge mass containing more oxygen, more fuel can be combusted and the power output of the engine will be increased.

In Figure 3 is a section view of the turbocharger. The turbocharger is assembled from specific components but the three main ones are center housing, compressor housing and turbine housing.
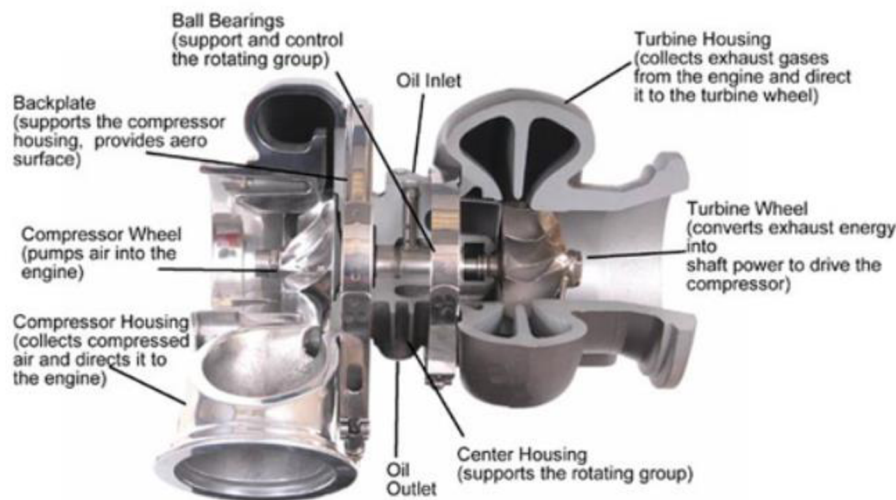

Figure 3 Section view of turbocharger [8]

2.1 METHODS OF TURBOCHARGING

The most commonly used methods are constant-pressure turbocharging and pulse turbocharging, combined with corresponding layout of exhaust system [2]. The principles of these methods will be covered on example of compression ignition turbocharged engine.

In the Figure 4, after the expansion phase 4-5 when the exhaust valves open at point 5 the cylinder content still has high pressure and temperature, which in naturally aspirated engine is wasted. If the gas could be expanded in the cylinder further down to point 6 the energy of the exhaust gases represented by the area 5-7-6, commonly referred as blowdown energy, could be theoretically recovered.

During the intake phase, air with a pressure value P_{intake}, higher than ambient pressure P_{amb}, enters the cylinder. At the bottom dead center, at point 5, expansion takes place via the exhaust valves and then the pressure in the cylinder drops down to the value of P_{exhst}, which is higher than ambient pressure, whereby a positive pressure ratio to the turbine drive can be achieved.
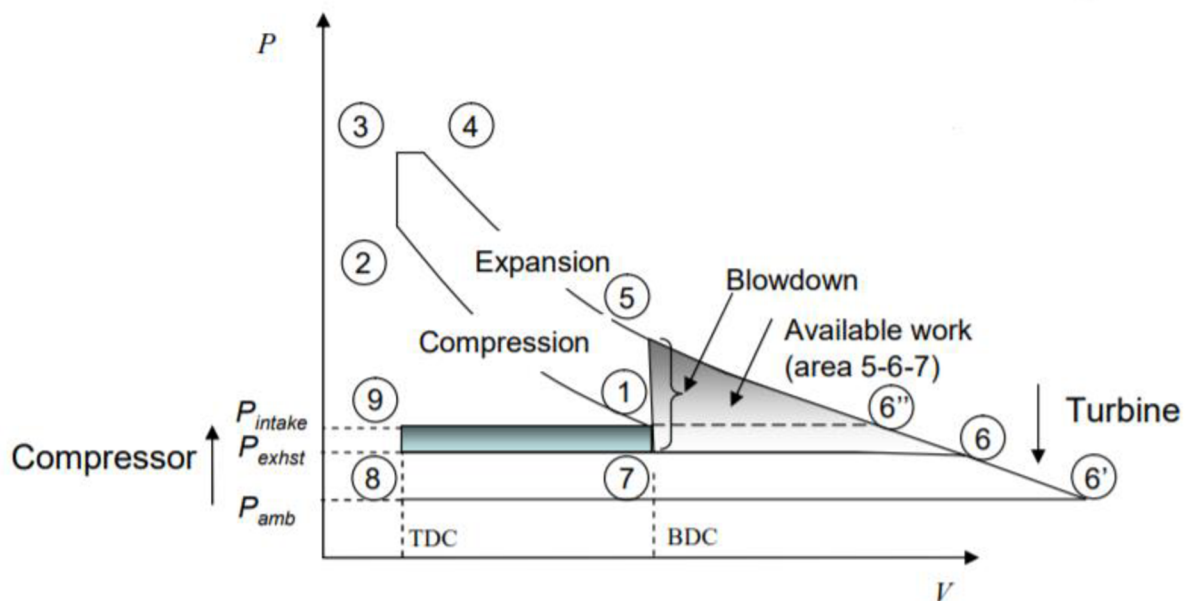

Figure 4 Ideal P-V diagram of supercharged engine (P – pressure, V – volume, P_{intake} – intake pressure, P_{exhst} – exhaust pressure, P_{amb} – ambient pressure) [5]

2.1.1 CONSTANT PRESSURE TURBOCHARGING

A constant pressure system is achieved if the exhaust manifold volume is large enough (larger than volume of the cylinder) to damp out any pressure pulsations from the exhaust valve events, see Figure 5. Meeting this condition, the turbine operates under steady state conditions during the constant pressure engine cycle. In Figure 4, during the exhaust stroke 7-8 the turbine inlet pressure is equal to P_{exhst} but then gas expand via the turbine and the output pressure will be equal to P_{intake} that means the turbine carried out the work to drive the compressor. The availability of energy from exhaust gases for the turbine is bouded by points 7,8 and pressures P_{exhst} and P_{amb}.

Without extending the expansion stroke in the cylinder from point 5 to point 6 the blowdown energy of the exhaust gases can not be utilized. However, it also affects that the additional exhaust energy, shown by points 7,6′ and pressures P_{exhst} and P_{amb}, cannot be used to perform the expansion process on the turbine.
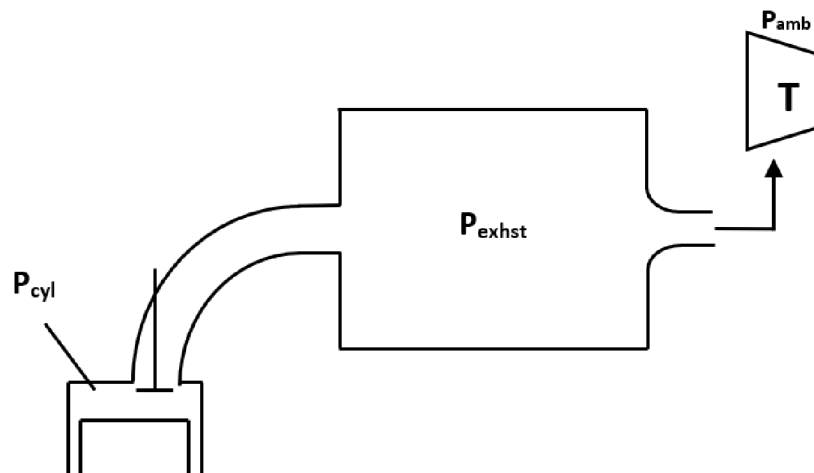
Figure 5 Principle schematic diagram with constant-pressure tubocharging
(P_{cyl} – cylinder pressure, P_{exhst} – exhaust pressure, T – turbine, P_{amb} – ambient pressure)

A serious disadvantage of constant-pressure turbocharging is the fact that with any change in the operating condition of the engine, the large exhaust manifold has to be brought to the new pressure and temperature level, which leads to significant problems under transient operating conditions [2]. If the turbine will be optimized to work under steady state conditions, a higher efficiency will be attained. Lower fuel comsumption and simple system for multicylinder engines are another advantages of constant-pressure turbocharging [2].

The major application of constant-pressure turbocharging is in highly charged slowspeed engines in stationary use (marine engines) and with load patterns where transient operation is either modest or not relevant [2, 6].

2.1.2 PULSE TURBOCHARGING

A way to recover a whole blowdown energy and addional exhaust gas energy, a pulse system can be used instead. In this case, the manifold volume is reduced to a minimum and the turbine is placed as close as possible to exhaust valves that will cause no damping of pressure pulsations, see Figure 6. In Figure 4 when the exhaust gas open at point 5, the pressure pulse caused by the cylinder pressure falling from 5-7 will be utilized by the turbine. The turbine inlet pressure then falls from 5 to 6 and then proceed ideally to the pressure value P_{amb} at point 6′. By this, the whole blowndown energy with additional exhaust gas energy, represented by the areas 5-6-7 and 6,7 with pressures P_{exhst}-P_{amb}, will be recovered.

This is the ideal case where the turbine inlet pressure would need to reach cylinder pressure instantaneously at point 5 and then the manifold pressure would need to expand completely down to ambient. In reality this is not possible since there are flow loses in the valves and the lower turbine efficiencies caused by transient gas admission to the turbine offside the turbine peak efficiency [2]. For the real application only a part of the theoretically available energy can be utilized because the turbine operates momentarily in ideal conditions.
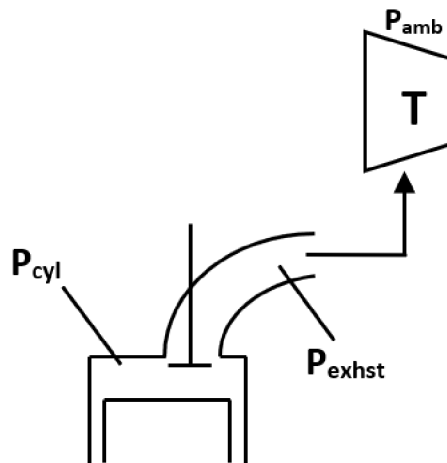
Figure 6 Principle schematic diagram with pulse turbocharging (P_{cyl} – cylinder pressure, P_{exhst} – exhaust pressure, T – turbine, P_{amb} – ambient pressure)

Advantage of the pulse turbocharging will be especially in transient engine operation, due to significantly improved acceleration behavior of the turbocharger and consequently the entire engine [2]. Study [37] presents a valve timing influence on controlling pulse turbocharging system resulting in good performance at both the low speed operation and high speed operation.

The major application area for pulse turbocharging is in engines with mostly transient operation, primarily in automobile engines and two-stroke engines [2,6].

2.2 CENTER HOUSING

Center housing also known as bearing housing is located between compressor housing and turbine housing. The center housing supports a bearing or bearings for rotation of turbocharger shaft which is coupled with turbine wheel housed by turbine housing and compressor wheel housed by compressor housing. CHRA is a well known short cut for center housing rotating assembly. Center housing also separates turbine housing and compressor housing due to their highly different temperatures, which in the hottest part (turbine housing) may exceed temperature over 1000 °C. Bearing housing is fastaned with the housings by bolts or V-band, which provides rotation of the housings towards each other and thus easier connection of the housings to the engine. Detail prediction model of sealing performance of turbocharger housings by V-band is presented in study [35].

Another essential role of the center housing is distribution of lubricating oil through oil inlet to the bearings of the rotor. These bearings control radial and axial motion of the rotor. They also have not negligible influence on turborcharger friction and and its impact on engine fuel efficiency [10].

Oil from the engine lubrication system enters the turbocharger and is distributed to the bearings. All turbochargers use two oil films, the first one between center housing and journal bearing, the second one between journal bearing and the shaft. Oil also feeds thrust bearing which controls the axial motion of the rotor. After flowing through the bearing

system, oil is collected and returned into the engine sump by oil throwers located at the turbine end and compressor end [11]. This abbreviated description of oil flow applies to hydrodynamic bearing system which contains one journal bearing and one thrust bearing.

Modern turbocharger bearing system can be split in two types, hydrodynamic bearing system and ball bearing system. The hydrodynamic bearing system contains a set of journal bearings or one journal bearing, mentioned above, and a thrust bearing. An innovation of ball bearing caused that ball bearing is now an affordable technology advancement which can provide significant performance improvements to the turbocharger in certain applications [12]. The advantages, possible applications and properties are presented [33, 34].

Journal Bearings   **Ball Bearings**

Figure 7 Illustration of turbocharger bearings [12]

Center housing is usually manufactured from grey cast iron or exceptionally of aluminium and is very often cooled by water from the engine own cooling system due to high temperatures. Even when the engine stops running the thermosiphon effect of the system continues to cool the turbocharger [11].

2.3 COMPRESSOR PART OF TURBOCHARGER

Compressor part of the turbocharger is consisted of housing or cover and impeller or wheel which is radial flow type in most automotive applications. In the Figure 8, filtered air enters in axial direction into a compressor housing and then proceeds to the compressor wheel. As air proceeds through the compressor wheel it makes a 90° turn thus changing its flow from axial to a radial direction. Air exits the compressor wheel and travels thought a narrow diffuser to the volute where gathers. After gathering, the flow of charged air leaves the compressor housing and continues though the intercooler to the engine intake manifold.
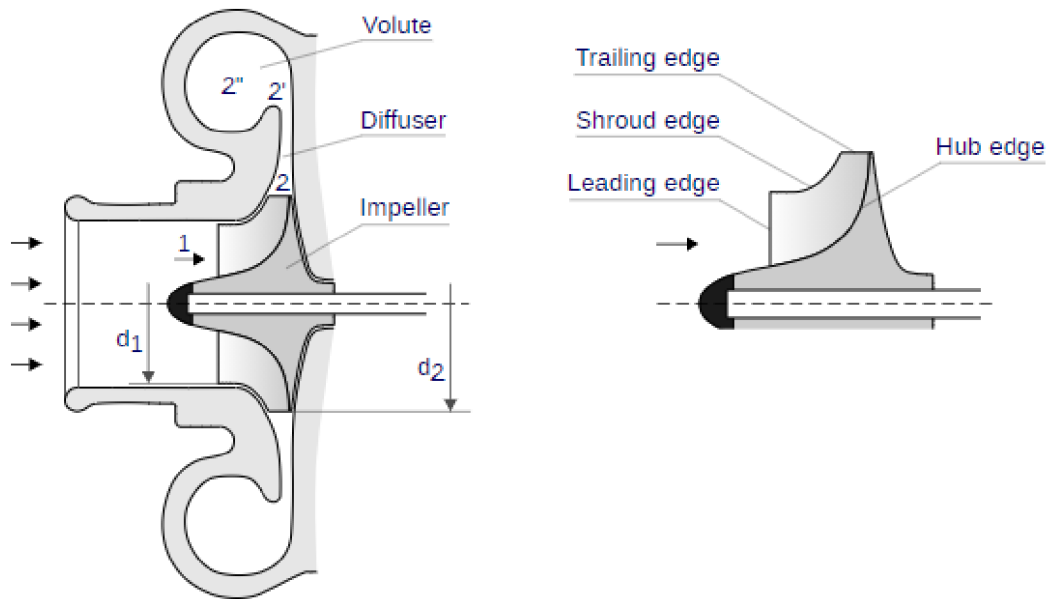
Figure 8 Cross section of radial flow compressor [13]
(d_1 – inducer diameter, d_2 – exducer diameter)

2.3.1 COMPRESSOR WHEEL

The compressor wheel is assembled from hub with curved blades. The curved blades are critical components of the compressor wheel and their purpose is changing the direction of the airflow from axial to radial and at the same time to accelerate it to a high velocity. The shape of the compressor blade profile from the impeller inlet to the impeller outlet can significantly impact performance and durability [13]. In the Figure 8 is viewed that the blade is bounded by hub edge and from the other side by compressor housing countour so-called shroud edge. Charged air enters in axial direction the leading edge and then leaves the compressor wheel in radial direction with higher velocity due to the curved blade trailing edge (blade tip).

Backward, radial and forward are three standard types of curved blades but the utilization of forward blades is nowadays very rare. Radial impeller blades were very common in the past due to the easier way of manufacturing and strenght against the centrifugal forces resulting from high rotation speeds. However, Figure 9 shows that efficiency is lower with radial blades and for maximazing the efficiency of the compressor are backward blades the best option for modern turbochargers.
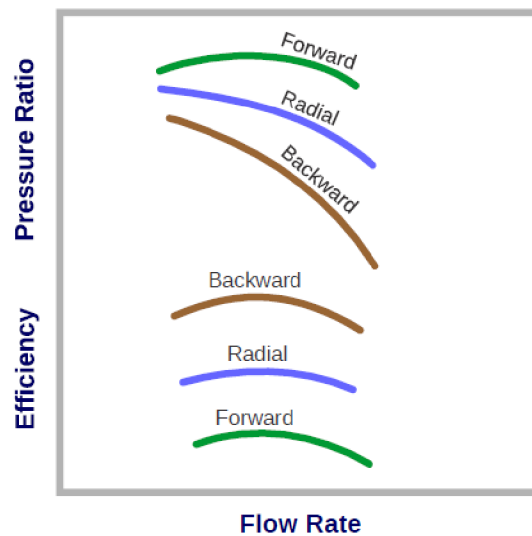
Figure 9 Effect of blade tip angle on efficiency and pressure ratio for given flow rate [13]

From the the Figure 9 is clear that backward blades has the highest efficiency but tend to provide the lowest pressure ratio for a given flow rate. The backward curvanture also means that blade tips can be subjected to significant bending forces at high rotation speeds with the bending stress increasing with backward sweep angle [13]. The influence of back sweep angle on performance and efficiency examined Wang et al. [14] in their study. Comparison of different back sweep angles resulting in different pressure ratios and efficiencies depending on engine speed.

Turbocharger compressors often benefit from a higher number of blades which can provide better flow guidance along the impeller but too many blades can cause a blockage at the inlet. Schwind and Abdallah [15] publication shows that addition of splitter blades is the solution for sufficient flow guidance while still keeping the number of blades at the inlet low.

Wheel trim is another aspect that have great influence on compressor performance. Wheel trim is an area ratio which express the relationship between inducer and exducer. Inducer is defined as diameter where air enters the wheel and exducer is diameter where air exits the wheel, see Figure 10.
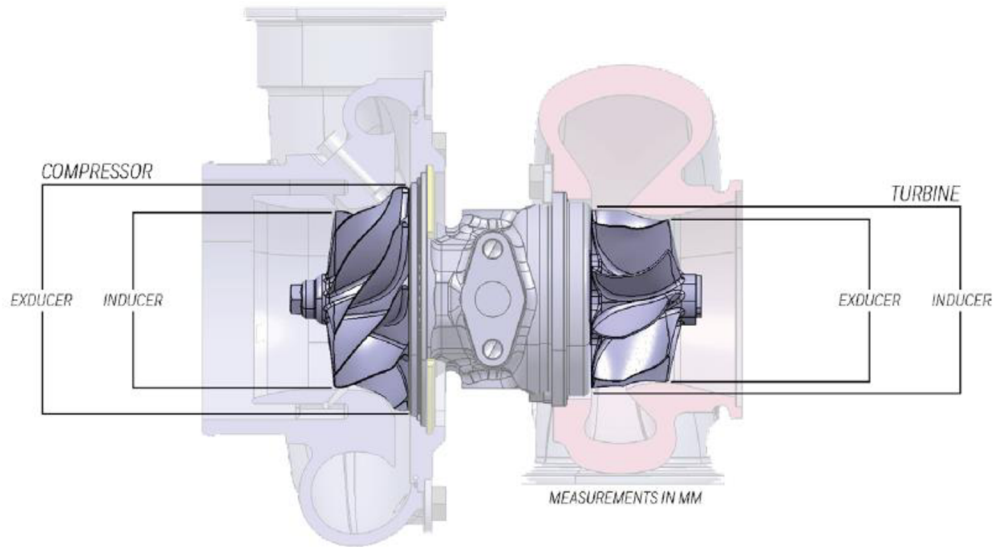
Figure 10 Exducer and inducer diameters of turbocharger [17]

$$Trim = \left(\frac{Inducer^2}{Exducer^2}\right) * 100, \tag{1}$$

is the equation for compressor wheel trim. Trim of the wheel affects performance by shifting the airflow capacity. If all other factors held constant, a higher trim wheel will flow more than a small trim wheel [17].

Compressor wheel is generally cast from alluminium alloys but titanium alloys are also used due to the higher pressure ratios, e.g. heavy duty vehicles. For fully machined compressor wheel, nickel plating is applied and provide better corrosion and erosion protection.

2.3.2 COMPRESSOR HOUSING

The compressor housing surrounds the impeller and addtitionally contains the inlet for the air flowing to the charger, the diffusor, the volute and possible air recirculation channels for flow-stabilization.

Diffuser, see Figure 8 could be vaned or vaneless and its main task is converting kinetic energy to pressure via volume expansion. Vaned diffusers are common in marine and generator applications where a high pressure ratio is often required [13]. Vaneless diffuser provides lower pressure recovery compared to vaned diffuser of the same diameter and it is used in most automotive type applications [13].
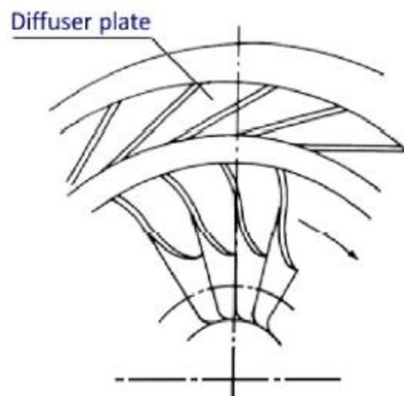
Figure 11 Radial compressor and vaned diffuser plate [13]

Spiral-shaped volute collects the flow from the diffuser and passes it to the compressor outlet. Related to the volute is A/R ratio which is expressed as the discharge cross-sectional area divided by the radius from the turbo centerline to the centroid of that area [17], see Figure 12. However, compressor performance is comparatively insensitive to changes in A/R ratio and probably the greatest influencer is wheel trim as it is mentidoned in Canove et al. [19] publication.

Compressor housing are cast from aluminium alloys but in the cases where compressor wheel is made of titanium alloys, the compressor housing is manufactured of ductile iron. Permanent mould or sand casting is usually utilized for compressor housings.
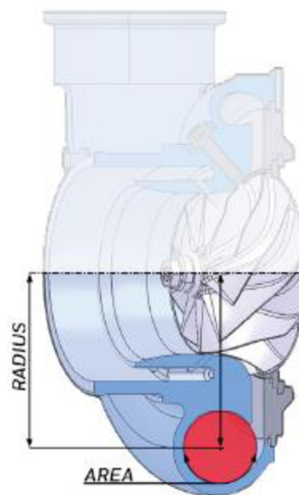

Figure 12 Area/Radius ratio of compressor housing [17]

2.3.3 COMPRESSOR MAP

Compressor map shows key characterictics of compressor which are needed for correct assignment of the wheel to the engine and provides operating envelope of the compressor over all stable operating points [13]. Key characteristics of compressor are measured on special test-bench facility called gas-stand. An example of data measurement and acquisition though specific senzors is described in Farrugia et al. [20] publication. There is a option to use CFD model resulting in flow solver which could be a prediction tool based only on the

machine geometry, offering the possibility of exploring the entire characteristic map of compressor, in this case [21] for marine application.
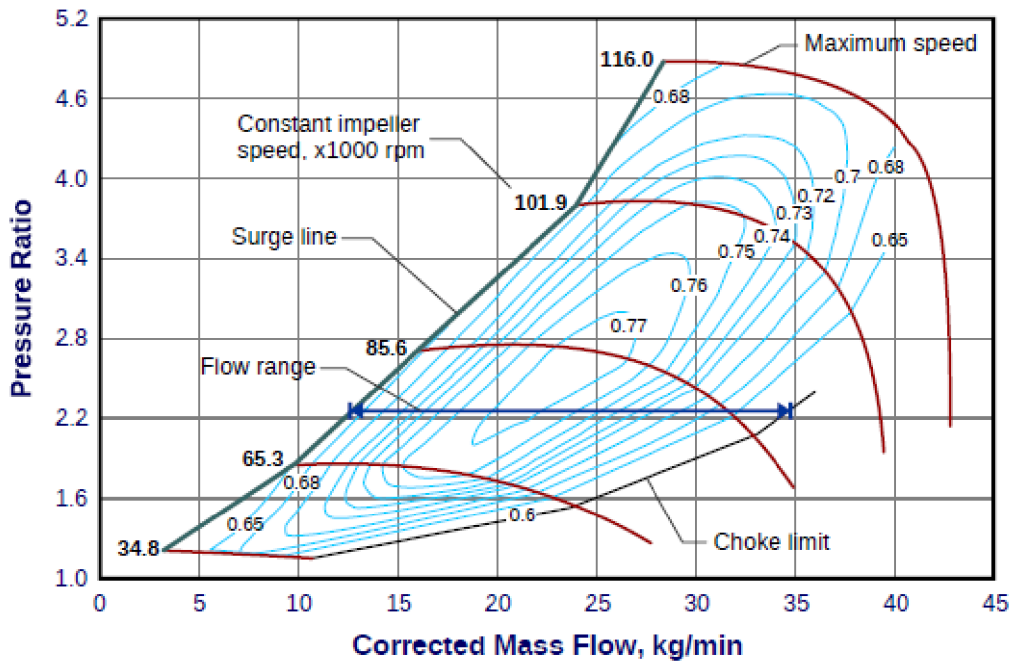

Figure 13 Compressor map illustration

The most important data of compressor is pressure ratio, plotted on the Y-axis and defining boost pressure of the engine. On the X-axis is plotted usable mass flow when compressor operates stably within acceptable limits effectiveness. Based on this range mass flow, it is possible to appropriately assign the compressor to the requirements of the engine. Commonly, contours of constant compressor efficiency are included on the compressor map.

The pressure ratio is a function of air flow, efficiency and turbocharger speed which are also shown in the compressor map as constant value curves. Speed and flow of air are corrected by pressure and temperature due to the different operating environments such as altitude or ambient air temperature. The correction is defined by the equations below.

$$\dot{m}_{\mathrm{ccor}} = \dot{m}_{\mathrm{c}} \frac{\sqrt{T_{\mathrm{in}}/T_{\mathrm{ref}}}}{p_{\mathrm{in}}/p_{\mathrm{ref}}}, \tag{2}$$

where $\dot{m}_{\mathrm{ccor}}$ is corrected mass flow rate, $\dot{m}_{\mathrm{c}}$ mass flow rate of compressor, T_{ref} and p_{ref} are the reference temperature and pressure, T_{in} and p_{in} are the temperature and pressure at the compressor inlet.

$$N_{\mathrm{ccor}} = N_{\mathrm{c}} \frac{1}{\sqrt{T_{\mathrm{in}}/T_{\mathrm{ref}}}}, \tag{3}$$

where N_{ccor} is corrected rotational speed and N_{c} rotational speed of compressor.

Figure 13 shows that there are three boundaries in compressor map. Surge line on the left, choke limit on the right and maximum compressor speed at the top.

Surge limit determines the minimum compressor flow for a given rotor speed. It occurs when the compressor stops operating stably, the air flow is reversed and air escapes before compressor inlet. This results in loud blows and pressure waves in the intake manifold leading to possible damage to the compressor [22]. The way to delay this behavior is in suitable adjustment of compressor housing and also correct geometry of the blades [22]. When selecting a compressor, it is essential that the conditions in which engine will operate were from this limit with a certain margin.

Choke limit occurs in a situation when the flow velocity at the narrowest entry area into the compressor reaches sonic speed. In this state it is no longer possible to increase mass flow of the compressor and in all tested speeds, the curve of the constant compressor speed in the limit case is close to the value pressure ratio 1 [22]. Resulting that the turbocharger is no longer able to exert any boosting pressure and air flows through it freely with high velocity [22]. The choke limit thefore determines the maximum flow capacity of the compressor and the narrowest entry is located either between the compressor blades or in the case of compressor housing with vaned diffuser is the narrowest are between them.

2.4 TURBINE PART OF TURBOCHARGER

Turbine part is consisted of turbine housing and turbine wheel. Job of the turbine housing is to guide exhaust gases into the turbine wheel. The energy from the exhaust gases turns the turbine wheel and then gas exits from the turbine housing through turbine exhaust outlet. There are different types of turbines which will be discussed in following subchapter.

2.4.1 TYPES OF TURBINE GEOMETRY

The task of the turbine wheel is to convert energy from exhaust gases to mechanical work as efficiently as possible and thus to rotate the shaft to which the wheel is welded. According to the direction of flow through the wheel, three types of turbine can be distinguished.
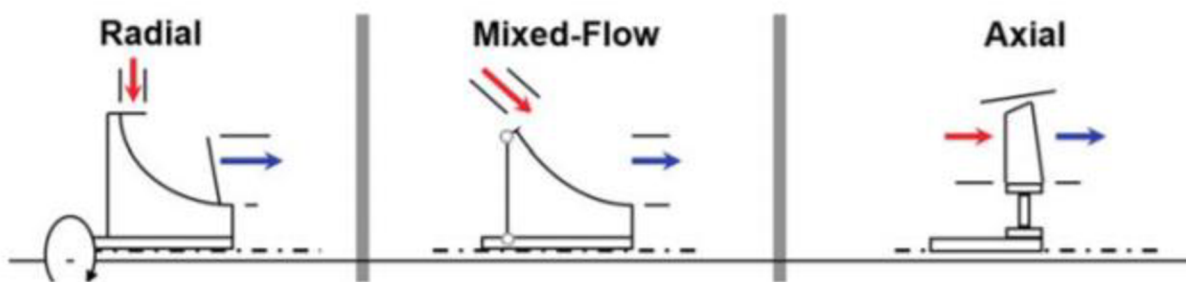

Figure 14 Types of turbines used in turbochargers [23]

In radial flow turbine gases enter in radial direction, perpendicular to the direction of rotation of the wheel and exit in axial direction. The wheel of the turbine is adjusted to operate with high efficiency in higher expansion ratios and lower gas flow. This turbine design provides compactness and strenght during high pressure, high temperature operations. Radial flow type turbine is most used in turbochargers for passenger and commercial vehicle applications.

Mixed-flow turbine has its place in commercial vehicle application where engines with large cylinder displacement are utilized. Turbine wheel is more efficient in conditions of higher expansion ratio and has higher flow capacity than radial. Gases enter and exit in direction

shown in Figure 14. An influence of number and angle of turbine wheel blades on performance and efficiency are presented in [23, 24] articles.

In axial flow turbine gases enter and exit the turbine wheel in axial direction, i.e. parallel to the axis of rotation of the turbine. Turbine wheel provides good efficiency in larger sizes engines where gas flow is high and expansion ratio low. The most common examples of application are medium and low speed engines, e.g. marine engines or stationary engines.

Energy extracted from the flow depends on the velocity vectors entering the turbine blade. Energy extraction is explained on example of radial flow turbine without losses in Figure 15. In this case, power output gained from working substance to the wheel is equal to the change in momentum cicumferential component of the input and output velocity vector and it is possible to apply Euler´s equation. Energy extracted is expressed as the difference between the product of blade speed and tangencial component of the absolute flow velocity. Output loss is the smalles for the zero velocity of the tangencial component $V_{6\theta}$ and therefore is it advisable to design the turbine output angle from the wheel to the axis of rotation as close as possible to zero. Euler´s equation and turbine power equation are

$$E_{\text{ext}} = (U_5 V_{5\theta} - U_6 V_{6\theta}),$$ (4)

where E_{ext} is actual energy extracted, U_5 and U_6 are blade speed vectors, $V_{5\theta}$ and $V_{6\theta}$ are tangencial components of absolute flow velocity where $V_{6\theta}$ is typically 0.

$$P_{\text{T}} = \dot{m}_{\text{T}} \cdot E_{\text{ext}},$$ (5)

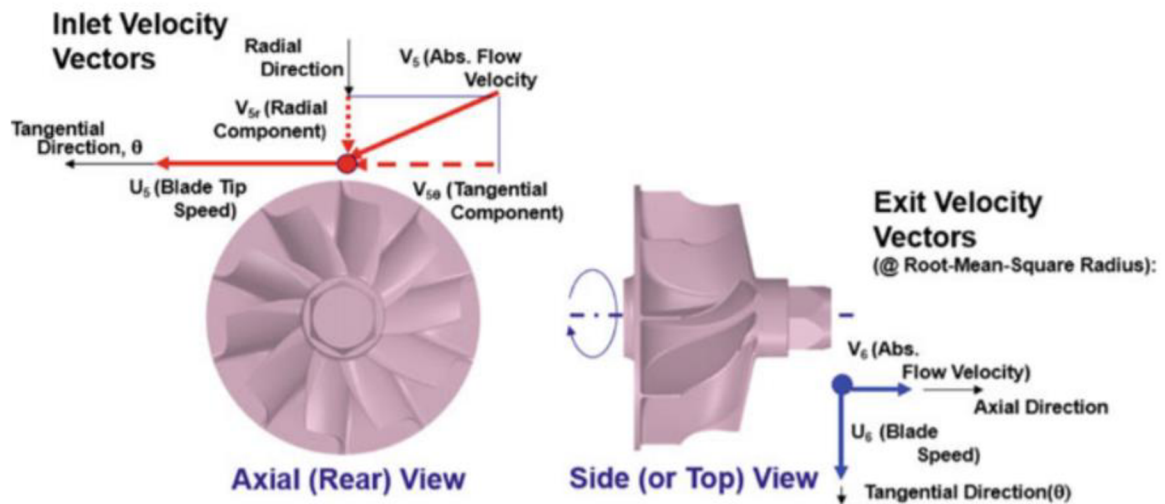where P_{T} is turbine power and $\dot{m}_{\text{T}}$ is turbine mass flow rate.

Figure 15 Velocity diagram of radial turbine [23]

For turbines, the trim is also an important parameter that influences flow capacity. A larger trim will handle a higher flow rate and result in less backpressure but will recover less exhaust energy and increase turbocharger lag [13].

Turbine wheels are usually cast from nickel-based super-alloys which must meet certain properties, especially high temperature strenght, fatigue resistance, good creep resistance, oxidation resistance etc.

2.4.2 TURBINE HOUSING

Turbine housing has the same spiral shape as compressor housing and its task is to accelerate and direct the exhaust gases to the wheel. Turbine A/R ratio has a much greater effect on performance of turbine than in the case of compressor housing. Turbine A/R ratio is the inlet cross section are divided by the radius from the turbo centerline to the centroid of that area and adjust the flow capacity of the turbine [17], see Figure 16.
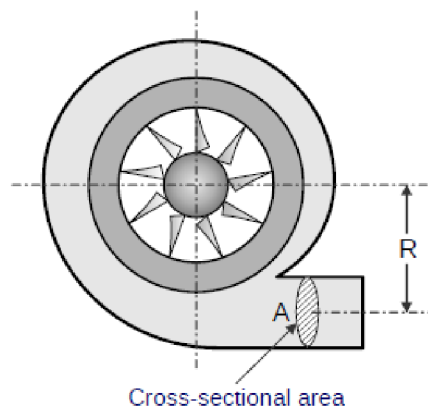

Figure 16 A/R ratio of turbine housing

As shown in [17] using a smaller A/R ratio will increase the exhaust gas velocity into the turbine wheel and it provides increase of turbine power at lower engine speeds, resulting in a quicker boost rise. The disadvantage of the smaller A/R ratio is that flow enters the wheel more tangentially which results in reduction of turbine wheel flow capacity. This reduction will cause increasing of exhaust backpressure and reduce engine ability to operate effectively at high speeds and also affect peak engine power. On the opposite larger A/R will lower gas velocity and delay boost rise due to the flow enters the wheel more radially. Large A/R also increase wheel flow capacity which results in lower back pressure and better power at higher engine speeds.
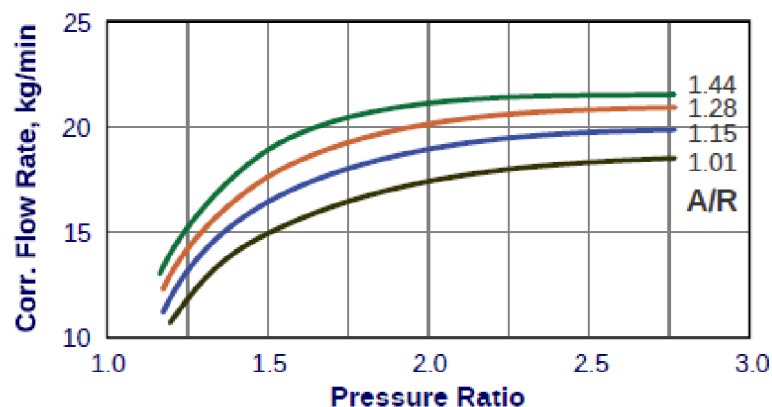

Figure 17 Effect of A/R ratio on swallowing capacity (definiton in subchapter 2.3.3) of an exhaust gas turbine [13]

Turbine housing must be optimized depending whether it is constant pressure type of turbocharging or pulse turbocharging. For constant pressure turbocharging the exhaust inlet of the housing is not splitted but for pulse turbocharging the inlet is splitted into two parts, where a seperation of exhaust gases from individual cylinders is relevant because of pulsations maintanance and their influence on performance [36]. This type of turbine is called twin scroll turbine and another option is dual volute turbine, see Figure 18.
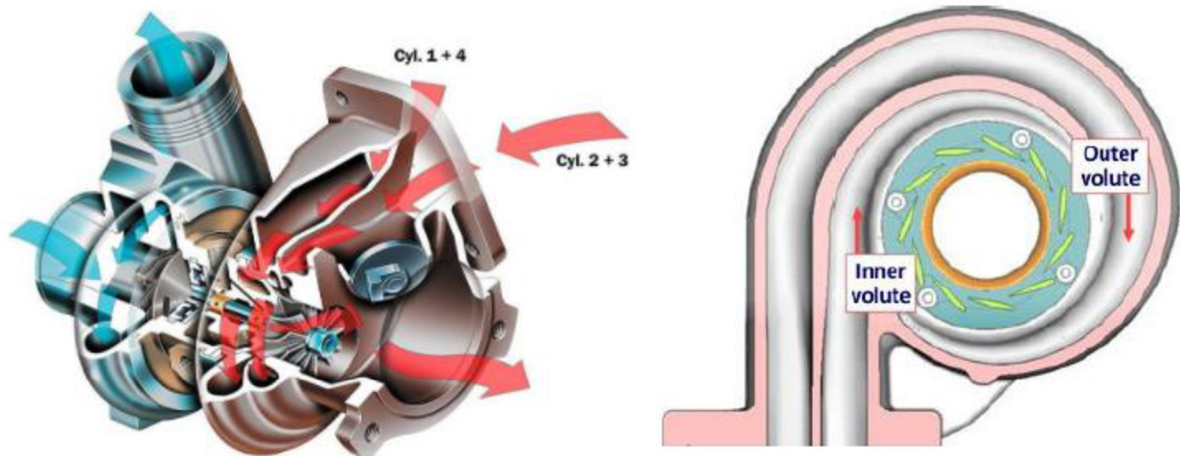

Figure 18 Twin scroll and dual volute turbine [26,13]

The utilization of asymmetrical twin scroll turbine in Figure 19 is very often, when a smaller part of turbine inlet is connected to energy gas recirculation (EGR) system and allows a greater pressure drop required to control gas recirculation.
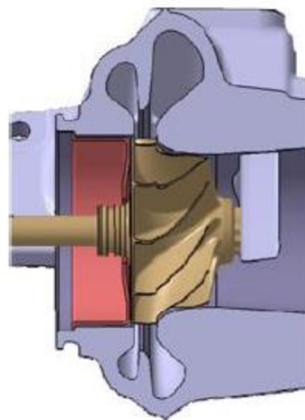

Figure 19 Asymmetrical twin scroll turbine [13]

2.4.3 TURBINE MAP

Similar to the compressor, turbine characteristics or so-called turbine map is used to assign the correct turbine to the engine. The map contains data of pressure ratio, corrected mass flow rate, efficiency and speed which is collected from gas-stand test.
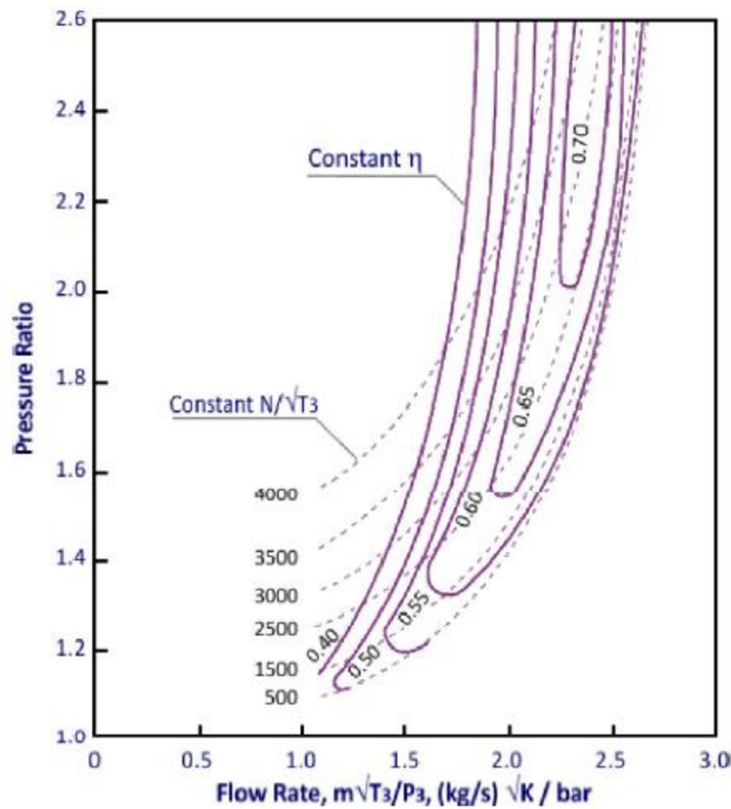
Figure 20 Example of full turbine map [13]

Rarely the entire map as in Figure 20 is shown and map in Figure 21 is more commonly found. When the pressure ratio versus mass flow characteristics at a number of turbine speeds are plotted in this way, they often form a curve that is almost continuous [13]. A line drawn through these curves at the peak efficiency for each turbine speed is sometimes referred to as the turbine swallowing capacity and represents the desired operating curve of the turbine [13].

Figure 21 Turbine swallowing capacity (lower curve) and efficiency (upper curve) [13]

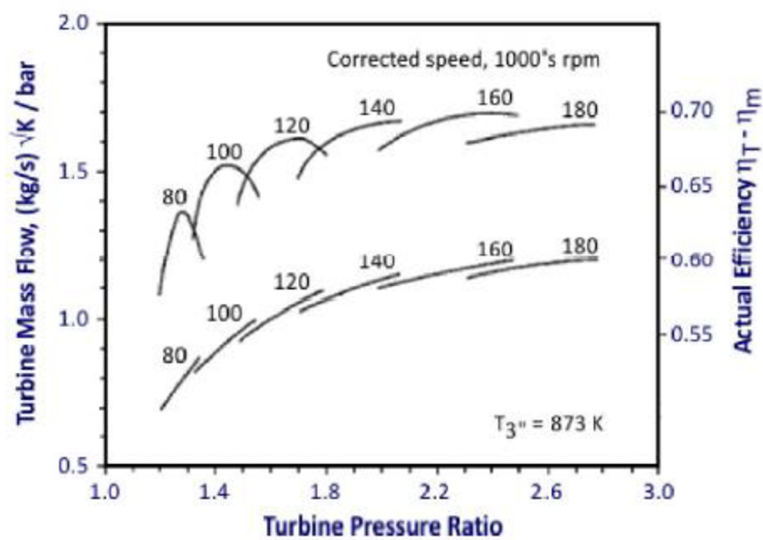For the comparison between turbines a number of dimensionless parameters exist, which are describing turbine properties from performance perspective. First of them is specific speed which is used to relate the performance of geometrically similar turbines of different size. Specific speed of a turbine is definied as

$$N_{\text{s}} = \frac{\omega \sqrt{Q_2}}{(\Delta h_{\text{ideal}})^{\frac{3}{4}}}, \tag{6}$$

where N_{s} is specific speed, ω is angular velocity of rotor, Q_2 is volumetric flow rate through the turbine at rotor exit conditions and Δh_{ideal} is ideal enthalpy change across the turbine.

Another less utilized dimensionless parameter is specific diameter which also as specific speed compares turbine performance. Specific diameter is defined as

$$D_{\text{s}} = \frac{d_{\text{tip}}(\Delta h_{\text{ideal}})^{\frac{1}{4}}}{\sqrt{Q_2}}, \tag{7}$$

where D_{s} is specific diameter and d_{tip} is tip diameter (largest) of turbine rotor (wheel).

Turbine performance can also be correlated against the blade-jet speed ratio (blade speed ratio), which is ratio between blade speed relative to the ideal stator exit velocity [13]. The ideal stator exit velocity C_0 is calculated assuming the entire ideal enthalpy change across the turbine is converted into kinetic energy [13].

Blade speed ratio is then calculated from

$$BSR = \frac{U}{C_0} = \frac{U}{\sqrt{2\Delta h_{\text{ideal}}}}, \tag{8}$$

where BSR is blade speed ratio, U is blade speed relative and C_0 is ideal stator exit velocity.
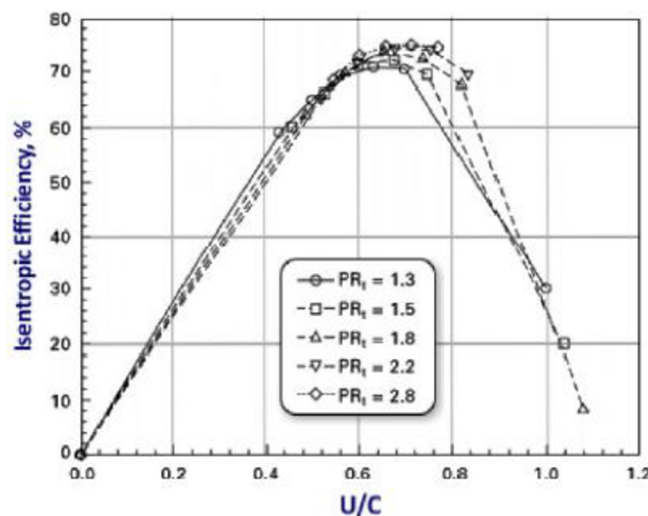

Figure 22 Turbine isentropic efficiency as function of blade speed ratio

2.5 TURBOCHARGER REGULATION METHODS

For the boost pressure control of the engine with turbocharger, there are three convential methods of turbocharger regulation used. Every type of turbocharger is suitable for precific type of the engine but in some occasions there could be more options for boost regulation of the engine and in this case the performance-prize ratio is the determining factor. There are engines where regulation is unnecessary but also engines which would not operate properly without regulation.

2.5.1 FIXED GEOMETRY TURBOCHARGER WITHOUT REGULATION

Fixed geometry no bypass is the simplest type of turbocharger and its boost pressure is entirely determined by the engine exhaust flow and turbocharger characteristics. This type of turbocharger is optimized for just one specific operating point of the engine. Turbocharger turbine size or A/R ratio tend tobe retively large for a given application because of the need to size the turbocharger so that at the highest flow conditions, the turbocharger does not overspeed or provide excessive boost pressure but for high altitude conditions, turbocharger speeds would tend to increase which could lead to problems with surge or turbocharger overspeeding unless accounted for by oversizing the turbocharger [27]. In Figure 23 is obvious that small fixed geometry turbocharger could overspeed the engine at retively low engine speeds. For engine applications operating primarily at a limited number of steady-state conditions e.g. marine engines or backup electricity generators could be fixed geometry no bypass turbocharger best solution in terms of price and reliability.
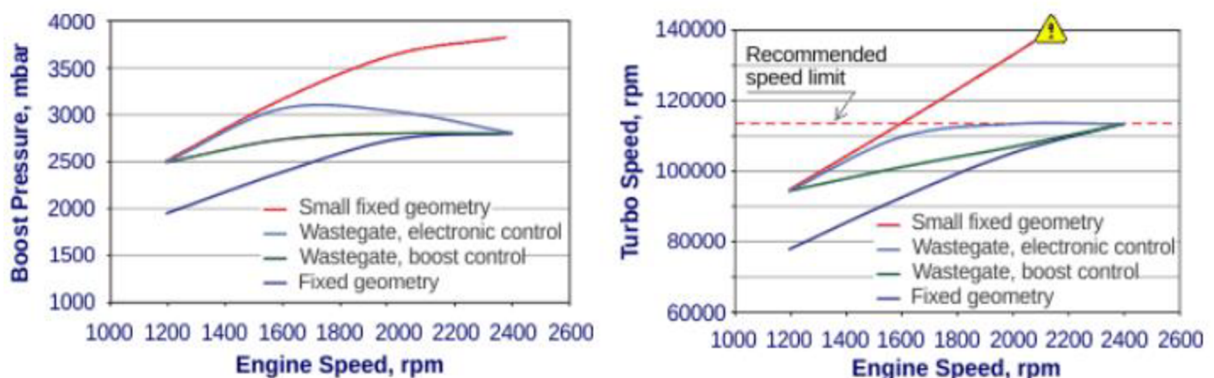
Figure 23 Boost pressure and turbo speed for various types of turbochargers depending on engine speed [27]

2.5.2 FIXED GEOMETRY WASTEGATE TURBOCHARGER

For applications that experience a wide range of operating conditions and must provide good dynamic response is controlling a boost pressure essential, e.g. in passenger car applications. Adding a bypass valve allowing some of the exhaust gas to bypass the turbine, thus control pressure boost produced by the compressor and avoid dangerous situations as overspeed mentioned above.
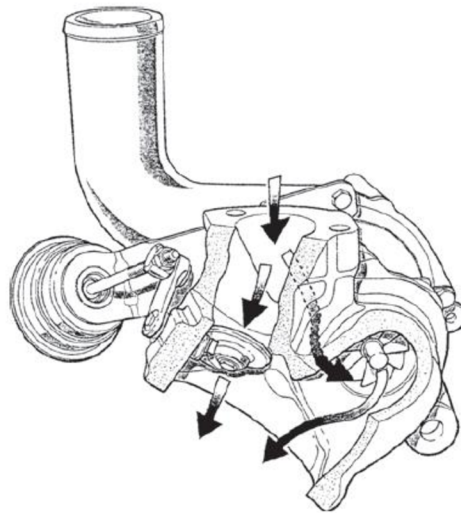
Figure 24 Gas flow though the turbine and wastegate [2]
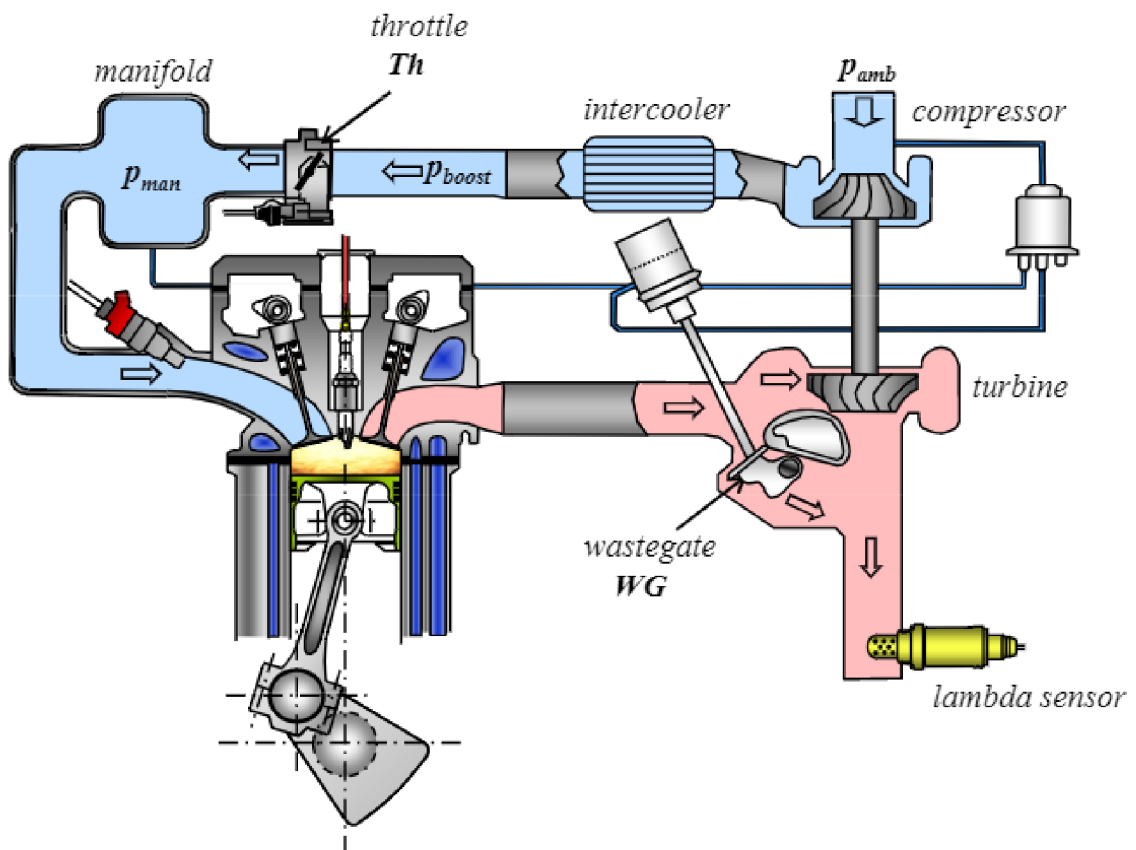
Figure 25 Wastegate turbocharger in spark ignition engine architecture

The effect of different wastegate valve openings on turbine plus bypass mas flow and turbine efficiency is illustrated in Figure 26. As the wastegate opens at a fixed pressure ratio, the total mass flow increases because of the increased amount of bypass flow while overall efficiency drops [27]. This efficiency drop is related to wastegate opening and bypassing the exhaust gases resulting in less compressor power input thus limiting speed of the rotor and boost pressure.
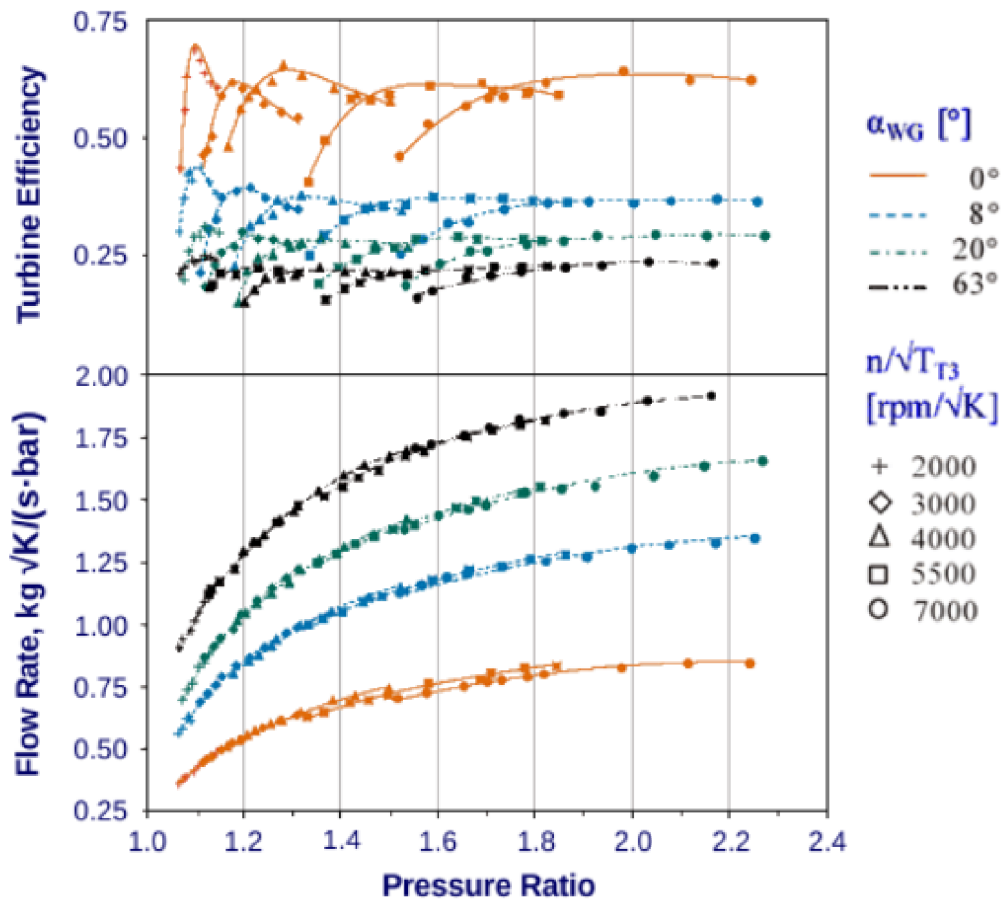
Figure 26 Effect of wastegate opening angle on turbine + bypass mass flow rate and overall efficiency [27]

Figure 27 shows full load boost characteristic in compressor map for wastegate and no bypass turbocharger. Each turbine is sized to provide the engine with the same boost pressure, intake air mass flow and rotationall speed at rated power [27]. Due to the boost control of wastegate turbocharger there is an advantage of being able to use a smaller turbine or lower A/R that is able to provide more power to the compressor at lower exhaust flows resulting in significantly improved transient response.
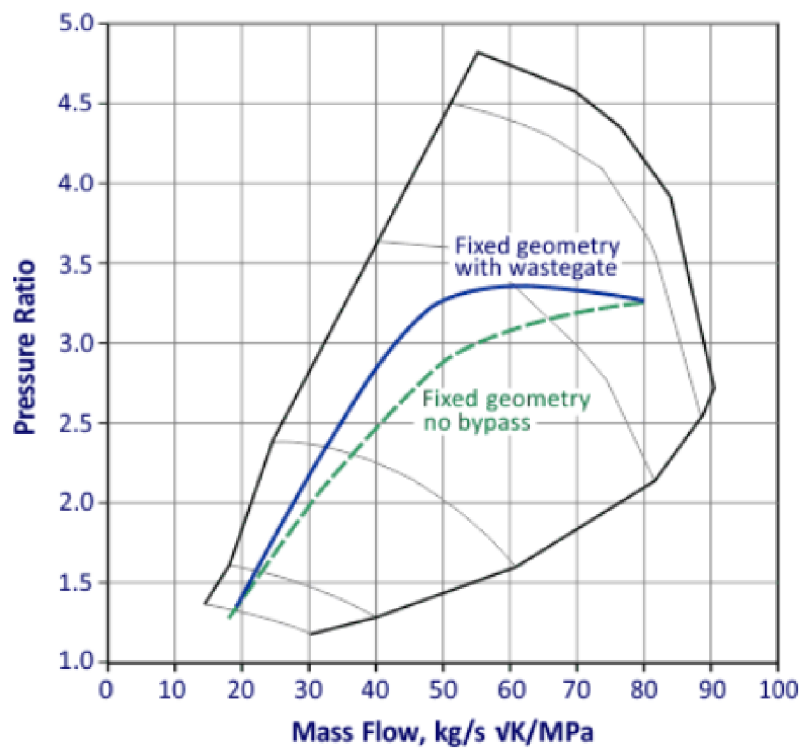
Figure 27 Full load boost characteristics with different turbine options [27]

A wastegate can be built into the turbine side of the turbocharger (internal wastegate) or a separate valve connected to the external plumbing (external wastegate) but the internal is preffered and shown in Figure 28 [27]. Wastegate valve is managed by pneumatic or electric actuator.
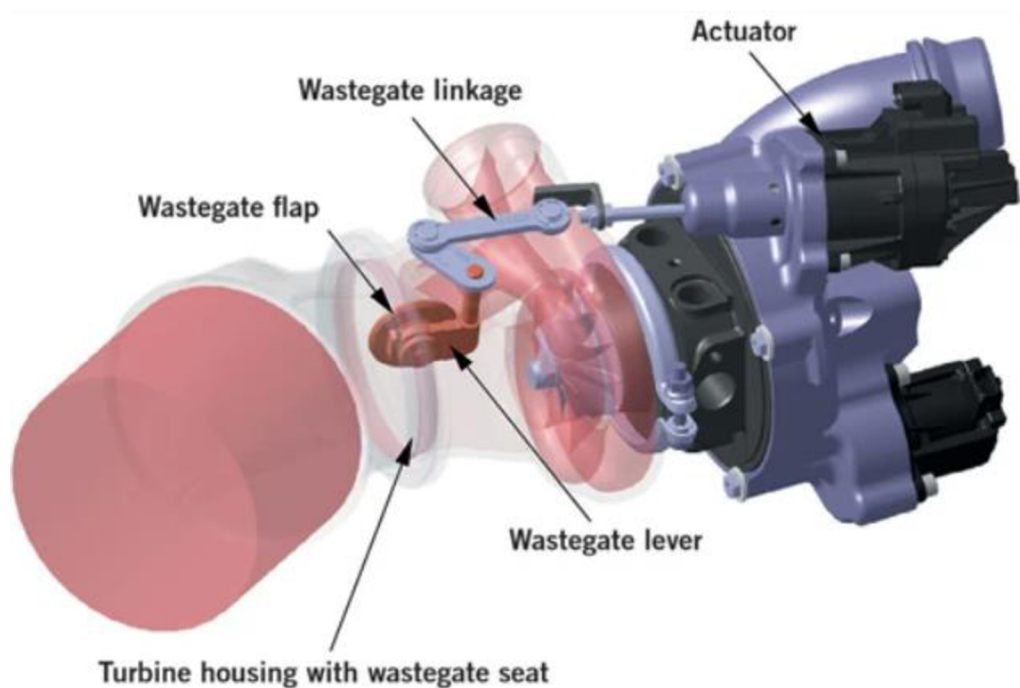
Figure 28 Wastegate turbocharger with electric actuator for BMW gasoline engine [30]

2.5.3 VARIABLE GEOMETRY TURBOCHARGER

Variable geometry turbine (VGT) is alternative to the fixed geometry turbine. There are a number of acronyms that are commonly used for variable geometry turbocharger depending on turbocharger manufacturer. Garrett Motion acronym for this type of turbocharger is VNT - Variable nozzle geometry.
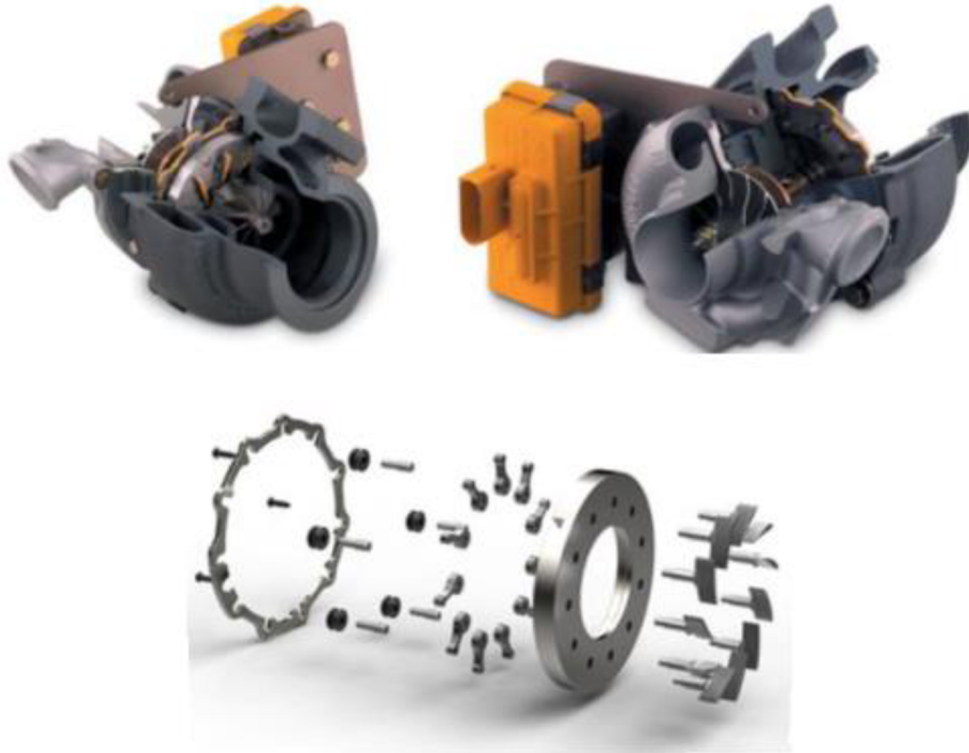
Figure 29 VNT turbocharger views at the top and pivoting vane type of VNT at the bottom [28]

VNT turbine has many benefits compared to fixed geometry turbine including possible change flow through the turbine caused by pivoting stator vanes (pivoting vane design) or variable width nozzle (moving wall design), both methods are shown below and described in Pesiridis et al. [38] study with future possible enhancements.
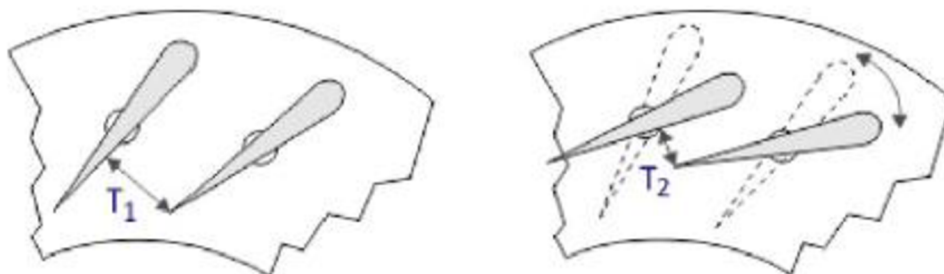
Figure 30 Pivoting vane variable geometry turbine [28]
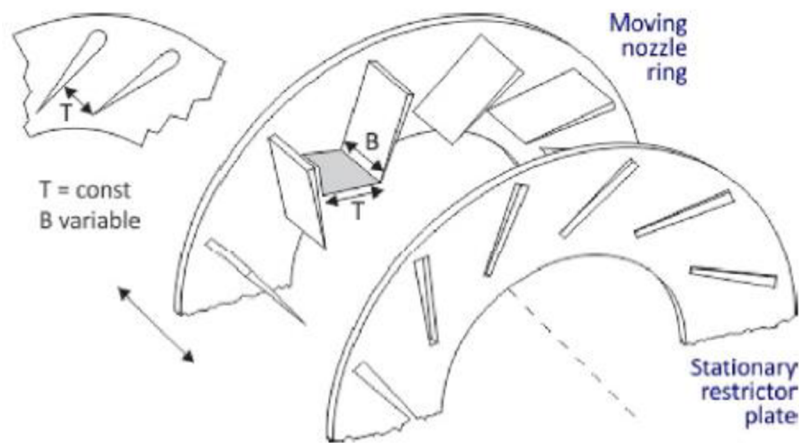
Figure 31 Moving nozzle or moving wall type variable geometry turbine [28]

Figure 32 shows full load boost characteristics of all described regulation types of turbines. It is clear that variable geometry turbine is able to provide a higher full pressure ratio over range of flows encountered if the turbine size is correct to handle all of the exhaust flow [28]. Also, since it is possible to control the boost pressure via the turbine's nozzle opening, a turbocharger with a variable geometry turbine can operate much closer to the surge margin without the risk of experiencing surge due to changes in compressor inlet conditions [28].
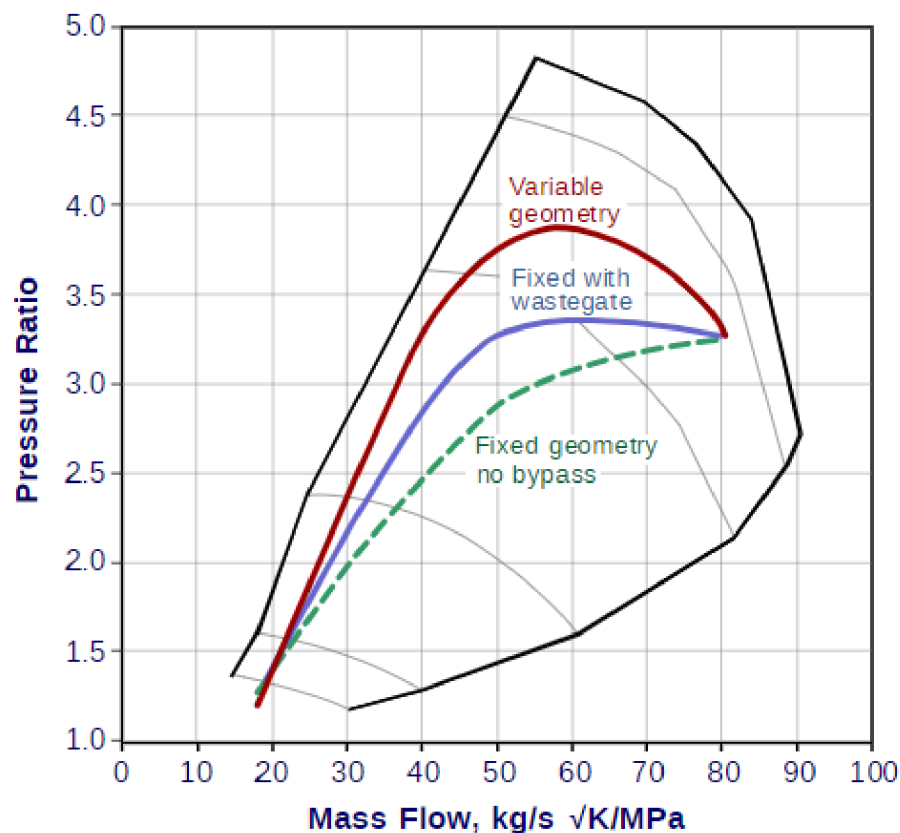
Figure 32 Compressor map showing full load boost characteristics with three different turbine options [28]

Variable flow rate reflects the effect of changing A/R ratio when at low engine speed the vanes are closing and with increasing engine speed thus higher exhaust flow the vanes are opening gradually. Closing the vanes at low engine speed results in an increase of boost pressure at turbine inlet which leads to higher turbine speeds and higher mass flow through the engine.
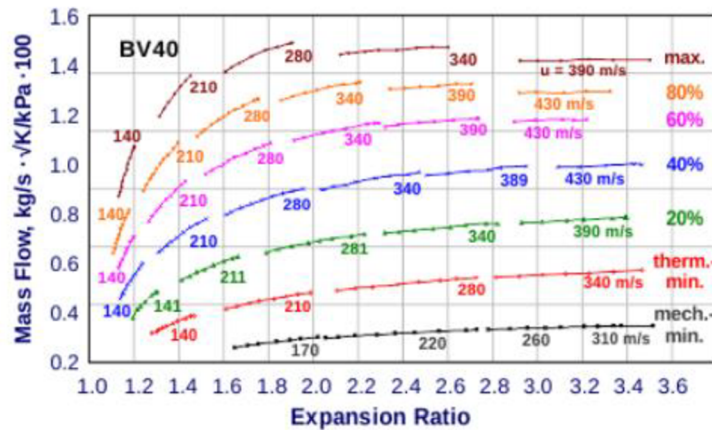
Figure 33 Variable vanes openings of VNT turbocharger in turbine characteristic

These facts are confirmed by examination in Figure 34 where turbine inlet flow and temperature are constant but inlet pressure is increased by closing the turbine vanes. As the vanes close, the available flow work represented by the turbine pressure ratio increases while turbine efficiency decreases [28]. The product of these two reflects the work extracted by the turbine and in this example, reaches a maximum when the turbine vanes are 80% closed [28].
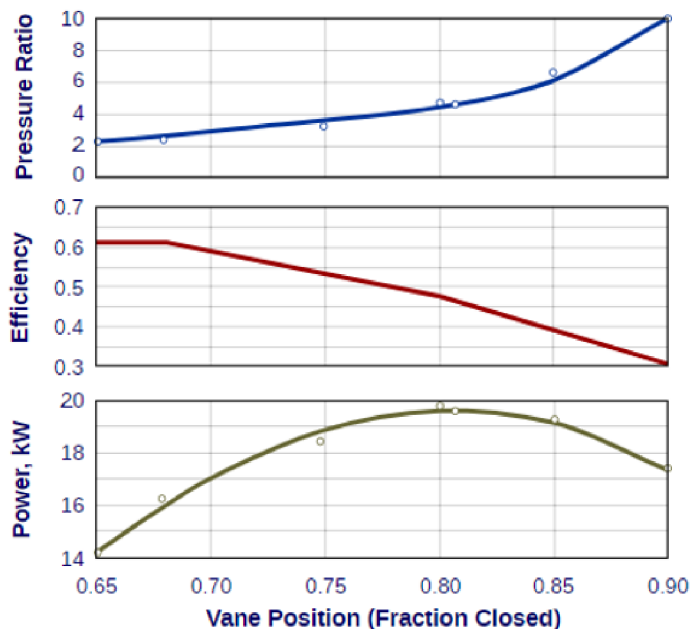
Figure 34 Effect of turbine vane position on the turbine pressure ratio, efficiency and power produced by turbine for given conditions [28]

Another advantage of utilization of VNT turbine is reduce turbocharger lag and improve engine trasient response, Figure 35.
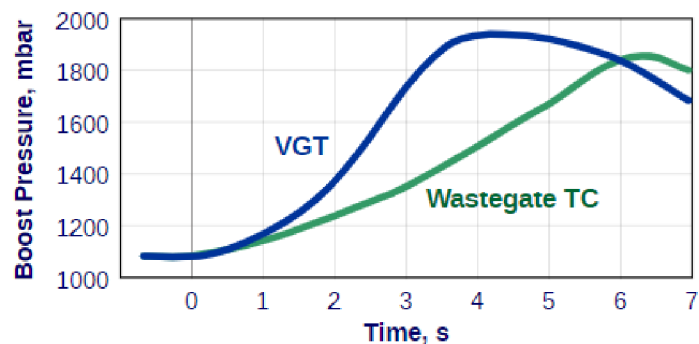
Figure 35 Improvement in transient boost pressure response is possible with a VGT [28]

Variable geometry turbochargers are usually combined with diesel engines in automotive application. The combination with gasoline engine is more complex, especially in terms of coping with higher exhaust temperatures [32]. An example of gasoline engine coupled with variable turbine geometry turbocharger and miller cycle with valve timing is Volkswagen EA211 TSI evo in Figure 36.
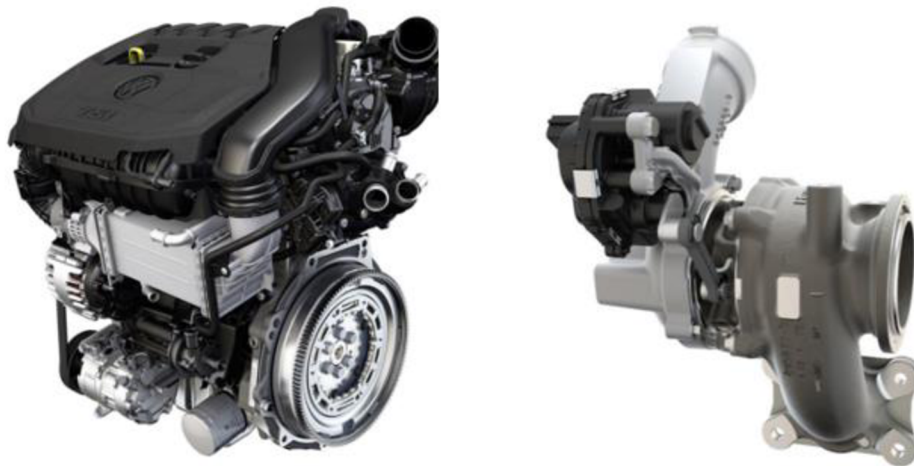
Figure 36 VW EA211 TSI evo and VNT turbocharger [31]

2.6 THERMODYNAMICS OF TURBOCHARGER

Thermodynamics plays a big role in turbocharger development. As Nguyen-Schäfer [1] refers, some essential thermodynamic characteristics of gases are needed to know in the turbocharging and expressed them in following equations where charge air and exhaust gas assumed as compressible ideal gases.

Total specific enthalpy of the flow is expressed as a sum of the gas specific enthalpy and specific kinetic energy of the gas

$$h_\mathrm{t} = h_\mathrm{s} + \frac{c^2}{2},$$ (9)

where h_t is total specific enthalpy, c is the gas velocity and h_s is gas specific enthalpy when

$$h_s = u + \frac{p}{\rho},$$ (10)

where u is the specific internal energy of gas and ρ is gas density.

Then total temperature T_t is the sum of static temperature T_s and dynamic temperature T_{dyn}. The static temperature is measured at the wall, where the gas velocity equals zero due to the viscous boundary layer and dynamic temperature is measured by probe in flow of air or exhaust gases. Based on the enthalpy equations, the equation for total temperature is

$$T_t = T_s + T_{dyn} = T_s + \frac{c^2}{2c_p},$$ (11)

where T_t is total temperature, T_s is the static temperature, T_{dyn} is dynamic temperature and c_p is the heat capacity at constant pressure.

For best possible power output of the turbocharger, high efficiencies of turbocharger components are required. High efficiency of turbocharger has also positive effect on engine efficiency. The compressor efficiency η_C is defined as the ratio of the isentropic total enthalpy change from 1t to 2st to the polytropic total enthalpy change from 1t to 2t [1], see Figure 37. The total-total isentropic efficiency of the compressor stage (compressor) is defined as

$$\eta_C = \frac{\Delta h_{s,tt}}{\Delta h_{12,tt}} = \frac{h_{2st} - h_{1t}}{h_{2t} - h_{1t}} = \frac{T_{2st} - T_{1t}}{T_{2t} - T_{1t}},$$ (12)

where η_C is total-total isentropic efficiency, h_{2st} is total specific isentropic enthalpy at the compressor outlet, h_{1t} is total specific polytropic enthalpy at the compressor inlet, h_{2t} is total specific polytropic enthalpy at compressor outlet, T_{2st} temperature after isentropic compression in compressor, T_{1t} temperature at the compressor inlet and T_{2t} temperature after polytropic compression in compressor.
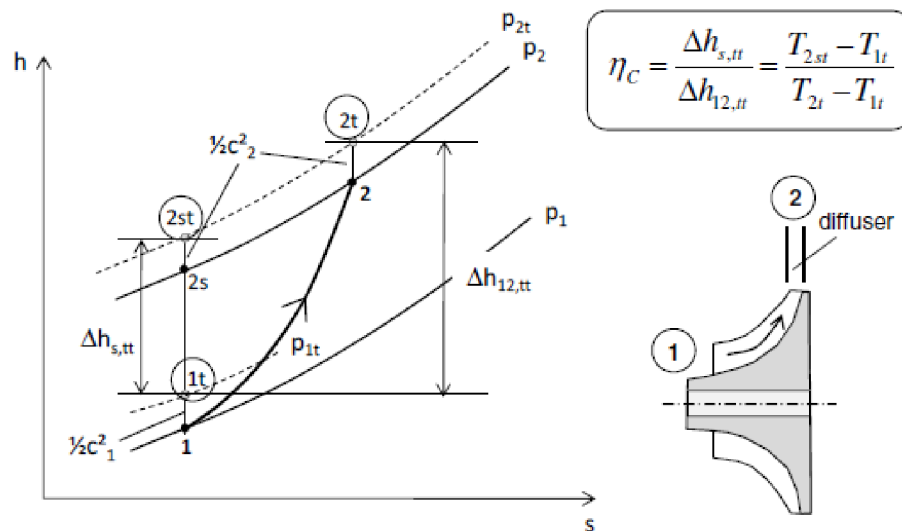

Figure 37 Compression process in the compressor stage [1]

The total-total isentropic efficiency is generally used in the compressor since the kinetic energy of gas in the state 2 is transformed into the pressure energy in the diffuser to further increase the pressure of charge air [1].

Expressing the isentropic temperature $T_{2\text{st}}$ based on pressure ratio and using equations for adiabatic process with equation of state the final form for $T_{2\text{st}}$ is

$$T_{2\text{st}} = T_{1\text{t}} \left(\frac{p_{2\text{t}}}{p_{1\text{t}}} \right)^{\frac{\kappa-1}{\kappa}} . \tag{13}$$

Substituting this form into compressor efficiency equation and subsequent adjustments, the compressor effiency can be written in the total pressures and temperatures at the inlet and outlet of the compressor and the isentropic exponent of the charge air.

$$\eta_{\text{C}} = \frac{\left(\frac{p_{2\text{t}}}{p_{1\text{t}}} \right)^{\left(\frac{\kappa-1}{\kappa} \right)_{\text{a}}} - 1}{\left(\frac{T_{2\text{t}}}{T_{1\text{t}}} \right) - 1} , \tag{14}$$

where $p_{1\text{t}}$ is total pressure at the compressor inlet, $p_{2\text{t}}$ is total pressure at the compressor outlet and κ_{a} (≈ 1.4) isentropic exponent of the charge air. The maximum total-total isentropic efficiency of the compressor η_{C} is normally between 70% and 80% at the design point of the compressor wheel [1].

The power input to the compressor is defined as

$$P_{\text{C}} = \frac{P_{\text{C,ideal}}}{\eta_{\text{C}}} = \frac{\dot{m}_{\text{C}} \Delta h_{\text{sC}}}{\eta_{\text{C}}} , \tag{15}$$

where P_{C} is power input of the compressor, $P_{\text{C,ideal}}$ is ideal compressor power at the isentropic compression, $\dot{m}_{\text{C}}$ is mass flow rate through the compressor and Δh_{sC} is the increase of isentropic entalpy in the compress.

The final equation for required compressor power of the charge air as function of the mass flow rate, inlet temperature and pressure ratio of the compressor [1] is

$$P_{\text{C}} = \frac{P_{\text{C,ideal}}}{\eta_{\text{C}}} = \frac{\dot{m}_{\text{C}} c_{\text{p,a}} T_1}{\eta_{\text{C}}} \left[\left(\frac{p_{2\text{t}}}{p_{1\text{t}}} \right)^{\left(\frac{\kappa-1}{\kappa} \right)_{\text{a}}} - 1 \right] . \tag{16}$$

Analogous to the compressor, the efficiency of turbine is resulted from the polytropic expansion process of the exhaust gas [1]. The turbine efficiency η_{T} is defined as the ratio of the polytropical total enthalpy change from 3t to 4t to the isentropic total enthalpy change from 3t to 4s [1].
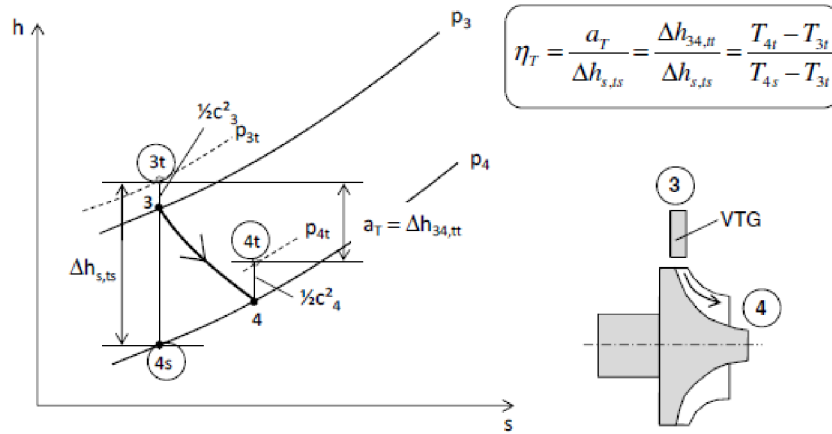
Figure 38 Expansion process in the turbine stage [1]

The total-static isentropic efficiency of the turbine stage (turbine) consisting of the turbine wheel and variable turbine geometry (VTG) or waste gate (WG) is written as

$$\eta_T = \frac{\Delta h_{34,tt}}{\Delta h_{s,ts}} = \frac{T_{4t} - T_{3t}}{T_{4s} - T_{3t}}, \tag{17}$$

where η_T is total-stacic efficiency, T_{4s} is temperature after the izoentropic expasion at the turbine outlet, T_{4t} is temperature after the polytropic expasion at turbine outlet and T_{3t} is temperature before turbine inlet.

The total-static isentropic efficiency is normally used in the turbine since the kinetic energy of gas in the state 4 does not generate the turbine power any longer [1]. As with the compressor, it is possible to utilizice the thermodynamics equations and express the turbine efficiency in the total pressure and temperature at the inlet and outlet of the turbine

$$\eta_T = \frac{1 - \left(\frac{T_{4t}}{T_{3t}}\right)}{1 - \left(\frac{p_{4s}}{p_{3t}}\right)^{\left(\frac{\kappa - 1}{\kappa}\right)_g}}, \tag{18}$$

where p_{3t} and p_{4s} are total pressures at the turbine inlet and outlet and κ_g (≈ 1.32) is the isentropic exponent of the exhaust gas.

The maximum total-static isentropic efficiency of the turbine η_T is normally between 65% and 70% at the design point of the turbine wheel [1].

Final power output genereted by the turbine is

$$P_T = \eta_T \dot{m}_T c_{p,g} T_3 \left[1 - \left(\frac{p_{4s}}{p_{3t}}\right)^{\left(\frac{\kappa - 1}{\kappa}\right)_g} \right], \tag{19}$$

where $\dot{m}_T$ is mass flow rate through the turbine and $c_{p,g}$ is heat capacity of gas at constant pressure.

Power can be considered in the case of steady state modes proportional to the flow thus performance balance where the compressor power is equal to the turbine power and bearing losses which represents the mechanical efficiency. This balance represents equation

$$P_C = \eta_m P_T \,, \tag{20}$$

where η_m is mechanical efficiency, P_C and P_T are compressor and turbine power.

The final equation for turbocharger efficiency is written as

$$\eta_{TC} = \eta_T \eta_C \eta_m \,. \tag{21}$$

3 E-TURBO

Hybridization of the base powertrain opens the possibility of electrifcation of the boosting system. Electrically assisted turbocharger or E-Turbo belongs into the group of E-Boosting systems [44, 18] which are electrically assisted systems of supercharing and possible energy recuperation. These systems and E-Turbo especially are in deep development phases because of their potential functionalities.

Figure 39 Possible functionalities of an electrified turbocharger for specific applications (Ligh vehicle gasoline, light vehicle diesel, light duty truck) [41]

E-Turbo is currently the most widely deleloped product of the E-Boosting group due to its possibilities of use for conventional powertrains. There are a few different designs of E-Turbo [39, 40] but the most common one is with motor-generator between the compressor and the turbine side [41], see Figure 40. This design is the most compact but it is necessary to note the fact that electrical part must withstand the high temperatures from the turbine side and thefore the stator of the electric part has to be cooled sufficiently.
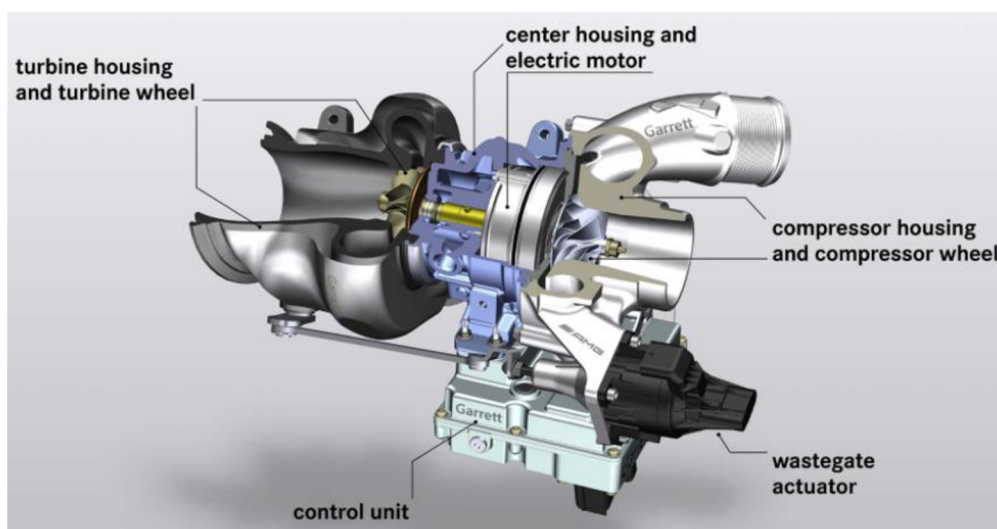
Figure 40 Garrett E-Turbo for Mercedes Benz AMG´s One hypercar [42]

Fully operable E-Turbo with motor generator providing electric power to boost the compressor of turbocharger and also energy recuperation was used for the first time in 2014 in Formula F1 application. As is shown in Figure 41, the hybrid F1 powertrain is equipped with two motor generator units which can recover energy. MGU-K generator unit recovers energy from braking, regenerative braking will be discussed in chapter 4. MGU-H generator unit which absorbs power from the turbine shaft to convert heat energy from the exhaust gases and pass it to the MGU-K (or the battery in case it needs recharging), but is also used to control speed of the turbocharger to match the air requirement of the engine by slowing it down in place of a wastegate or accelerating it to compensate for turbo lag [43].

Figure 41 F1 V6 hybrid powertrain with MGU-K and MGU-H generator units for energy recovering [43]

For the commercial and passanger car it is ordinary to have one turbocharger in engine area for simplicity and compactness. In this case E-Turbo with motor-generator on turbocharger shaft is the best option and must be able to recuperate the energy and also deliver it to the compressor if it is needed. The schematic layout of this system is presented in Figure 42.

Figure 42 Schematic layout of engine with electrically assisted turbocharger [44]

3.1 ENERGY RECUPERATION
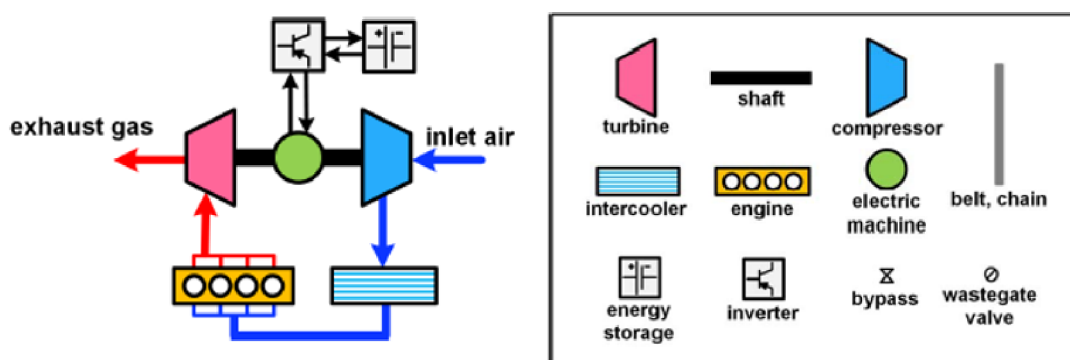
As shown in Figure 39, energy recuperation is one of the funclionalities of electrically assisted turbocharger. Enthalpy of conventional turbocharger is utilized for air compression but with E-Turbo it is possible to convert part of the enthalpy into electric energy. High temperatures and high pressure before turbine is the most effective way to convert enthalpy of exhaust gases into electric energy. On the other hand it can cause increasing the work required to engine scavenging. The amount of power generated through the recuperation is difference between the change in turbine power and change in scavenging power. This difference is at sufficiently high exhaust temperatures always positive and the equation is

$$P_{\text{recu}} = \left(\Delta P_{\text{T}} - \Delta P_{\text{pump}} \right) \cdot \eta_{\text{trans}} , \tag{22}$$

where P_{recu} is the amount of power recuperated, ΔP_{T} is turbine power change, ΔP_{pump} is scavenging power change and η_{trans} is efficiency of conversion to electrical power.

$$\Delta P_{\text{T}} = \eta_{\text{T}} \cdot \dot{m}_{\text{T}} \cdot c_{\text{p}} \cdot T_3 \cdot \left(\frac{p_3{'}}{p_3} \right)^{\left(\frac{n-1}{n} \right)} \left[1 - \left(\frac{p_3}{p_3{'}} \right)^{\left(\frac{\kappa-1}{\kappa} \right)} \right] , \tag{23}$$

where T_3 is the temperature at turbine inlet, p_3 is pressure at turbine inlet, $p_3{'}$ increased pressure at turbine inlet and n is polytropic coefficient.

$$\Delta P_{\text{pump}} = (p_3 - p_3{'}) \cdot \frac{\dot{m}_{\text{a}}}{\eta_{\text{vol}}} \cdot \frac{r \cdot T_2}{p_2} , \tag{24}$$

where $\dot{m}_{\text{a}}$ air mass flow, η_{vol} volumetric efficiency.

If it is considered VNT E-Turbo which could provide more benefits than wastegate, the efficiency of the turbine will have large influence of the system. Efficiency of VNT turbine depends on position of the stator vanes. With higher turbine efficiency it is possible to recuperate more energy.

Increasing the pressure before turbine can be achieved by decreasing of flow (flow area) or turbine wheel trim and closing of turbine stator vanes. For energy recuperation is has to be considered ratio between turbine size and scavenging power which is adversely affected by VNT closing. Because the flow through the turbine is various for every operating point of engine, the VNT turbocharger with motor-generator appears to be best option with another degree of freedom.

In Dimitriou et al. [45] simulation study of gasoline engine with wastegate E-turbo is confirmed that smaller turbine with increased pre-turbine pressure can provide better energy harvesting conditions across the whole area of engine´s load map / speed map. There is also a energy balance study for different types of driving cycles e.g. NEDC,WLTC, US06 resulting in amount of recuperated energy during these cycles, see Figure 43. It has to be mentioned that none of the results presented in the study take into account any electrical losses, such as converter or battery losses, which will obvisously reduce the net amount of harvested energy [45].
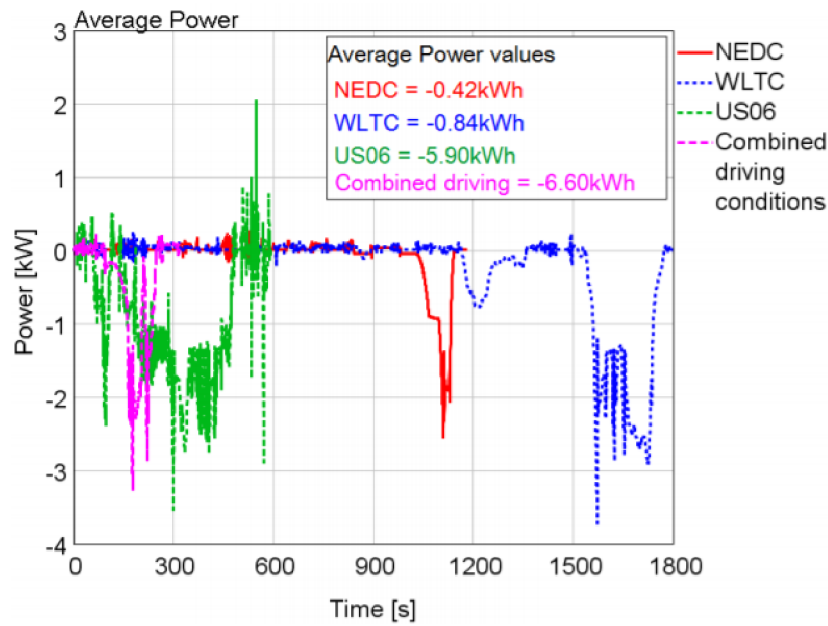
Figure 43 Average power provided / harvested by the motor-generator where negative values indicate energy harvesting [45]

Results in Figure 44 from another simulation [46] of 2.0L gasoline engine with electrically assisted turbocharger in shows that electrified turbocharger is capable of recuperating as much as 3x the eletrical energy in the acceleration phases, if the rotor is braked electrically in the braking, over-run and idle phases of the WLTC cycle. This means that the electrified turbocharger will not be a consumer of electricity from the vehicle electrical network, but on the contrary, will become net contributors to the state of charge of the battery [41, 46].

Figure 44 Kinetic energy recover from electrified tubocharger [46]

3.2 ELECTRIC BOOSTING

Instead of energy recovery, it is possible to utilize the motor-generator as electric boosting assistance. Because of the immediate availability of maximum electricity power, it is possible to accelerate the turbocharger rotor in a significantly shorter time than in the case of conventional turbocharger, thereby reducing the response to the accelerator pedal.

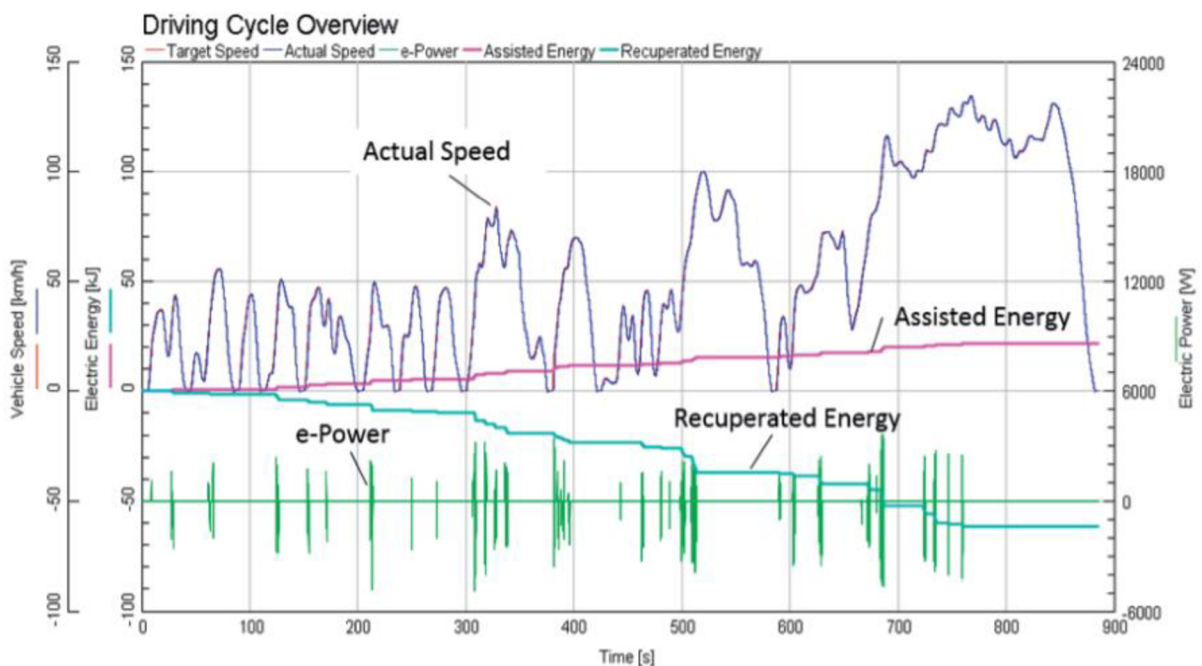The electric assistance will be exploited especially in low engines´s speed. The amount of air depends on the boosting pressure created by compressor, whose power input depends on the power generated by the turbine. At lower engine speed, the power of the turbine is limited by the amount of exhaust gas energy. Because of the electric motor-generator, it is possible to increase the power input of the compressor and thus ensure a higher air supply to the engine. The resulting effect of increasing the boosting pressure will allow more injectors fuel and increase engine torque. In Figure 45 is comparison of turbocharger types for improving low speed torque.
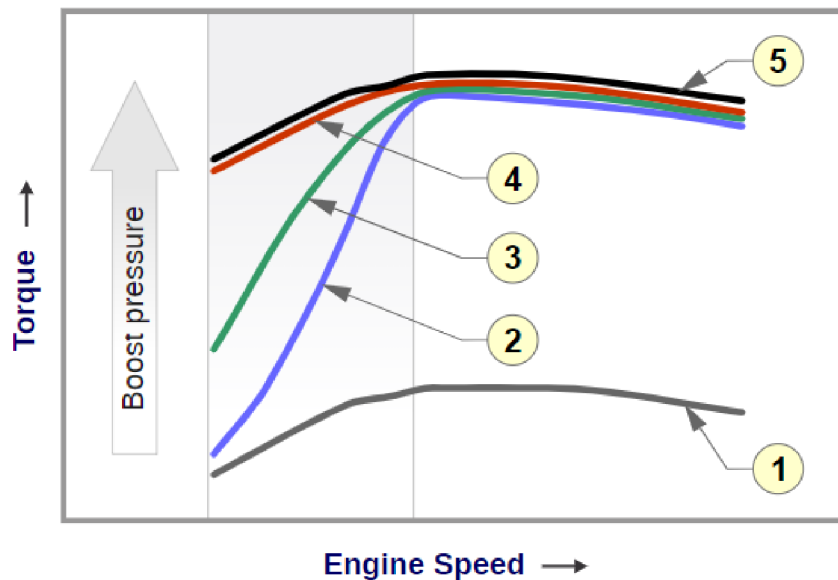
Figure 45 Turbocharger assistance for improving low speed torque in downsized engines
1-Downsized engine, 2-Conventional turbocharger, 3-Variable geometry turbocharger,
4-VGT with motor assist, 5-Large displacement engine

Results from Pesyridis et al. simulation [48] of 1.5L 3-cylinder engine with electric assisted turbocharger show that electrically asssited turbocharger (EAT) engine model improved the overall performance of the engine compared to baseline engine. The engine torque improvement from low engine speed is presented in Figure 46. Improvement of torque transient response obviously depends on the amount of energy providing to the compressor.
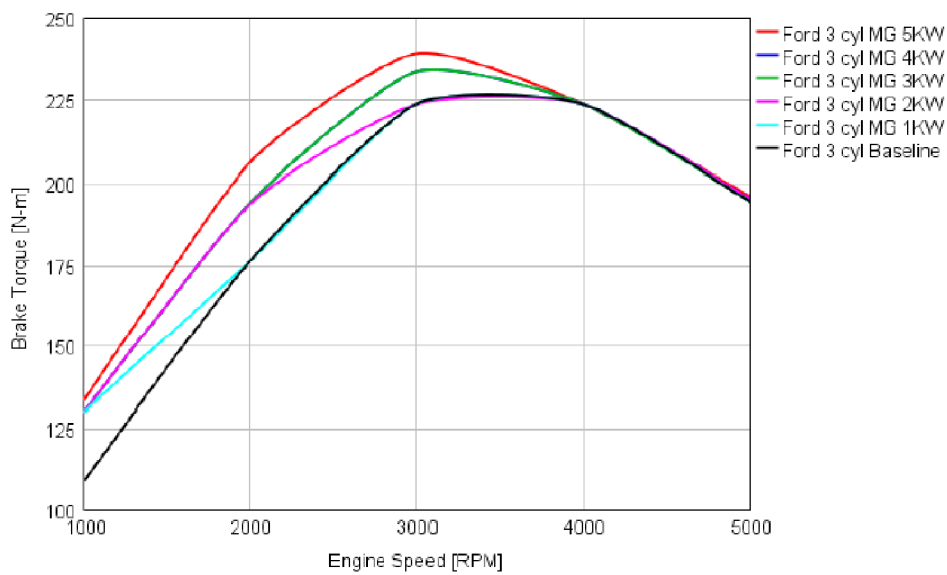
Figure 46 Brake torque response for Ford 3-cylinder engine with elecrically assisted turbocharger [48]

In Garrett Motion comparison study [41] for Audi 2.0L gasoline engine with electrically assisted turbocharger (red line) and series application turbocharger (black line) is also shown the benefits of EAT in trasient operations. For example for 1500 RPM (revolutions per minute) the provided electric power (limited up to 6 kW) can cause a significantly faster rotation of turbocharger which corresponds with faster intake pressure and engine torque.
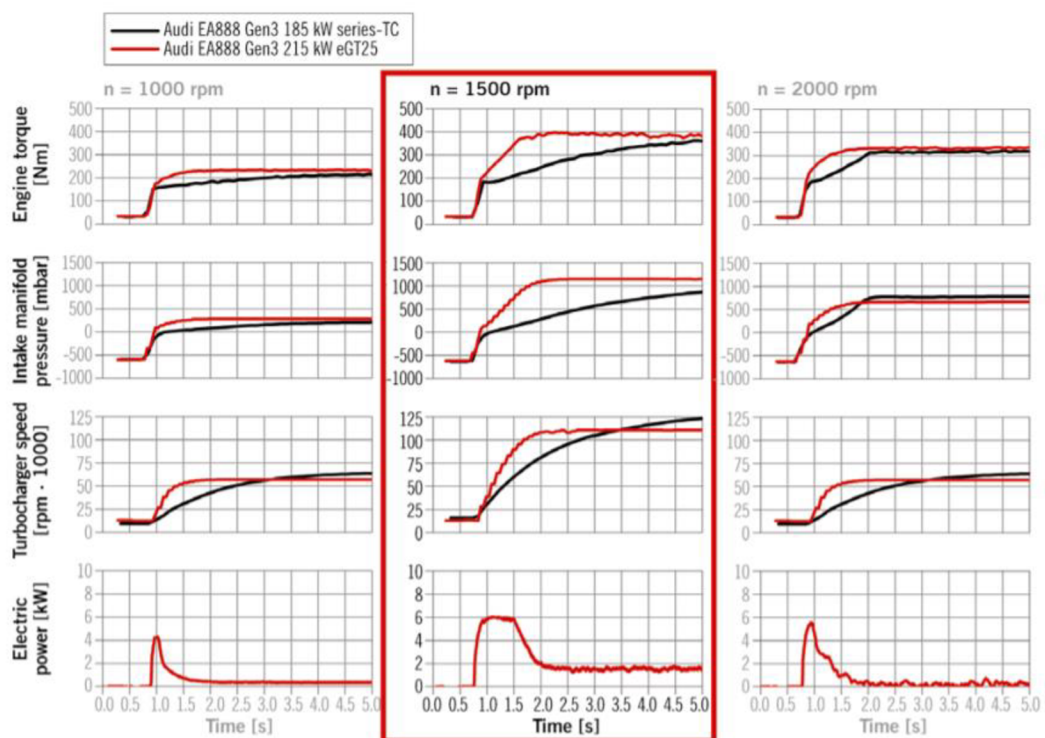
Figure 47 Comparison study of EAT and conventional turbocharger [41]

4 HYBRID VEHICLES

Hybrid vehicles are an intermediate stage in the transition from an internal combustion engine to a purely electric one. Due to the presence of emission-free electric motor in hybrid vehicles which draw energy from batteris or fuel cells, it is possible to lower the emissions and fuel comsumption. The hybrid vehicle is usually consisted of two powertrains, where electric motor allows bidirectional flow of the energy while the internal combustion engine only unidirectional flow of the energy [7]. Hybrid vehicles can be categorized according to the degree of hybridization also called hybridization factor [9, 16]. Degree of hybridization (DOH) depends upon the power supplied by internal combustion engine and electric motor where ratio of power developed by an electric motor in a hybrid vehicle to the total power consumed by the vehicle [8].

$$HF = DOH = \frac{P_{EM}}{P_{EM} + P_{ICE}} * 100 \, , \qquad (25)$$

where HF is the hybridization factor, DOH is degree of hybridization, P_{EM} is power of electric motor-generator and P_{ICE} is power of internal combustion engine.

4.1 HYBRID VEHICLES SUITABLE FOR ENERGY RECOVERY FROM E-TURBO

In this chapter will be introduced types of hybrid vehicles from most suitable to the least suitable in terms of energy recovery from electric assisted turbocharger.

4.1.1 PLUG-IN HYBRID VEHICLE

Plug-in hybrid vehicle also know as PHEV are combining diesel or gasoline engine with an electric motor and large rechargeable battery. PHEV is the only type of hybrids that can be plugged in and recharged from and outlet, allowing the vehicle to drive extended distances just in full electric mode [9]. When the battery is emptied, the conventional engine turns on and the vehicle operates as a convetional, non plug-in hybrid [9]. Due to the bigger battery and larger capacity, the power output of the electric motor can be higher and that means DOH of plug-in electric vehicle will be greater than in case of fully hybrid vehicle [9, 16]. PHEV can be built using all architecture that will be mention below [51]. Detailed description of PHEV based on fuel consumption in different driving cycles is presented in [56].

Electrically assisted turbocharger will most likely have the greatest utilization in plug-in hybrid vehicle and can provide many benefits. As it was mentioned, energy recovered from the turbocharger can be supply the battery of the vehicle and extend the distance of fully eletric drive or hybrid drive where conventional engine with electric motor work jointly.

4.1.2 FULL HYBRID VEHICLE

DOH of full hybrid vehicle varies according to position of electric motor arrangement defined in subchapter 4.2. For parallel arrangement DOH is 10-50 % and for series it is 50-75 % [9]. Electric motor and battery are bigger which cause a reduction of required size of conventional engine [9]. Motor supplies power circa 50 kW at 200-300 V.

Utilization electrically assisted turbocharger in full hybrid vehicle will depend on position of electric motor in hybrid vehicle arrangement. Paralell configuration will be best option for achieving energy recovery and other benefits of EAT in full hybrid vehicle.

4.1.3 MILD HYBRID VEHICLE (MHEV)

Electric motor in MHEV also replace starter and alternator but in this case is integrated to provide around 10% of maximum engine power [9]. MHEV can operate with higher voltage levels of 100-200 V but for safety most of mild hybrid systems operate of 48 V with electric motor power from 10 to 20 kW.

EAT in MHEV vehicle can be provide turbo lag reduction and energy recuperation. Energy recuperation has to be considered due to the contain of regenerative braking system in MHEV vehicles. Because of limiting capacity of battery in MHEV, the regenerative braking system can recuperate a sufficient amount of energy and store it into battery and thus a full potential of energy recovery from EAT will may not be reached.

4.1.4 MICRO HYBRID VEHICLE

In micro hybrid vehicles are automotive starter and alternator superseded by a motor-generator. The electric motor-generator usually supplies power of 2,5 kW at voltage of 12 V, so the DOH is about 5%. Electric motor functions to start or stop the system to automatically shut off the engine while idling and does not provide additional torque to the vehicle [9]. Utilization of EAT in micro hybrid is possible and can reduce the turbo lag, however it won´t achieve full potential of energy recovery in this hybrid system.

4.2 HYBRID VEHICLE ARCHITECTURES

The architecture of a hybrid vehicle is loosely defined as the connection between the components that are define the energy flow routes and control ports [7]. Traditionally hybrid electric vehicles were clasified into two basic types – series and parallel, but since 2000 they are presently classified into four kinds – series hybrid, parallel hybrid, series-parallel hybrid and complex hybrid [7].

4.2.1 SERIES HYBRID VEHICLE

As Figure 48 shown, the components of series hybrid powertrain are arranged one behind the other. Series hybrid powertrain is one in which two electric power sources feed a single electrial power plant in the case the electric motor that propels the vehicle [7].
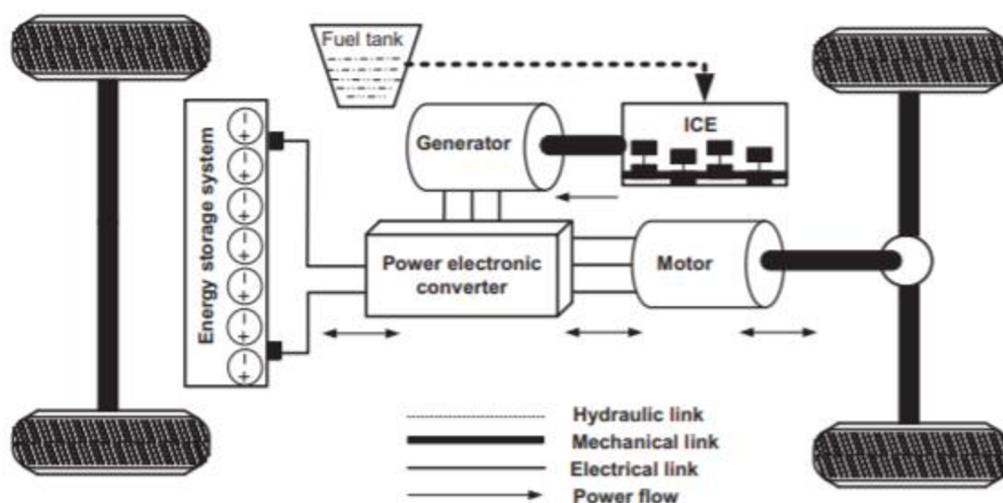

Figure 48 Architecture of series hybrid vehicle [52]

One source is ICE, its energy is transformed into electrical power with help of generator and the transformed energy can be distribuded to the electric motor. The second source is battery pack which powers the electric motor. In this case, DC/DC converter is energy node that ensures the distribution of energy between generator, battery pack and electric motor [7, 50].

One of the advantages of series architecture is no mechanical connection between the engine and the drive wheels, so the engine could be potentionally at any point on its speed-torque (power) map which cause that engine can operate in maximum efficiency region [7]. Furthermore, the mechanical decoupling of the engine from the drive wheels allows the use of high-speed engines, where it is difficult to directly propel the wheels through a mechanical link, such as gas turbines or power plants that have slow dynamic responses (e.g., Stirling engine) [7].

Another advantage is that drivetrain may not need a multigear transmission due to the almost ideal torque-speed profile of electric motor for traction. There are also disadvantages of this architecture such as double conversion of energy from ICE to generator (mechanical to electrical) and from electric motor to drive wheels (electrical to mechanical) which can cause significant losses [7, 52]. For power gain it is necessary to have three units (ICE, generator, electric motor) and that will have influence on weight and diameters of powertrain system [7].The maximum power output is also limited by electric motor due to the series architecture and not possible combining power of units.

Utilization of electrically assisted turbocharger in this type of hybrid architecture will not be probably effective due to high possible efficiency of the ICE. Another point can be complexity of the system with EAT and dependence of the compressor input on the turbine output.

4.2.2 PARALLEL HYBRID VEHICLE

In parallel hybrid configuration, internal combustion engine and electric motor are connected in parallel to deliver power to the wheel as shown in Figure 49. The powers of the engine and the electric motor are coupled together by mechanical coupling [7]. The distinguishing feature of this architecture is that two mechanical powers from the engine and the electric motor are added together by a mechanical coupler [7].
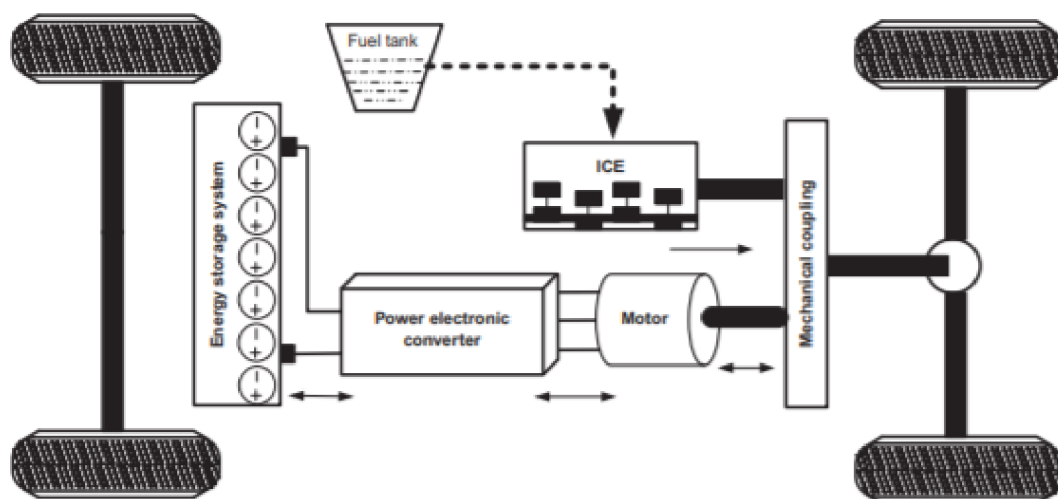

Figure 49 Architecture of parallel hybrid vehicle [52]

As compared to series HEV, elimination of generator leads to single-stage power conversion that increases efficiency and reduces the weight and cost of the vehicle [52]. Another advantage is that both the engine and the electric motor directly supply torques to the drive wheels, so no complicated energy conversions occur and energy losses will be lesser [7, 52]. Major disadvantage is mechanical coupling between engine and drive wheels, since then the engine operating points cannot be fixed in a narrow speed and torque region [7]. Due to the help of electric motor it is possible to move the operating point of combustion engine into area with highest efficiency in certain speed and load. This process is so-called load point shifting.

EAT in parellel hybrid vehicle could have great utilization, especially due to the energy recovery and possible battery pack charging thus pure electric drive or hybrid drive extension. The suitability of EAT in hybrid vehicle is described in [53] publication based on fuel economy and acceleration performance.

Architecture of parallel vehicle can be further subdivided according to position of electric motor on its way from internal combustion engine to the wheels as is shown in Figure 50.
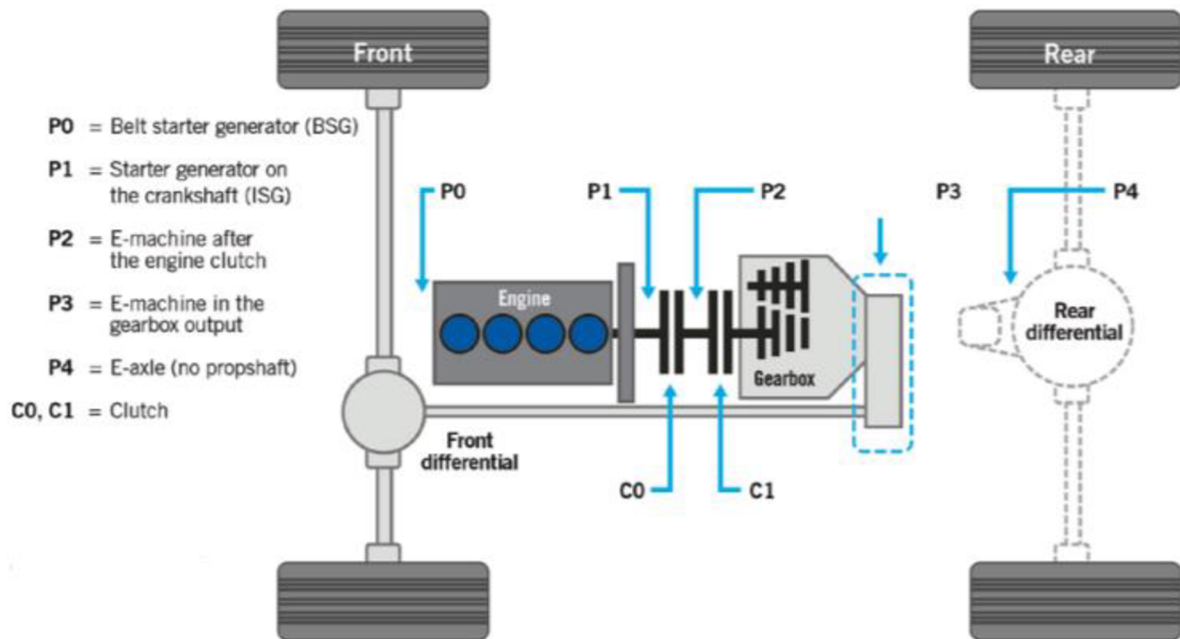
Figure 50 Position of electric motor in parallel hybrid architecture [54]

All positions have their advantages and disadvantages presented in [55] article but from the recuperation view, pure electric drive and utilization of EAT will be probably the P2 position of electric motor the best. In [54] are also benefits of CO_2 reduction presented on base of MHEV.

In P2 configuration, the electric motor is placed behind the clutch which separetes ICE from gearbox which lead to possible mechanical disconnection of ICE from electric motor. Electric motor can be pernamently connected with gearbox input shaft. The most common configuration is where the electric motor is placed between ICE and transmission. In this case two clutches are used, primary C1 disconnect the ICE and electric motor, secondary C0 electric motor and gearbox. In this configuration, when primary clutch is disengaged and

secondary is engaged, the pure electric drive is possible. When both clutches are engaged, combination of ICE and electric motor could happen. The main disadvantage is the higher integration cost of such a system [55].

The parallel configuration in plug-in hybrid vehicle will be probably the best option for placing the electrically assisted turbocharger and reaches its full potential.

4.2.3 SERIES-PARALLEL HYBRID VEHICLE

Series-parallel HEV is an integration of the series and parallel hybrids as shown in Figure 51. The configuration contains an additional mechanical link and additional generator to facilitate the advantages of both configurations [7]. Using DC voltage bus and the planetary gear set, a series-parallel HEV can operate as series or parallel in terms of energy flow [50] where planetary gear set distributes power of ICE, electric motor and generator. Although series-parallel HEVs have the features of both the series and parallel HEVs, they still require three motors and a planetary gear set, which makes the powertrain somewhat complicated and costly [50]. In addition, controlling this architecture is quite complex. EAT utilization in this configuration is possible, however it will be another stage to an already complicated system.
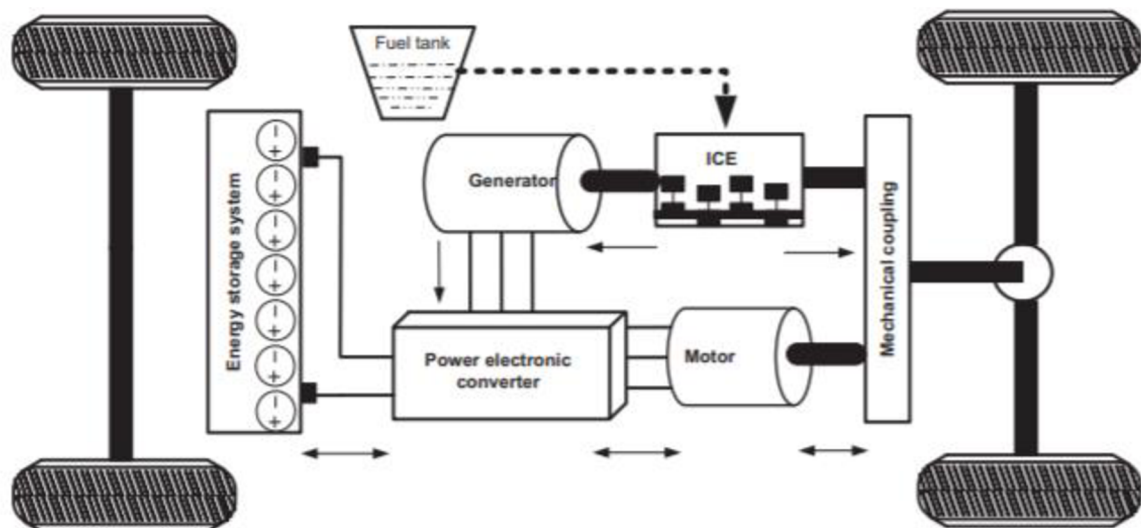
Figure 51 Series-parallel architecture of hybrid vehicle [52]

4.2.4 COMPLEX HYBRID VEHICLE

Complex configuration is designed for dual-axle propulsion where both the front and rear wheels propel the vehicle [52]. Front-wheel and rear-wheel axles are decoupled from each other so there is no mechanical link between them and both axles are driven independently. The front wheels are propelled by hybrid propulsion system and rear wheels are propelled by electric propulsion system or vice versa, but in case where front wheels are propelled by electric system, only front wheels are driven at starting [52]. Electric generator in this configuration in Figure 52 offers bidirectional power flow. Planetary gear arrangement is used to coupled ICE, front electric motor and front axle together [52]. Independent control of front and rear wheels provides smooth vehicle operation but increases complexity and costs [52].

Figure 52 Architecture of complex hybrid vehicle [52]

4.3 REGENERATIVE BRAKING SYSTEM
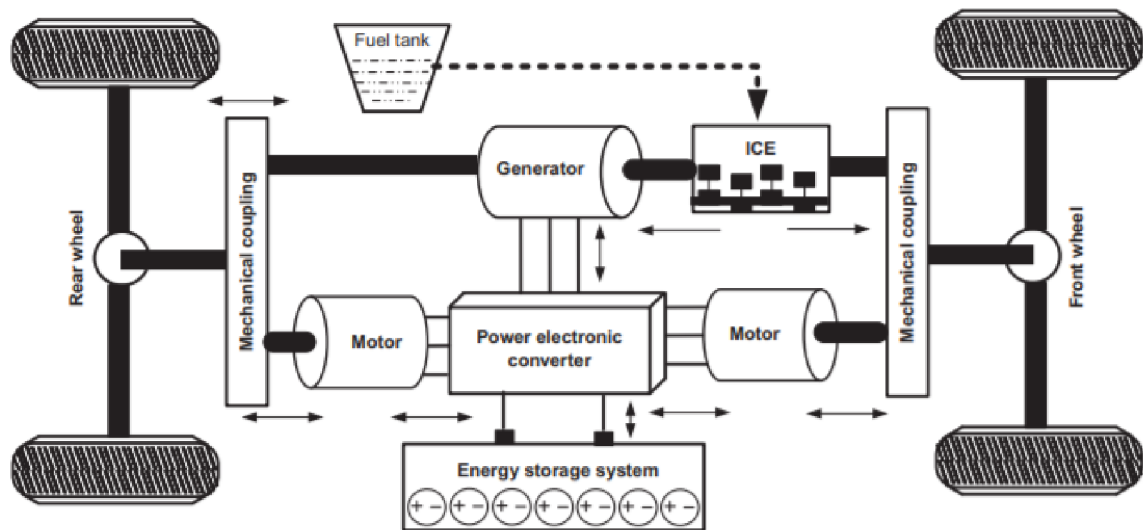
The future viability of electric powertrains is greatly dependant on their range and battery storage capacity. Electric vehicles will achieve ranges that are sufficient for everyday use only with efficient batteries, intelligent energy management and the recovery of braking energy [57].

As Bosch [57] presented in their article, braking in a conventional vehicle, the friction brakes convert much of the kinetic energy into heat that is emitted unused into the environment. Hybrid [58-61] and electric [62-64] vehicles with regenerative braking system are different in that. When braking in a hybrid or electric vehicle, the electric motor switches to generator mode. The wheels transfer kinectic energy via the drivetrain to generator. The generator transform part of the kinetic energy into electrical energy, which is stored in a high-voltage battery. At the same time, generator resistance produced from the electricityc reated, slows the vehicle. When more braking torque is required than the generator alone can provide, additional braking is accomplished by friction brakes.

This process of transforming energy from braking is know as recuperation or regenerative braking [56]. The electric motor can then use this stored energy when driving off or accelerating. Regenerative braking makes it possoble to increase the range of electric vehicles and reduce fuel consumption and carbon footprint of hybrid vehicles.

Regenerative braking systems control the interaction between the friction brakes and the generator to guarantee efficient energy recuperation. They also ensure that deceleration behaviour and pedal feel are identical to conventional braking systems. The generatos´s braking potential is dependent on the engine driving speed. At low engine speeds, maximum brake torque is available. At high speed or very low speed, e.g. just before coming to a stop, sufficient brake torque cannot be provided meaning the friction brake must be activated. Generator brake torque is proportional to the generator´s output and is also influenced by the battery´s level of charge. Brake torque from the generator is only available when the high-voltage battery is not full charged.
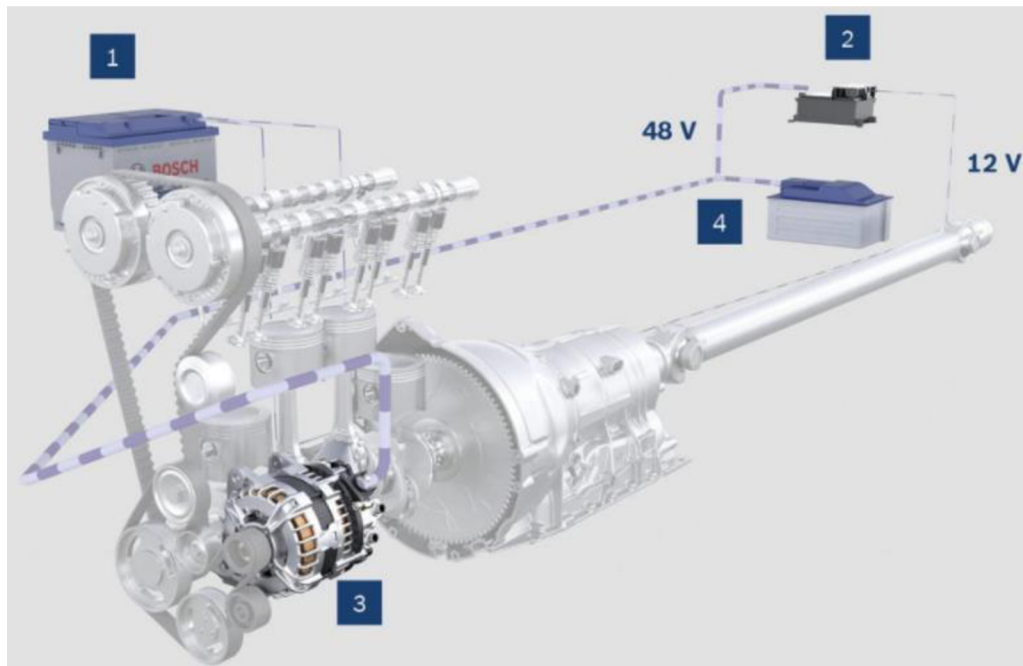
Figure 53 Bosch 48V MHEV – components of the boost recuperation system 1 – low voltage battery (12V), 2 -DC/DC converter, 3 – electric motorgenerator, 4 – high voltage battery (48V) [55]

Vehicles that are mostly powered by combustion engines, such as mild hybrids and full hybrids, produce vacuum which can be used by conventional brake boosters. In contrast, plug-in hybrids and electric vehicles are not able to provide sufficient vacuum for brake boosters to operate. This is the reason why Bosch for example offers products including vacuum-based and vacuum-independent regenerative braking systems [57] tailored to meet the individual requirements of various drive concepts.
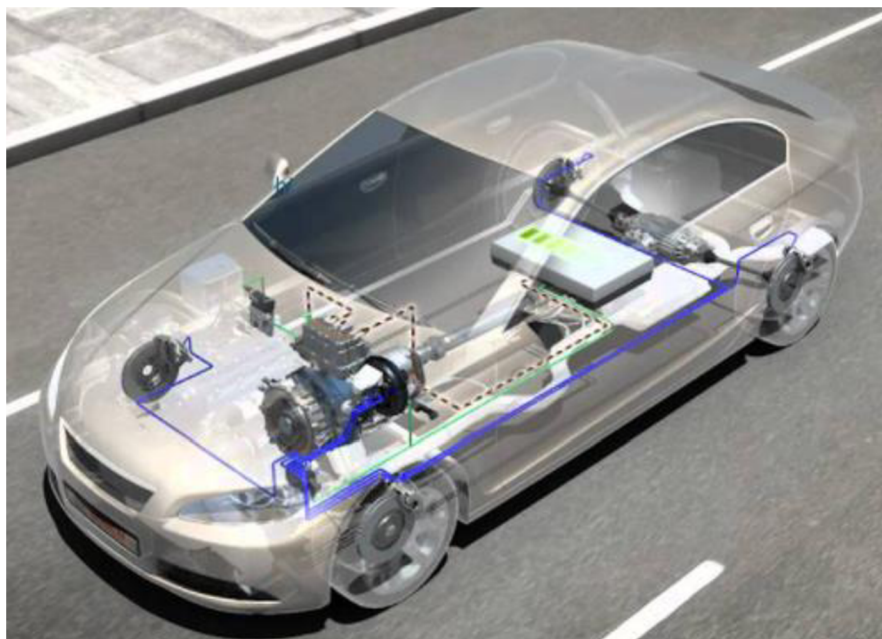
Figure 54 Bosch regenerative braking system [57]

5 DEFINITION OF THE OBJECTIVES OF THE DIPLOMA THESIS

First goal of the thesis was describe a group of hybrid vehicles and sort them for possible utilization of electrically asissted turbocharger in them, especially in terms of energy recovery and thus reduce of fuel consumption and emissions.

From the chapter 4 is clear that best way to utilize EAT is in case of plug-in hybrid vehicle. Plug-in hybrid vehicle with EAT has the biggest potential in form of energy recovery and thus extention of purely electric drive or hybrid drive.

In the second part of the thesis will be examined influence of different turbine or compressor wheels on possible energy recovery and energy flow of electrically asissted turbocharger for different operating points of the engine at full load and part load simulations. The comparison will be based on different turbine or compressor diameters and their effect on energy recovery.

6 ENGINE CALIBRATION

In this practical part of the thesis will be analyzed an influence of different turbine and compressor wheels sizes (diameters) on energy recovery of electrically asssisted turbocharger with variable geometry turbine. This type of turbocharger is used for delivery vehicle in this case for Iveco Daily where replace a conventional variable geometry turbocharger. The engine model with EAT will be created and studied in computational software GT-SUITE. All datas about engine and turbocharger are provided by company Garrett Motion.

Figure 55 Iveco Daily [65]

6.1 ENGINE AND TURBOCHARGER SPECIFICATION

Iveco Daily belongs to the group of light-duty or medium-duty vehicles, operating both in and outside of the urban areas. For this turbocharger study will be placed four cylinder diesel engine with parameters shown below in Table 1.

Table 1 – Engine parameters

Engine Type	4-stroke, 4-cylinder, diesel
Displacement	2.998 [dm^3]
Compression Ratio	17.5:1
Cylinder bore	95.8 [mm]
Cylinder stroke	104 [mm]
Valves per cylinder	4
Injection system	Common Rail
Engine position	in line
Exhaust Gas Recirculation	High Pressure EGR
Max Engine power /rated speed	150 [kW] @ 3500 [RPM]
Max Torque / rated speed	470 [Nm] @ 1600 [RPM]

Supercharging of the engine is mediated by variable geometry turbocharger with intercooler. Parameters of turbocharger are shown in table 2.

Table 2 – Turbocharger parameters

Turbocharger type	Variable geometry turbocharger
Architecture	1 Stage turbocharger
Turbine wheel diameter	47 [mm]
Compressor wheel diameter	56 [mm]

6.2 ENGINE MODEL IN GT-SUITE

GT-Power is part of simulation package software GT-Suite which is used in many branches of industry especially in automotive and development engineering. GT-Power contains large library of examples, tutorials and manuals for beginner users of this software which will be very helpful for further engine creation or adjustment.

Nowdays GT-Power is another level of simulation software providing thermodynamic simulations of internal combustion engines with e.g. compressors, turbochargers, intercoolers, afterthreatment parts and many others. This software also incluces simulation of whole vehicle with all kinematic parts in different driving cycles, also includes hybrid and electric vehicles.

As it was mentioned GT-Power includes a lof of engine examples but also informs that not all data and results from their examples are valid and serves only for example purposes. First of all, it will better to choose an example engine model from GT-Power library than creating a whole new engine model. After choosing a valid example, it is necessary to adjust and calibrate the engine model for steady-state for best possible comparison with results of engine model from Garrett Motion. This comparison will be done on a base of results of engine full load speed map and few other parameters. After engine validation can be added a motor-generator for possible energy recovery.

6.2.1 EXAMPLE CHOOSING

GT-Power has pretty much turbocharged diesel examples and for purposes of this thesis was chosen predictive combustion engine model with displacement of 1.998 dm^3, VGT turbocharger, EGR and intercooler. Model is illustrated in Figure 56. It also contains PID contollers which ensure that the required values of engine parameters are reached at the individual points of the engine load, which are characterized by a constant operating speed as the input into to the crank mechanism. In this engine model PID controllers are targeting BMEP, boost pressure, EGR rate (for EGR are used two PID controllers).

Table 3 – PID controllers

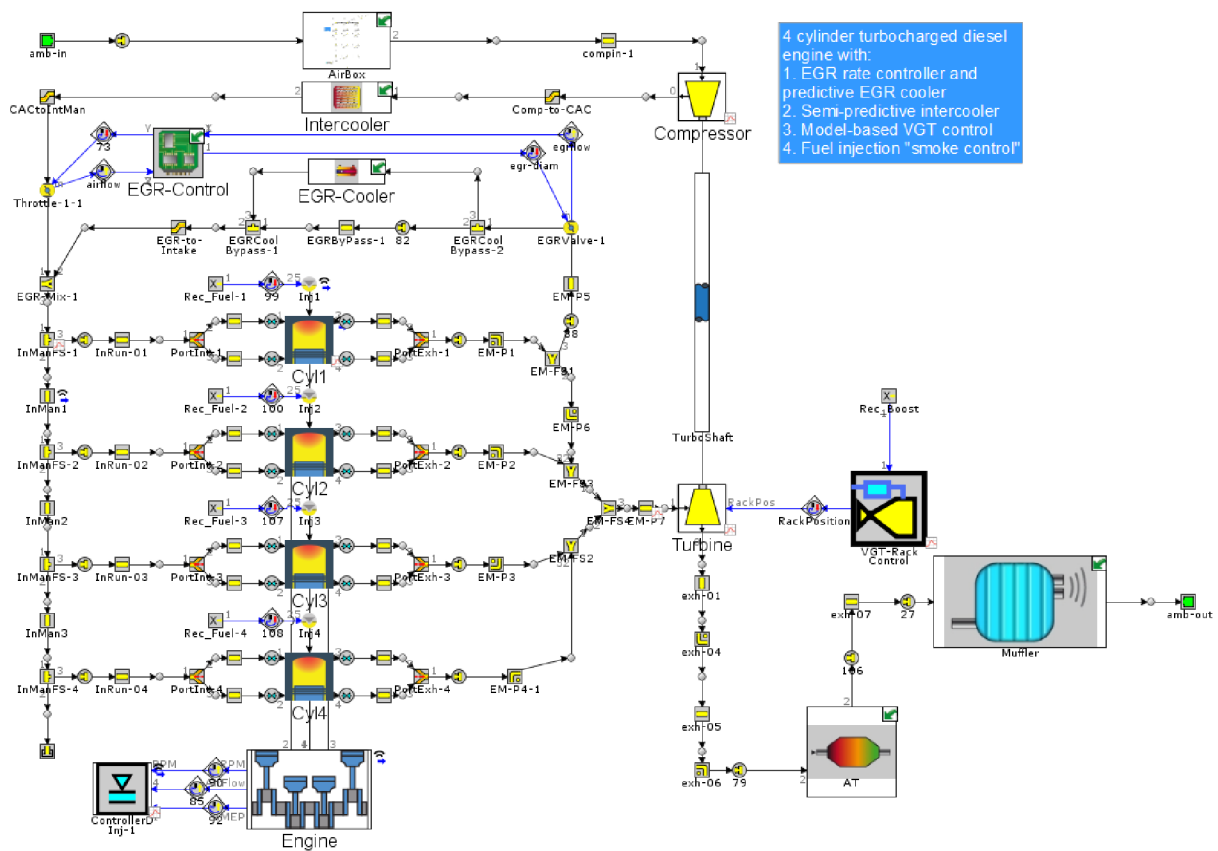| Targeting parameter	Regulating value
BMEP [bar]	injected mass [mg/cycle]
Boost pressure [bar]	VNT position [-]
EGR [%]	EGR valve diameter [mm]

Figure 56 Example of diesel engine model from GT-Power library

6.2.2 ADJUSTING ENGINE MODEL

After choosing an example model, it is necessary to adjust it for engine specification of Iveco Daily. Firstly AirBox and Muffler were removed because they prolong simulation time. Small pressure drop caused by AirBox was modified by flow coefficient for each engine speed in connection before Airbox in Figure 56. Another step was simplification of EGR system because the original example model includes two PID controllers for EGR which can lead with other controllers to "battle" between themselves. Too many badly configured controllers can cause oscilations in signals and they won´t be able to reach targeting values and steady state. Adjustments of EGR system and other parts of the model is shown in Figure 57. There were done some other modifications in model e.g. pipes diameters, engine and cylinder object adjustments, turbocharger and intercooler configuration etc.
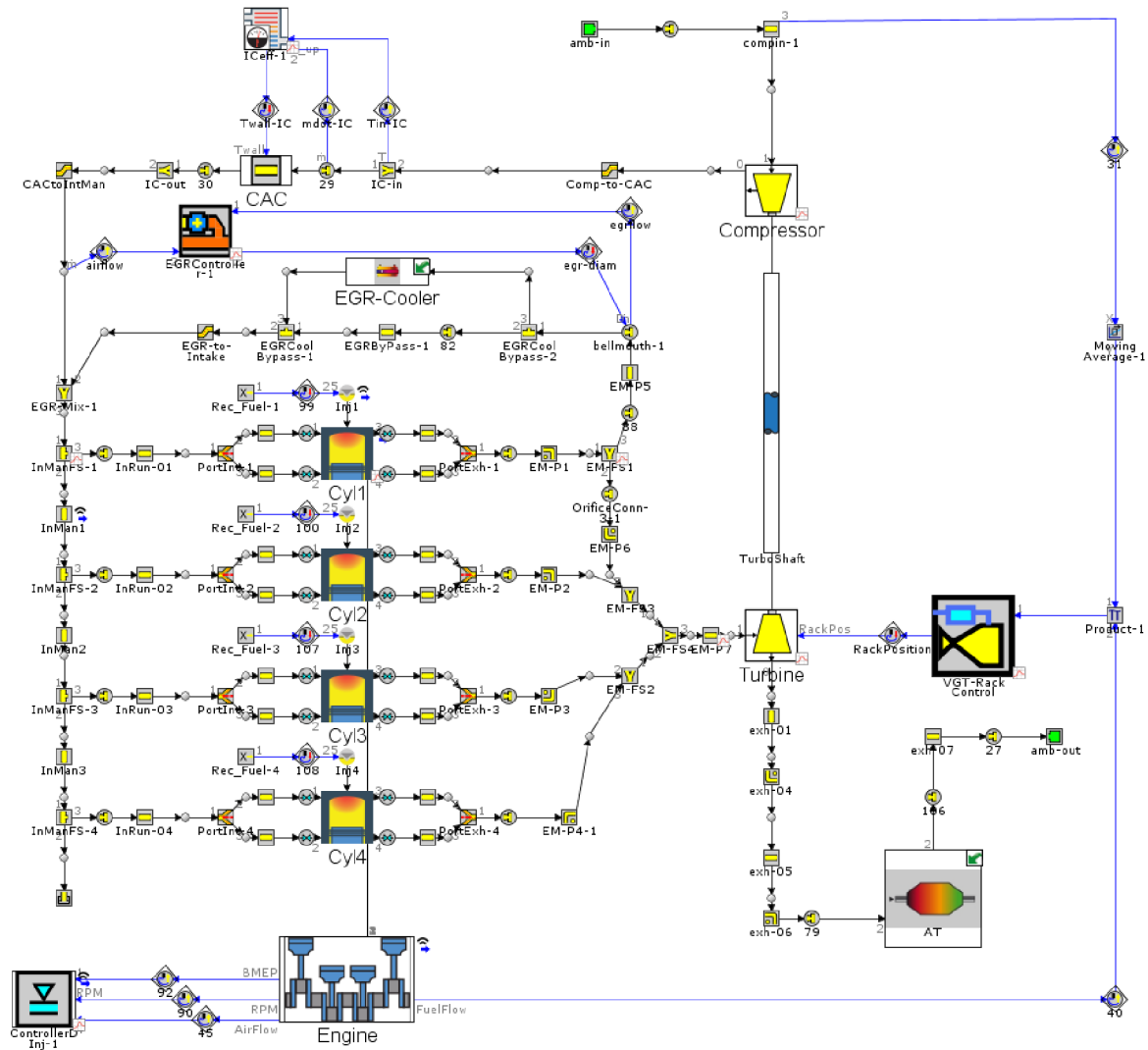
Figure 57 Modified engine model with Iveco Daily parameters

EGR PID Controller

EGR-Control unit with two PID controllers inside (Figure 56) from original example was replaced by one PID controller which also simplify EGR system. EGR controller is targeting EGR rate value for for specific operating point of the engine. There were no modifications in EGR-Cooler or pipes of EGR system except expansion diameter and characteristic length of EGR-Mix flow split volume according to the manual.

Injection PID Controller

Injector controller (Figure 57 next to Engine object) controls amout of fuel per cycle which should be injected for different load conditions of the engine according to the signals from the engine object. Controller send signal to the reciever which via the actuator controlls amout of fuel which will be injected. For this engine model, injection controller is targeting BMEP and therefore torque curve for different loads.

Turbocharger VGT Rack Controller

This template is specially created for controlling variable geometry turbocharger which is used to targer various engine performance parameters e.g. boost pressure, BMEP, air-fuel ratio, brake power, brake torque etc. In this concrete engine model will be targeted air-fuel ratio. To meet the target value of A/F it is necessary record the values of air flow and fuel flow thought sensors. Fuel flow is taken from the engine object and air flow from the pipe before the compressor because air flow from the engine object is influenced by EGR system. These values will be devided in Product object (Figure 57) and than the output is sended to the controller.

6.2.3 COMPARISON WITH TESTED ENGINE

For engine validation were used three PID controllers mentioned above. These controllers are configured to reach target values via actuating units with a permissible deviation and for certain number of engine cycles to meet the convergence criteria. The criteria are defined in the Table 4.

Table 4 – Convergence criteria

Targeting parameter	Regulating value	Convergence criteria (CR)
Air-Fuel ratio [-]	VNT position [-]	CR < 0.5 % - 5 cycles
BMEP [bar]	injected mass [mg/cycle]	CR < 0.5 % - 5 cycles
EGR [%]	EGR diameter [mm]	CR < 0.5 % - 5 cycles
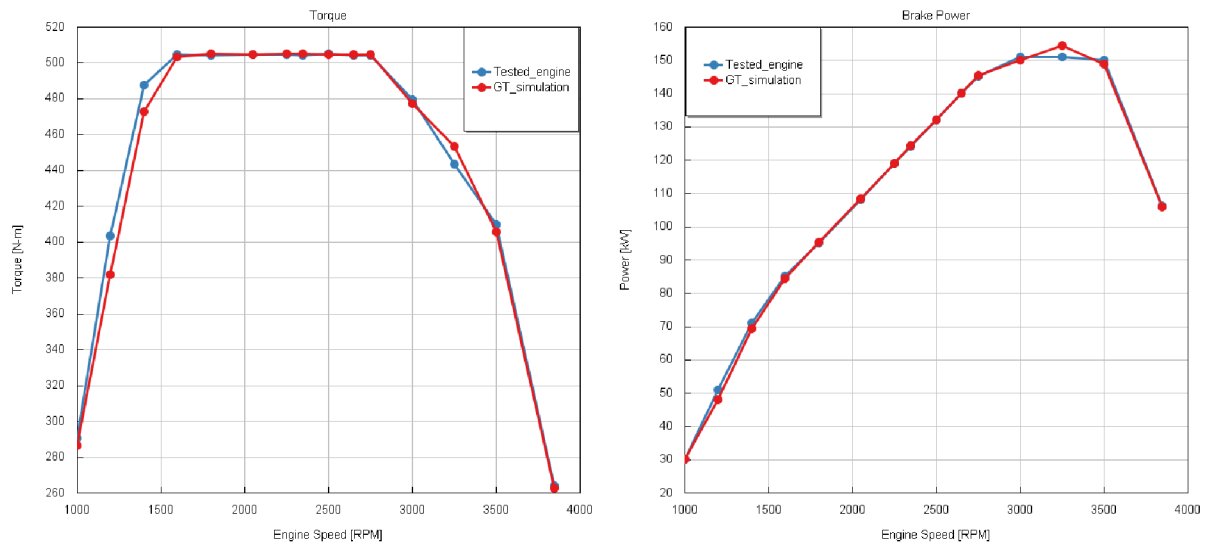
Figure 58 Results of engine calibration

Torque curve is almost the same as for tested model, little differences are at low RPM which is probably caused by engine imperfections. Brake power curve from GT-Power simulation is also very similar to the tested model and reach higher power at one of the peak points of engine speed. Figure 59 plots the points of engine full load into the compressor and turbine map.

Figure 59 Compressor and turbine map with full engine load points

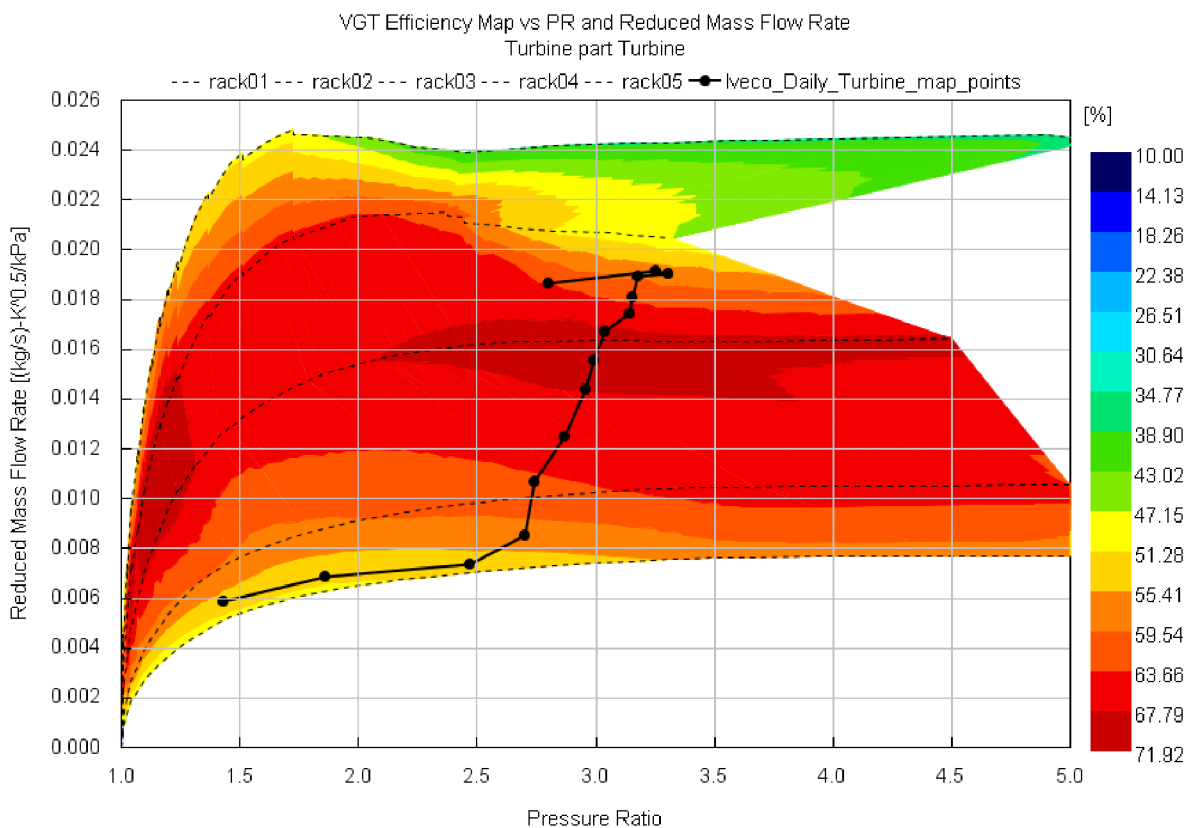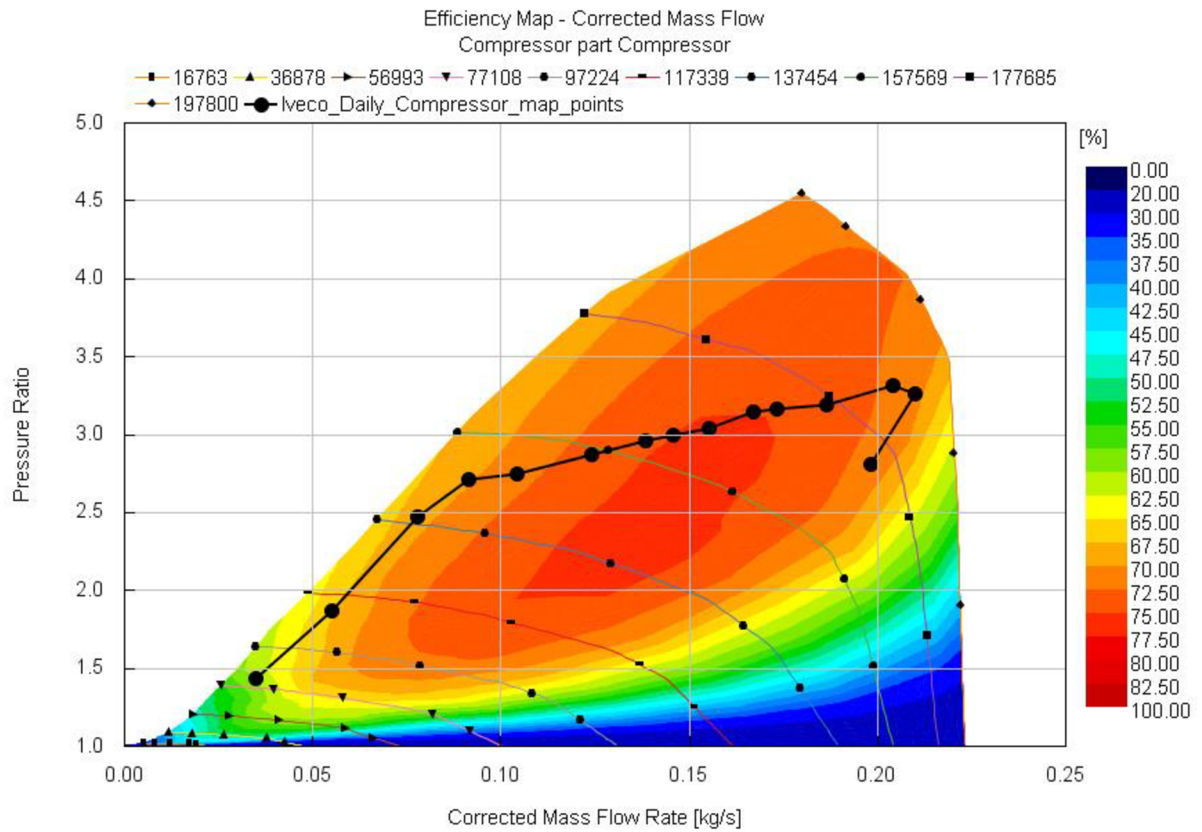From the turbine characteristic it is obvious that for every rack position of the turbine, the turbine wheel efficiency based on pressure ratio and reduced mass flow is different. Adding a motor-generator which will take the energy, the rack position will be probably even smaller and the efficiency point of the turbine will change which could have impact on turbucharger performance and thus engine fuel consumption.
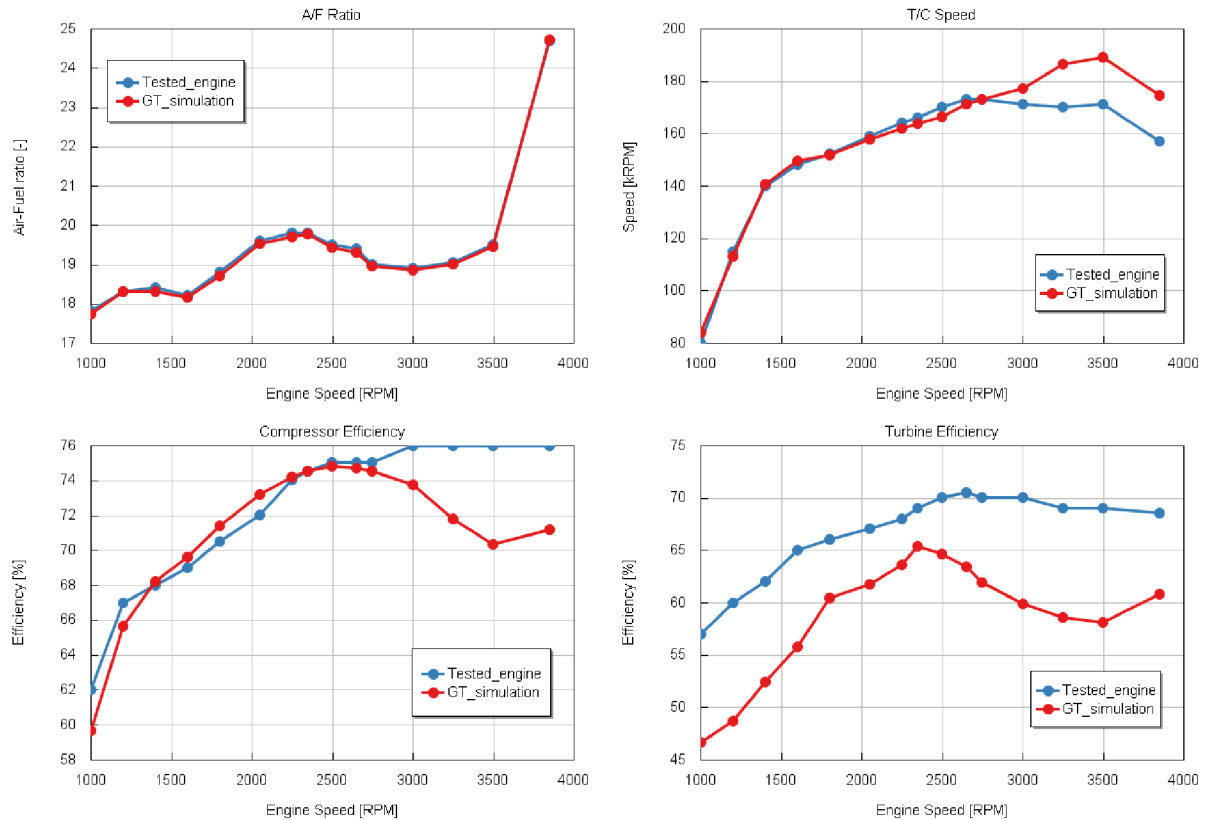

Figure 60 Engine parameters comparison

Figure 60 shows that targeted air-fuel ratio was reached in every operating point of the full load speed map. Turbocharger speed differs from 3000 RPM operating point which could be caused by engine imperfections but it is also a point where the engine will operate very rarely. Differences also arised in comparison of compressor and turbine efficiency. This could be adjusted by using compressor and turbine efficiency multiplier but it was not been done because it can affects other factors of the engine. Nevertheless, it has to be counted with lower turbine efficiency in terms of energy recovery in EAT with motor-generator. As it was mentioned in chapter 3.1, turbine efficiency has great influence on turbine performance and thus possible energy recovery, so the future results of recoved energy would be slightly larger for the original tested engine.

7 ELECTRICALLY ASSISTED TURBOCHARGER

In this part will be added motor-generator device which is able to recover energy from exhaust gases. This recovered energy is taken from turbocharger shaft and then converted into the electric power which could be utilized to charge batteries in hybrid vehicle or electricity of the vehicle.

7.1 MOTOR-GENERATOR

Because it was not available defined motor-generator for this engine speicification, it was necessary to create one and customize it to the turbocharger especially in terms of speed. It was chosen motor-generator from GT-Power examples for hybrid vehicle. For this engine application, the motor-generator will be customized for maximum brake power of 15 kW and maximum speed (turbocharger speed) 173 kRPM (kilo revolutions per minute) because these are maximum revolutions of turbocharger of tested engine (Figure 60) and further simulations will take place at lower engine speed.
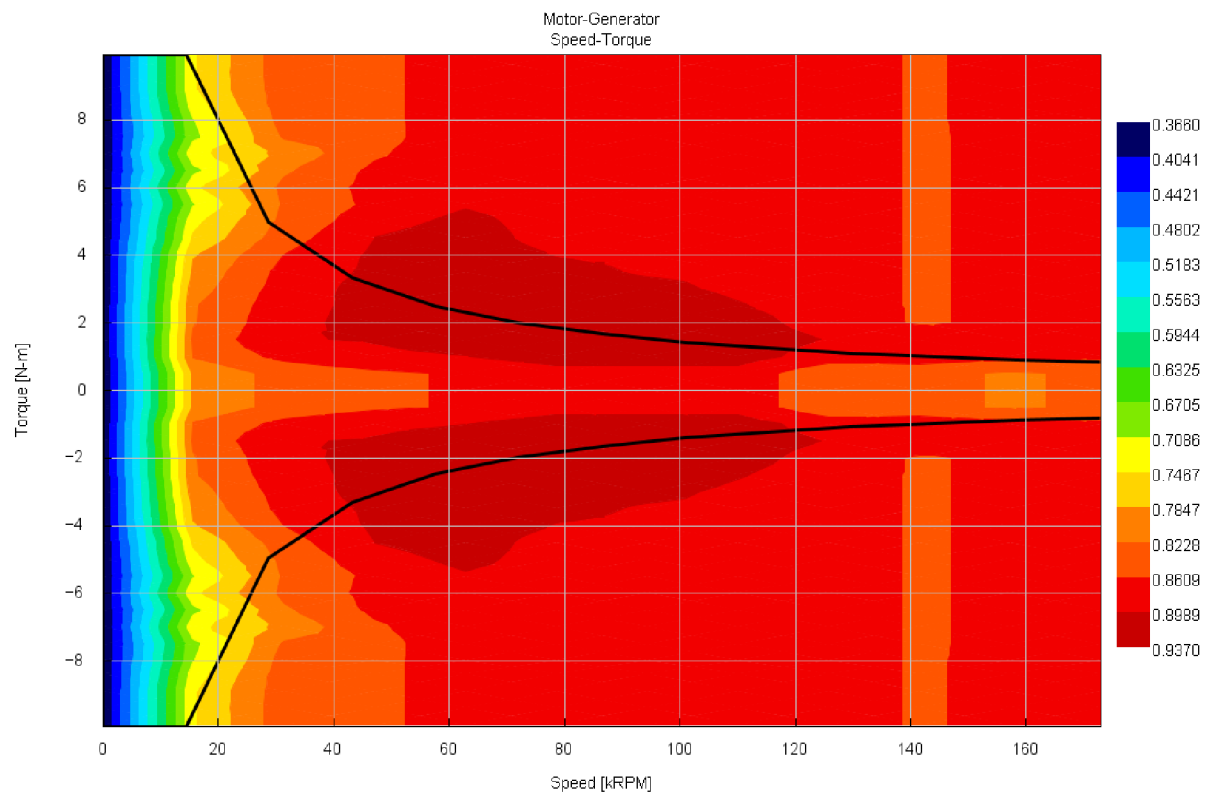
Figure 61 Motor-generator speed-torque efficiency map

After the adjustment of original motor-generator, it was created new motor-generator characteristic in Figure 61. This characteristic indicates the amount of power (energy) at defined rotor speed which is possible to recover or supply. Efficiency map remains the same as for original motor-generator. Positive part of the map shows power which could be utilized for conversion of electrical energy to mechanical energy and negative part indicates the mode where is possible energy recovery (mechanical energy to electrical).

7.2 BATTERY AND POWER LIMITER

The amount of electrical energy whether it is recovered or utilized must be taken into or from the battery. Battery limiter object (Figure 62 connected to the battery) has to limit the current and voltage limit to avoid incorrect results. The limit voltage has been set to 48 V for charging and also for discharging the battery.

Battery capacity is 100 A-h and initial state of charger was set to 10 %. Battery circuit voltage and internal resistance for charging and discharging were utilized from the example model. Battery temperature was left at 300 K. It has to be mentioned that model will not count with inverter losses which may also occur.
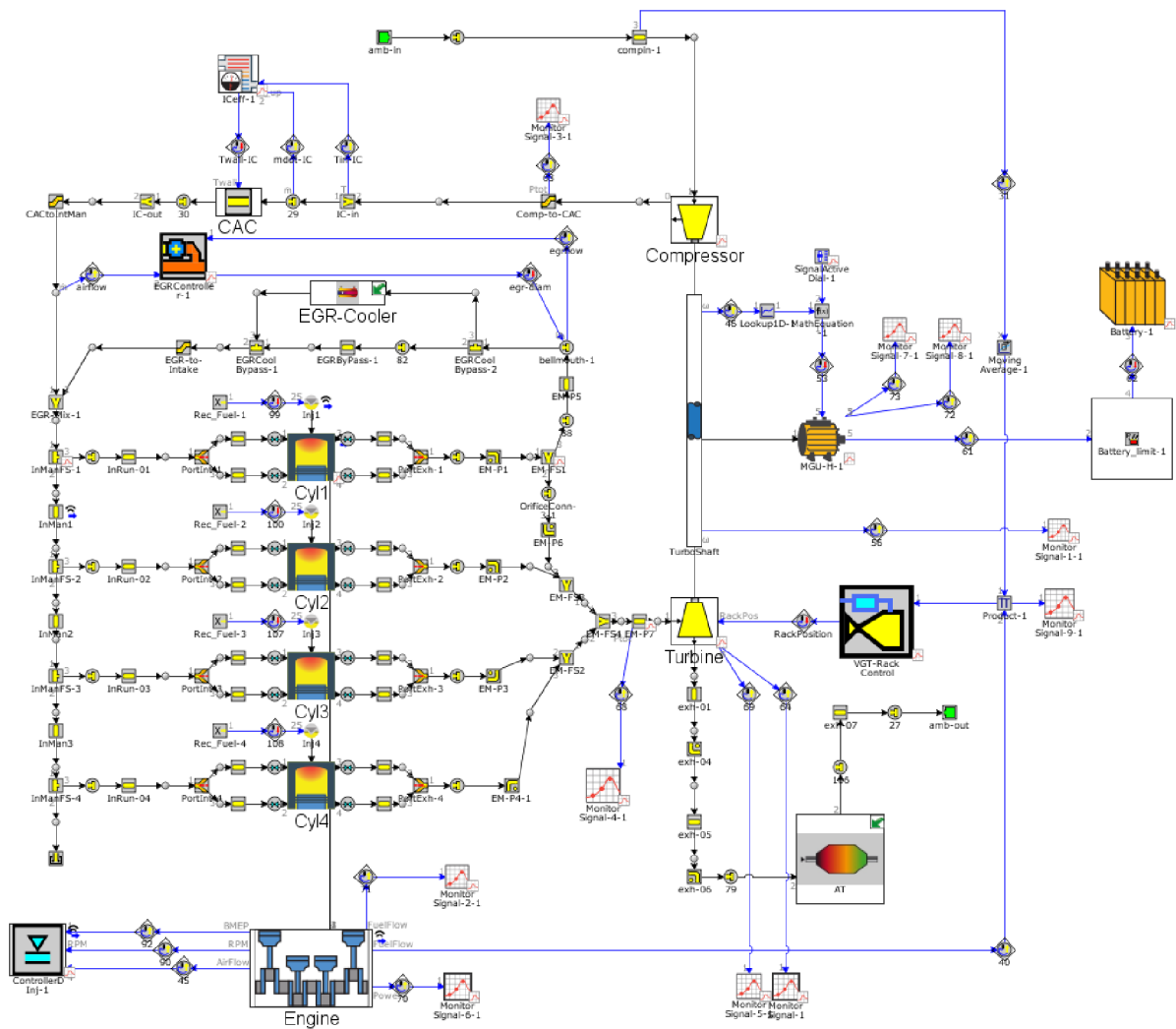

Figure 62 Engine model with motor-generator and battery

7.3 VNT CONTROL

For tubocharged model with motor-generator, the VNT control can be handlel in several ways.

First option is to supplied or recover power to turbocharger shaft through electrical energy, so that the compressor power demand would be satisfied to target air-fuel ratio or boost pressure but the rack positions will be fixed. This type of controlling requires specially configured PID controller which could be very difficult to do. Instead of this was utilized second option.

Second option is that rack position is controlled by already used PID controller to reach target value of air-fuel ratio and motor-generator unit will be gradually loaded. This flow is described in Figure 63 and corresponds with engine model in Figure 62.
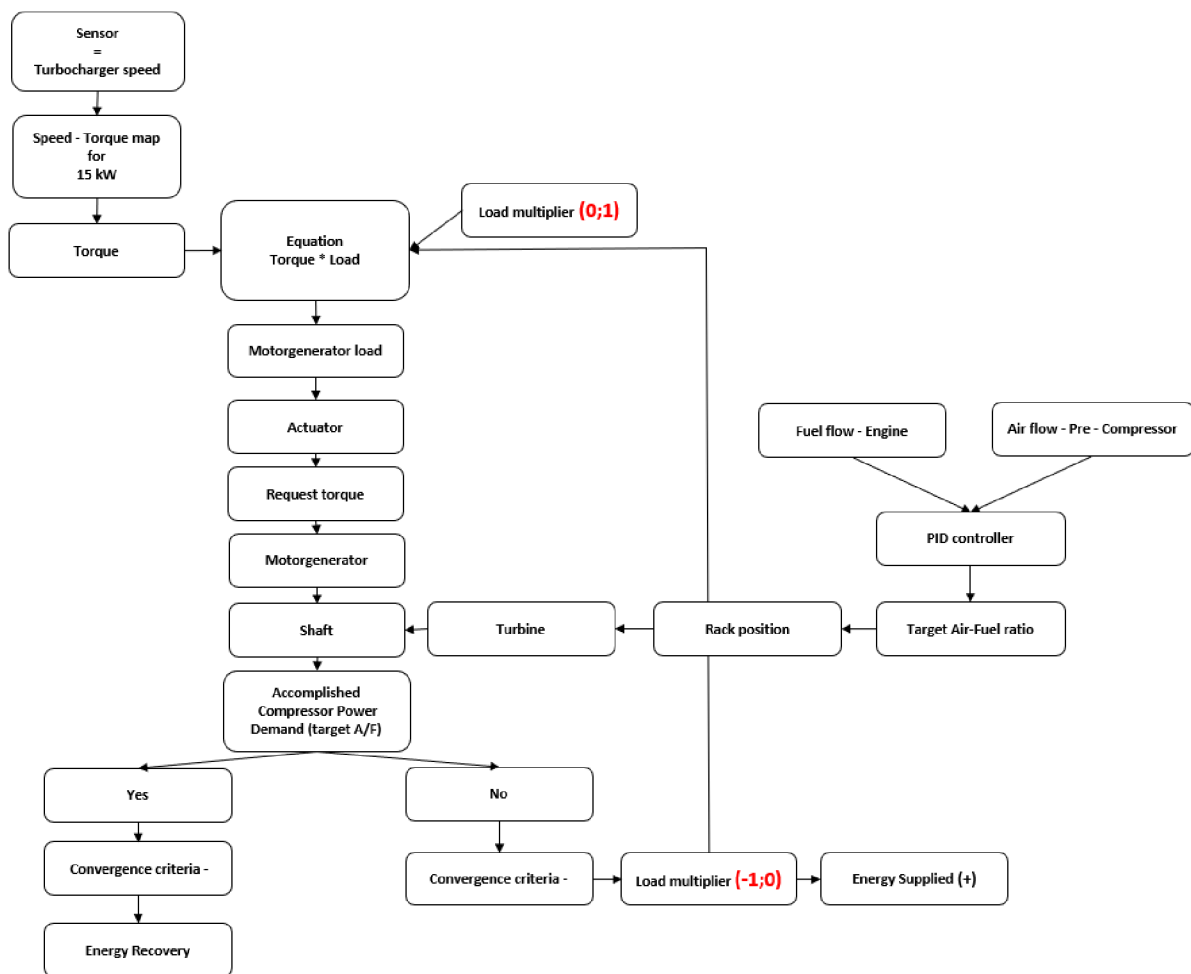

Figure 63 Flow chart map of controlling motor-generator load (2nd option)

For changes in load of the motor-generator, it was created control panel (Figure 64) which can alter load during the simulation and it is possible to observe changes in engine parameters during the simulation, especially for PID controllers and their targeting values.
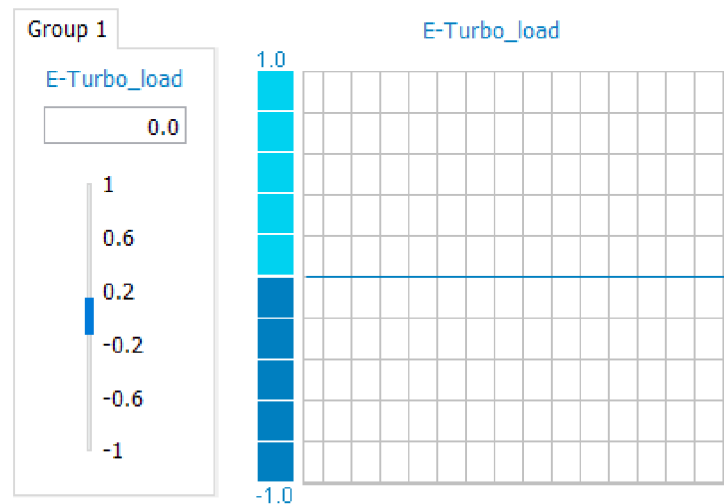
Figure 64 Motor-generator load controller

Load of the motor-generator is specified value of the multiplier from -1 to 1 (-100% to 100%). Due to this multiplier it is easier to find out the limit value of the load at which could motor-generator recover or supply energy. Recuperated or supplied power by motor-generator is then given based on turbocharger speed and efficiency in operating point of load according to the motor-generator characteristic in Figure 61.
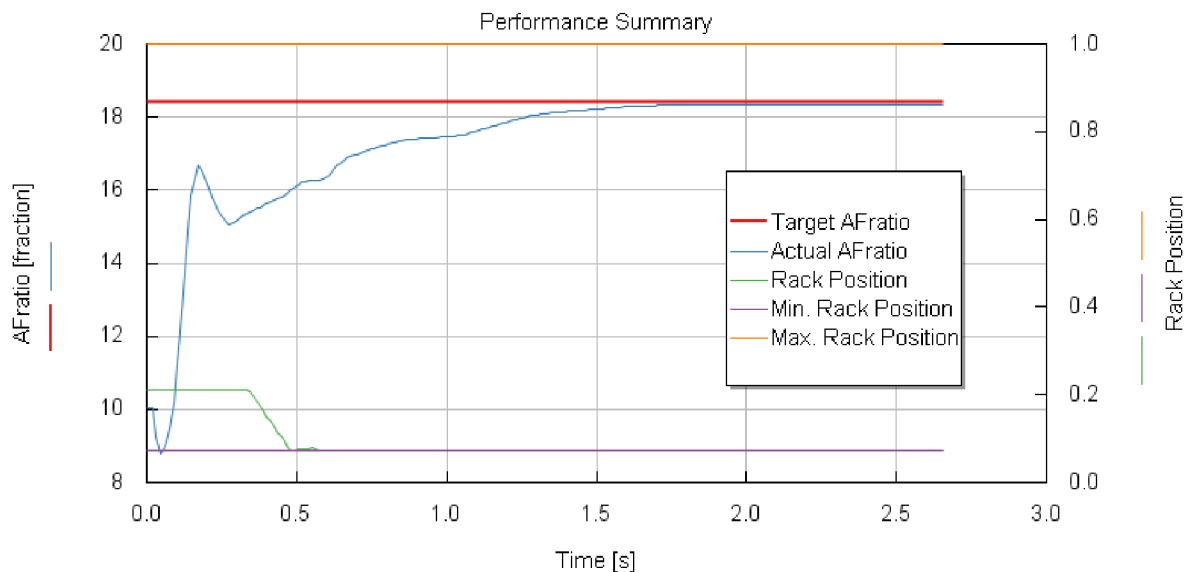
Figure 65 VNT controller for air-fuel ratio

Example of VNT controller is shown above where target value of A/F ratio is reached and the rack position is at its lowest value. In this case the convergence criteria which are set the same as for engine without motor-generator unit are accomplished.
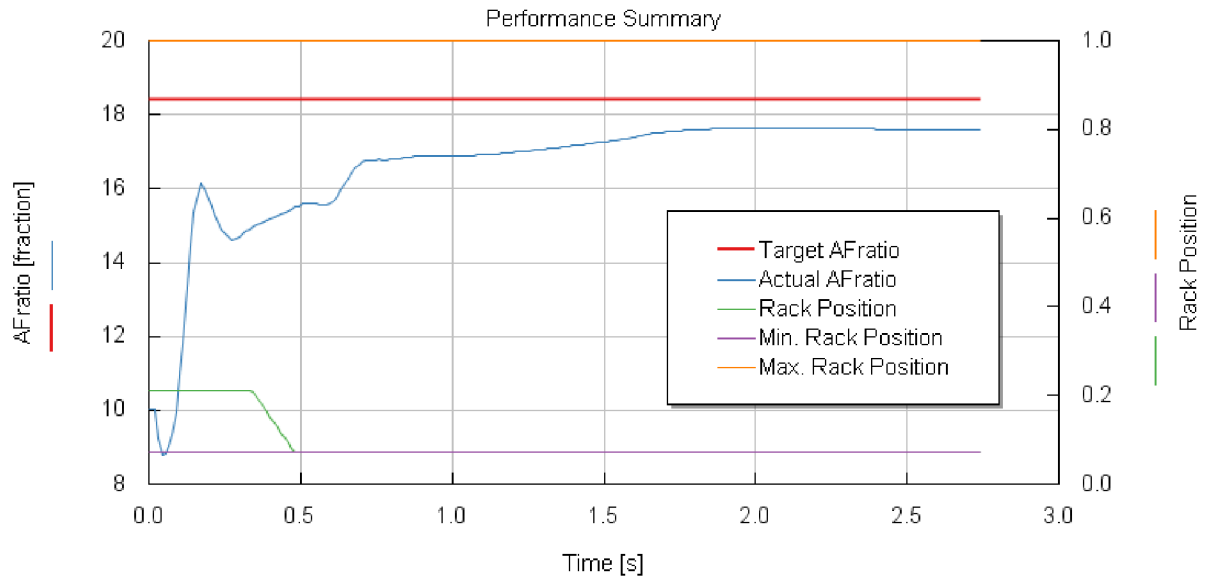
Figure 66 Too high E-turbo load

On the other hand, there will always be a situation where the E-turbo load for energy recovery is too high which means that the turbine is not able to supply the required power for the compressor for the target A/F ratio and that means the convergence criteria will not be met.

8 ENERGY RECOVERY STUDY

In this energy recovery study will be compared different diameter combinations of compressor and turbine wheels and their influence on possible amount of recovered energy. The combinations were selected based on recommendations from company Garrett Motion which also provided compressor and turbine maps for this study.

First of all, it has to be found the border of load where E-Turbo is capable of reaching the targeting value of air-fuel ratio for engine operating point as it was done in Figure 65, that means turbocharger recovers the hightest amount of electrical energy and still meet the convergence criteria for steady state. On the other hand, if convergence criteria will not be met, the motor-generator will have to supply energy to meet the criteria. For this recovery study were chosen operating points at full engine load and one operating point for partial load which are shown in Table 5. These points were selected because of low RPM operation ranges of the engine.

Table 5 – Operating points for the study

Load	Percentage of load	RPM
Full load	100 %	1000,1200,1400,1600,1800,2350
Part load	75 %	1800
	50 %	1800
	30 %	1800

8.1 BASELINE ENGINE VS. ENGINE WITH MOTOR-GENERATOR

For the first combination were used compressor wheel and turbine wheel diameters as for original engine, diameters are in Table 2. There will be compared baseline engine from simulation without motor-generator (Figure 57) and with motor-generator (Figure 62) to see resulting changes.

8.1.1 FULL LOAD

For each operating point above was found the border of load of motor-generator and possible energy recovery. As it was mentioned, with energy taken from the turbocharger shaft, the VNT mechanism is forced to close vanes (rack position) so turbine is capable to supply enough power for compressor. This is exactly what can be seen in Figure 67 where the rack position of all operating point remains the same or it is smaller. The amount of recovered electrical power is increasing with higher engine speed and thus turbocharger speed.
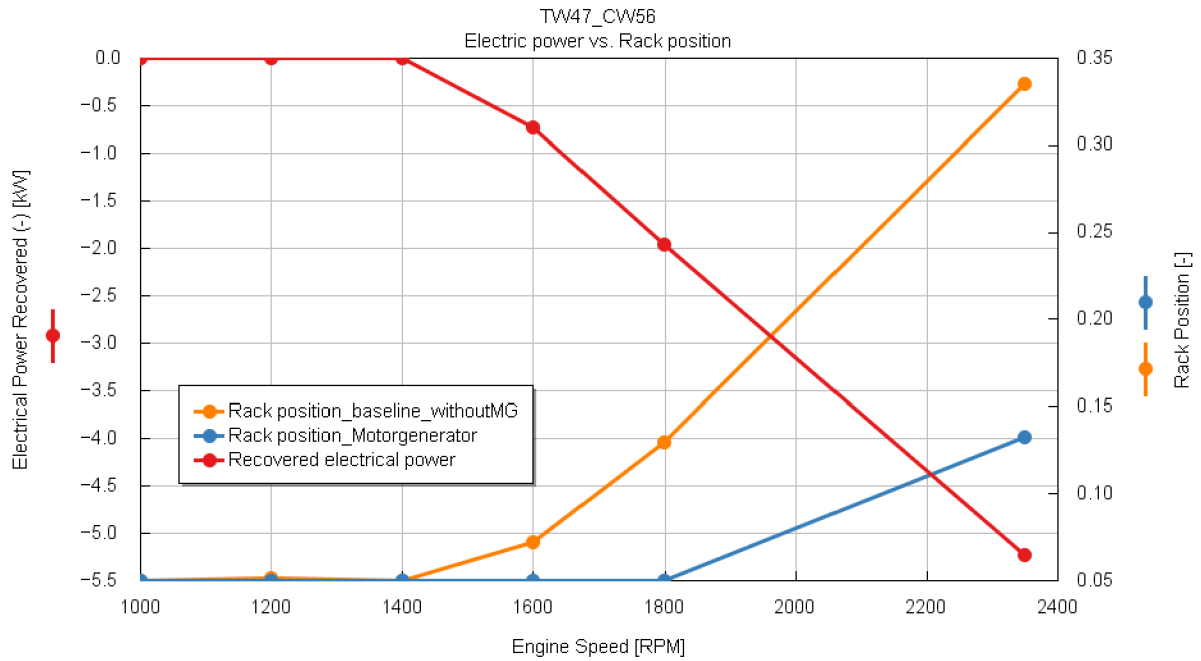
Figure 67 Differences in rack postion for engine models

Rack position is also related to the pressure and temperature (chapter 3.1) which are higher for engine model with motor-generator due to that the turbine have to produce more power to meet compressor power demand and at the same time recover energy. The temperature starts to rise exactly at the point of engine speed where engine can recover energy. Small pressure drop at 2350 RPM is than caused by slightly opened rack position.
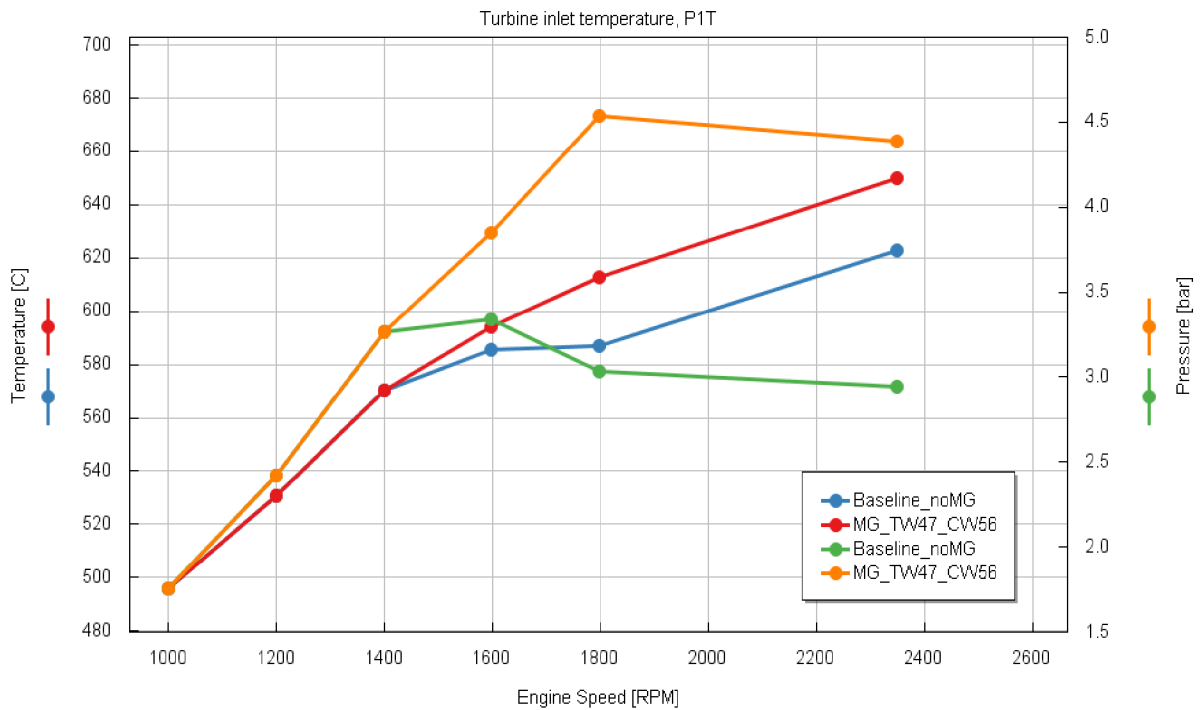
Figure 68 Pre-turbine pressure and temperature comparison

With increased pre-turbine pressure is also related post compressor pressure which have to meet targeted air-fuel ratio. Figure 69 shows that when turbocharger starts recovering energy, post compressor pressure and turbocharger speed are increasing. Turbocharger speed at 2350 RPM reaches the limit value of motor-generator speed-torque map as was mentioned in chapter 7.1 so the amount of recovered power is limited, but with extended map of motor-generator and allowed higher turbocharger speed, the amount of recovered power may be higher.
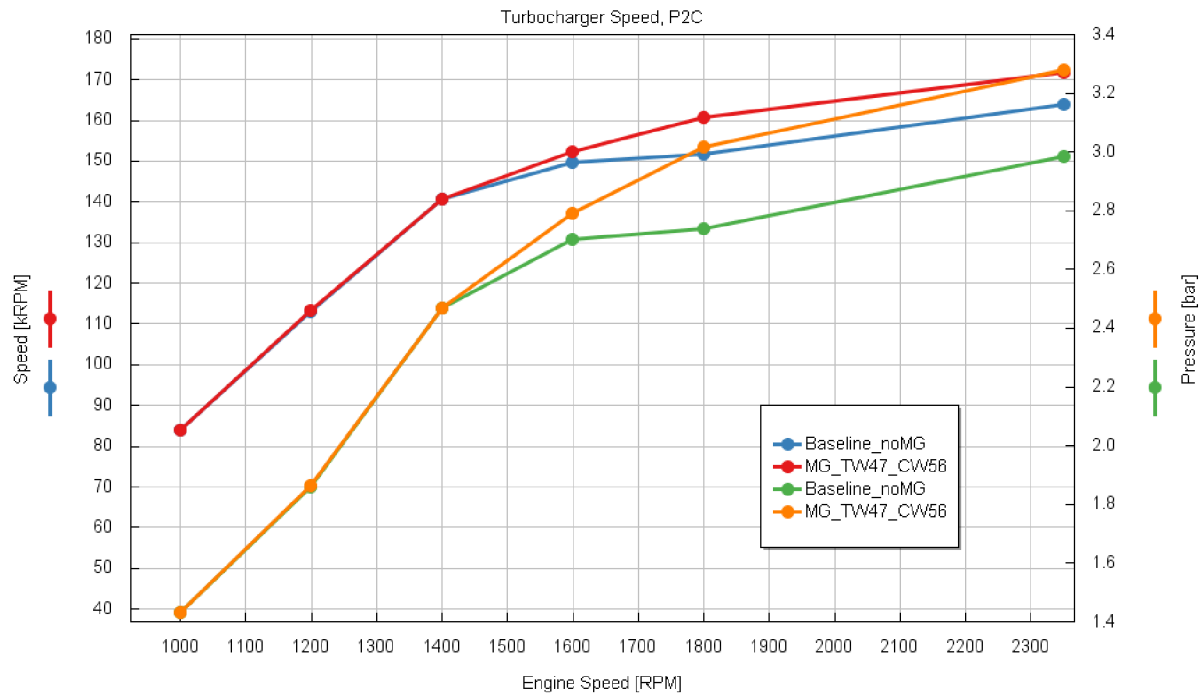
Figure 69 Turbocharger speed and post compressor pressure

8.1.2 PART LOAD

For part load simulation was chosen engine speed point described in Table 5. The rack position in Figure 70 copy the rack postion of full load which means for energy recovery the vanes are at their minumum rack position and the turbocharger can recover energy at all three levels of load.
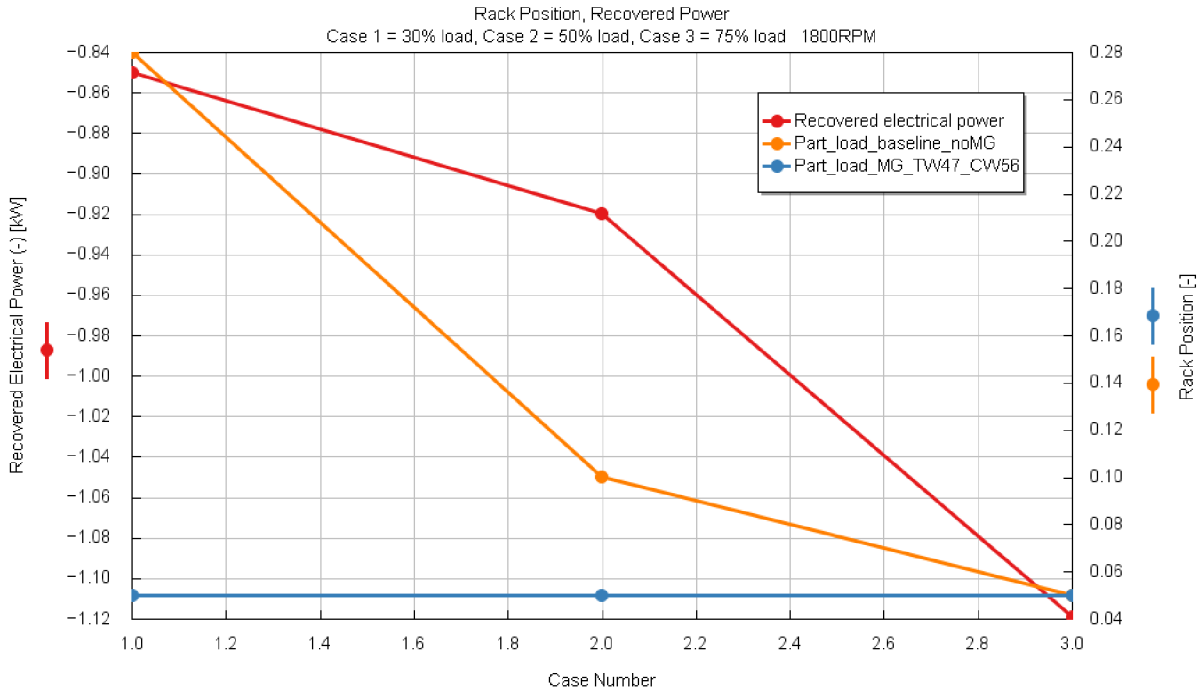
Figure 70 Part load comparison for 1800 RPM

At part load, it is also visible that turbine inlet temperature and pressure increase with increasing load and recovered amount of energy.
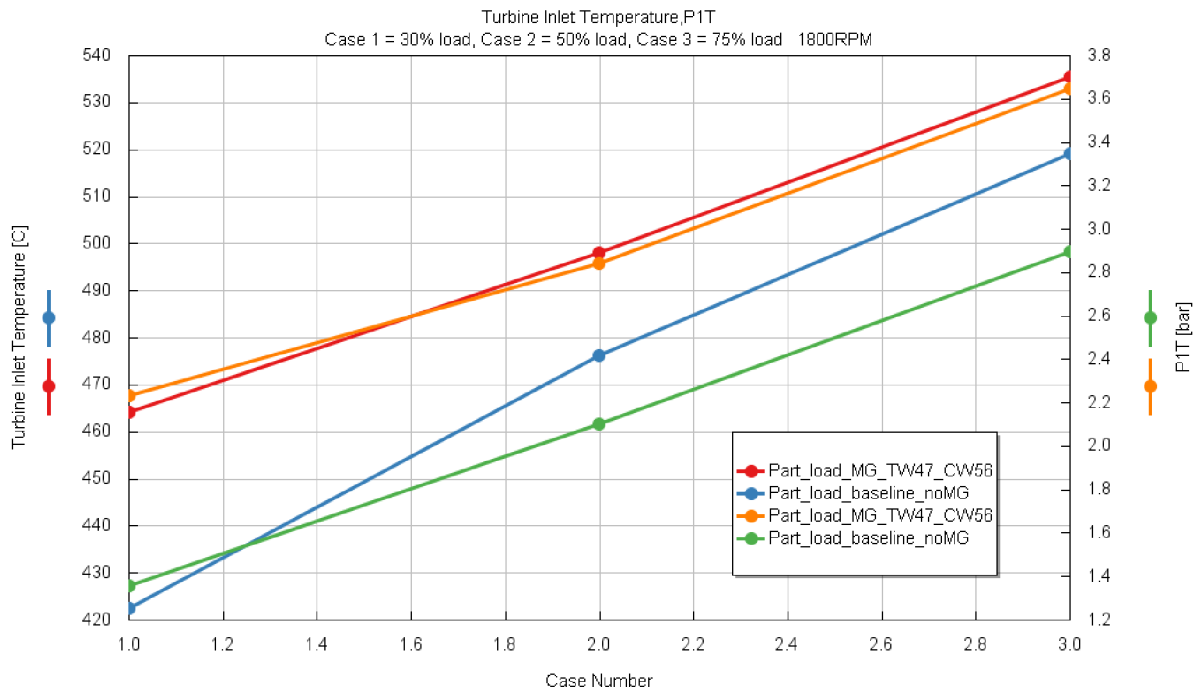
Figure 71 Part load comparison of turbine inlet pressure and temperature

With higher turbine pressure and temperature, the outlet compressor power and turbocharger speed have to higher too which may be seen in Figure 72.

Figure 72 Part load comparison of turbocharger speed and compressor outlet pressure

8.2 COMPARISON OF DIFFERENT WHEELS DIAMETERS COMBINATION

For this comparison will be used combination of compressor and turbine wheel presented in Table 6. These combinations are recommended based on previous applications and will be simulated for full load and partial load operating points in Table 5.

Table 6 – Turbine and compressor wheels diameters for comparison

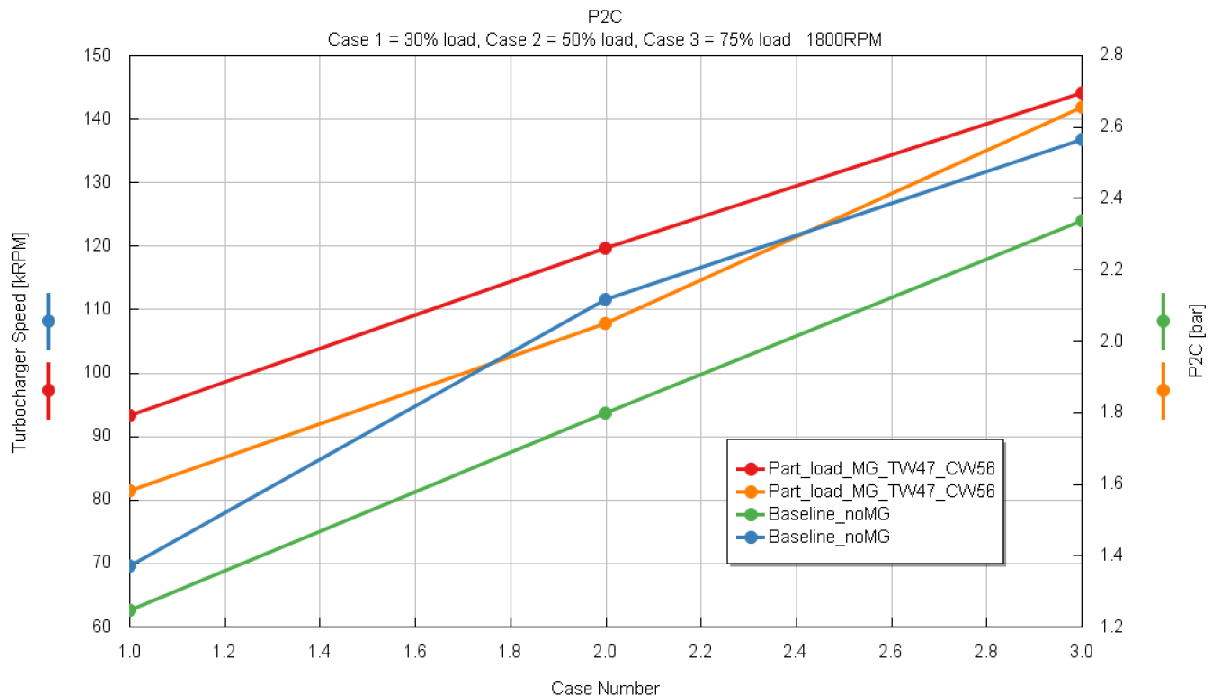|	Turbine wheel diameter [mm]	Compressor wheel diameter [mm]
Combination 1	47	56
Combination 2	47	52
Combination 3	47	60
Combination 4	50	60

8.2.1 FULL LOAD

From power comparison in Figure 73 with original combination 1 the turbocharger can recover energy and no energy needs to be supplied. Combination 2 can recover a small amount of energy at low engine speed but the energy has to be supplied at few operating point due to the turbine could not reach compressor power demand without supplied power from the motor-generator. For combination 3 and 4 it is necessary to supply energy for almost all operating points, 2350 RPM is the only operating point where these combination are capable of recover some amount of energy because of optimum turbocharger speed. Combinations 3 and 4 or even higher diameters of turbine and compressor make no sence for this engine application. The best combination will be probably the original combination 1 or combination 2 because of engine operating range when driving in urban city areas rarely exceeds 2000

RPM. But this would be tested for specific driving cycles and also on the intended use of the engine.
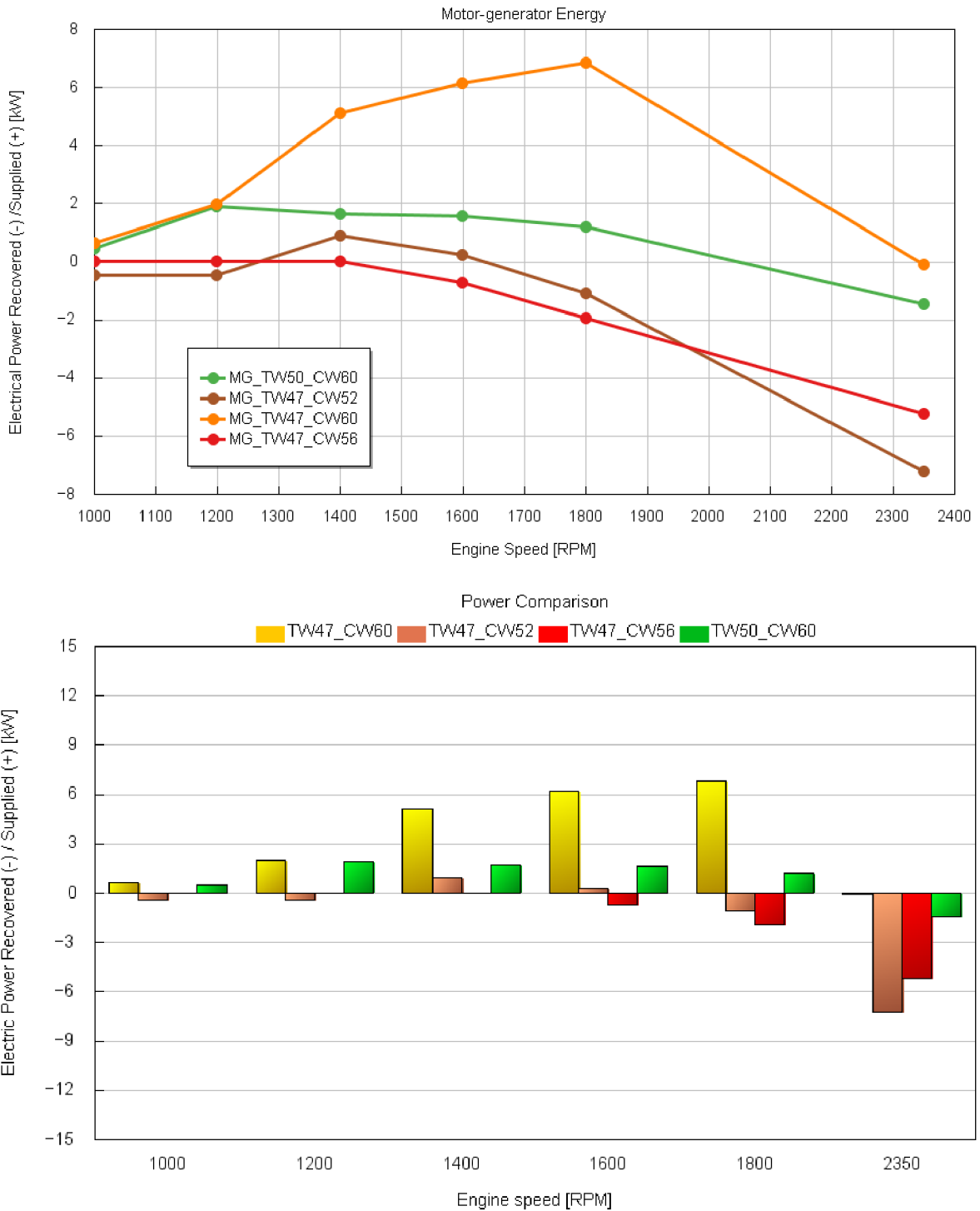
Figure 73 Energy recovery/supply comparison

Rack position at low engine speed usually remains in the smallest possible position to meet compressor demand even when the turbocharger recover energy or if the energy is supplied. At 2350 the rack position is more opened due to the larger flow of exhaust gases and thus

turbocharger speed. Exception is combination 2 where the turbocharger can operate at wide range of speed at low rack position.
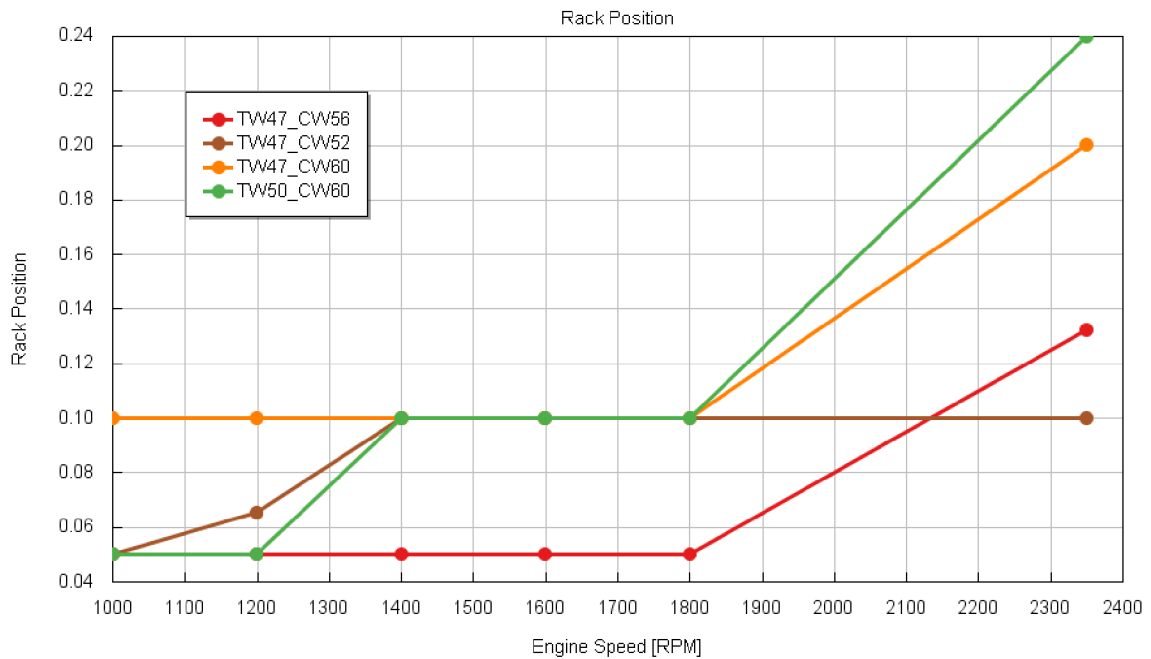
Figure 74 Rack position comparison

Turbine inlet pressure corresponds the rack position with energy recovered or supplied and increases during higher engine speed. The pressure drop of combination 4 (green line) at 1400 RPM is caused because of less energy is supplied and the rack position is more open versus previous engine operating point. Engine model have to be always restricted for maximum turbine inlet pressure to prevent damage or turbocharger speed to prevent for overspeed.
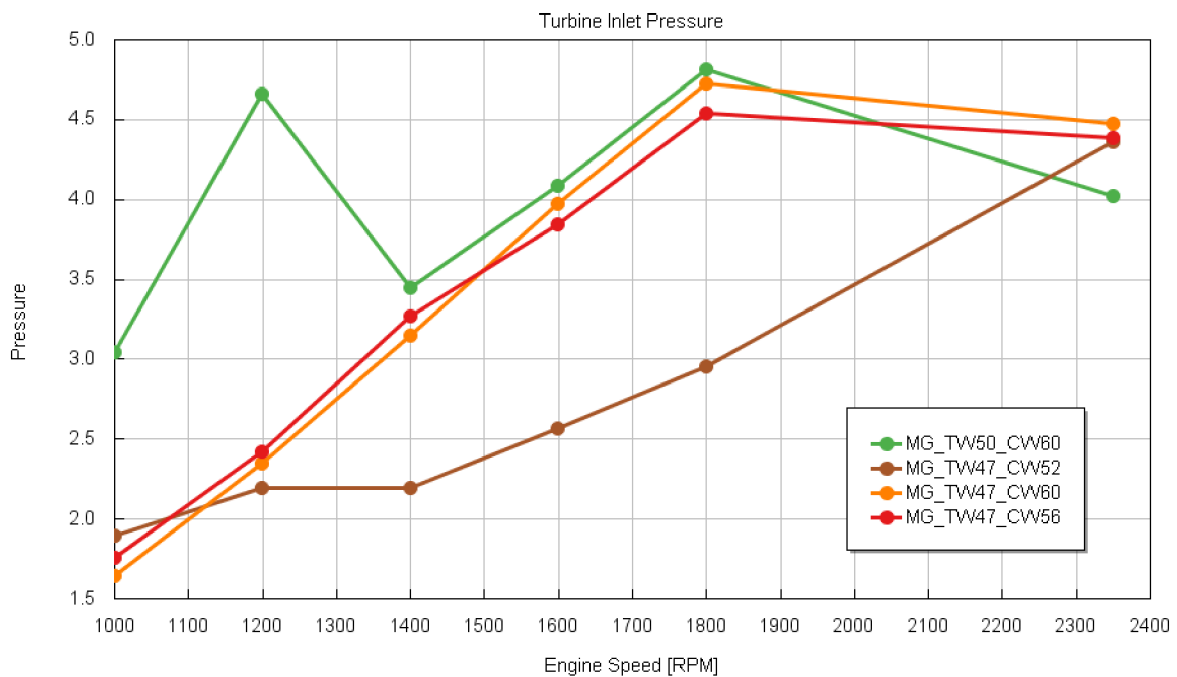
Figure 75 Turbine inlet pressure comparison

Turbocharger speed (Figure 76) increases though whole engine speed map and combination 2 also exceeds the maximum motor-generator speed map which means the recovered value of power is extrapoled from the motor-generator speed-map. In this case the speed-torque map of motor-generator should be enhanced to fit this turbocharger speed.
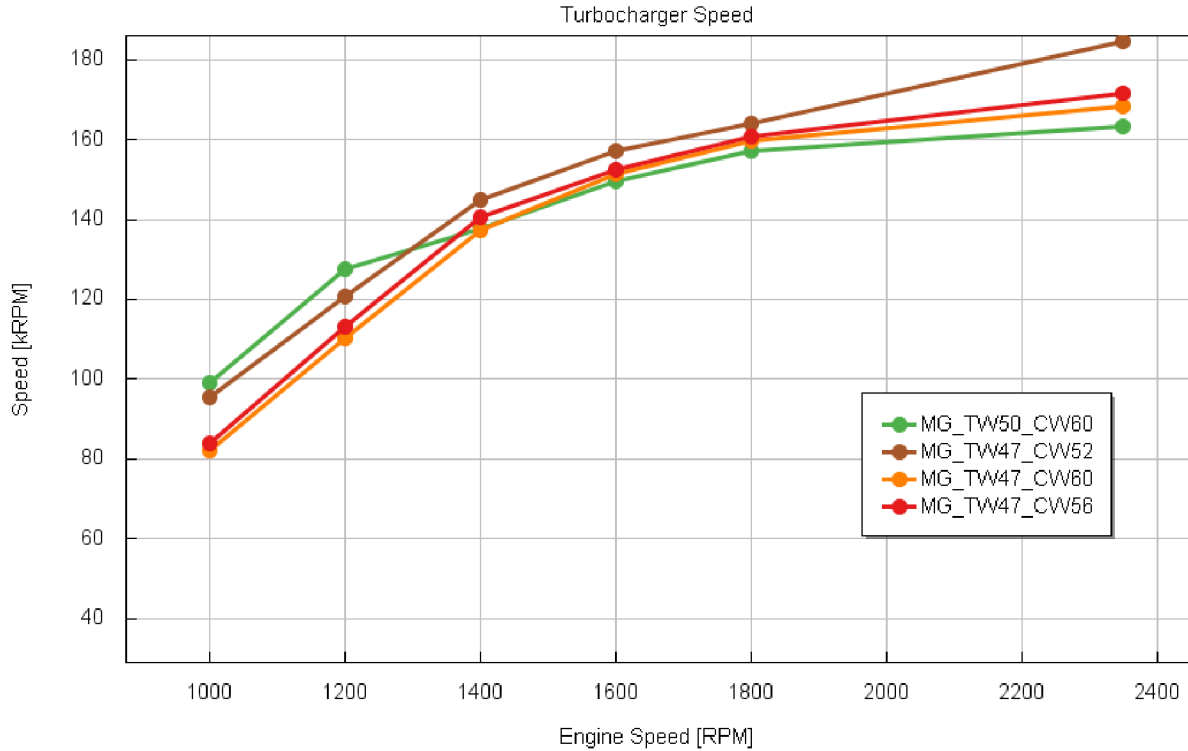
Figure 76 Turbocharger speed comparison

It is clear that from BSFC (Figure 77) perspective combination 3 and 4 have no utilization sence for this engine application. Combination 1 has higher BSFC primarily at 1800 RPM but this could be changed if the load of motor-generator will be reduced, this option will be presented in chapter 9. Combination 2 results in lower BSFC in whole engine speed operating points which could be also interesting for further studies. BSFC was calculated accrording to the equation

$$BSFC = \frac{\dot{m}_{\text{fuel}}}{P_{\text{ICE}} + (-P_{\text{EM}})},\qquad(26)$$

where $\dot{m}_{\text{fuel}}$ is fuel mass flow rate, P_{EM} power of electric motor-generator and P_{ICE} power of internal combustion engine. Equation indicates that if energy is recovered the BSFC will be lower due to the energy which is produced and which will be utilized for battery charging. This energy than will be used in future needs. Opposite if the energy is supplied from the battery the BSFC is lower due to the energy utilization.
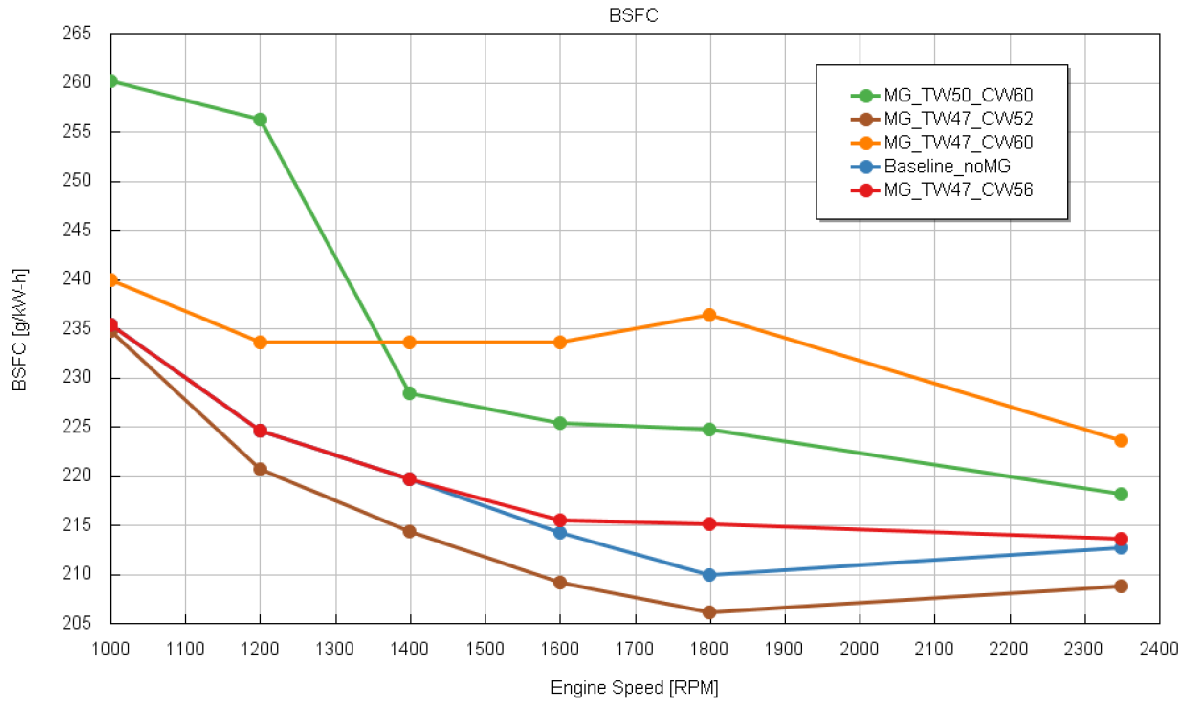
Figure 77 BSFC comparison

8.2.2 PART LOAD

For part load study will be used same information as for full load from tables 5 and 6.

As could be seen in Figure 78 at least for one load of combination 3 and 4 is necessary to supply energy from battery. Combination 1 and 2 are enable to recover energy at all part loads. Reason that combination 2 is able to recover more power at lowest load is primarily due to the rack postion (Figure 79) and high turbocharger speed at 30 % load.
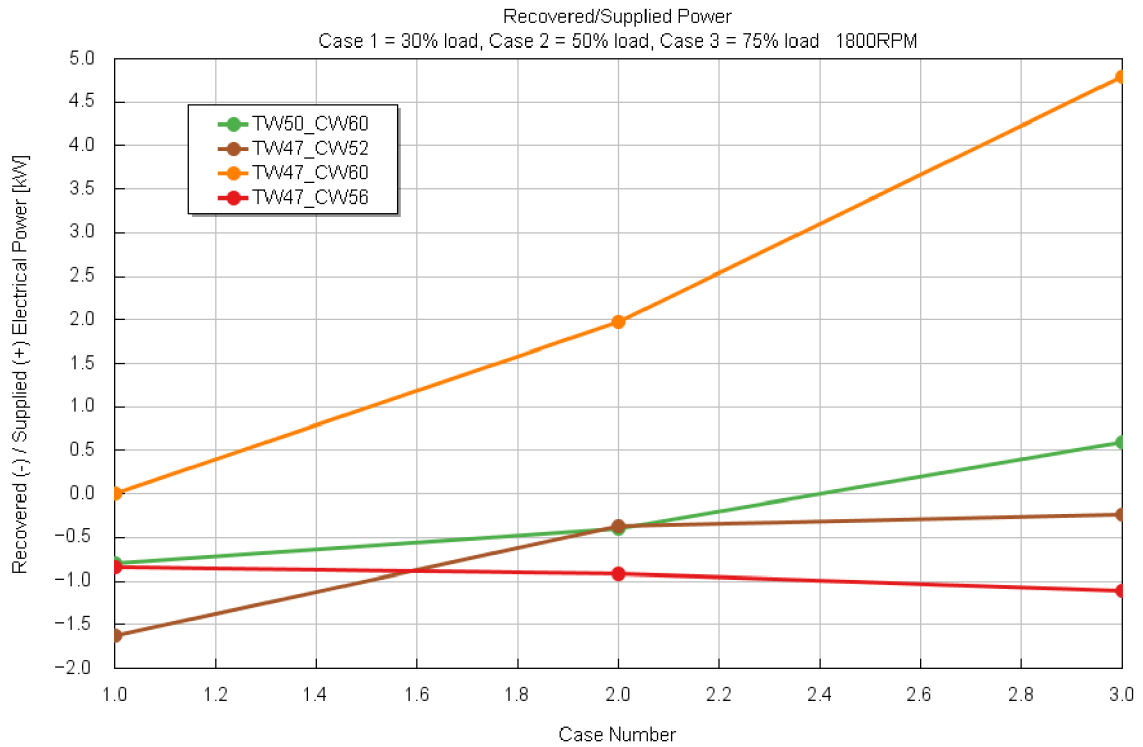
Figure 78 Energy recovery/supply comparison

The rack position in Figure 79 corresponds with both combinations where energy recovery is possible at all part load. For combination 1 the rack position stays at the lowest position for all loads. Combination 2 changed the rack position due to the higher exhaust gas mass flow and thus turbocharger speed and the vanes had to be opened.
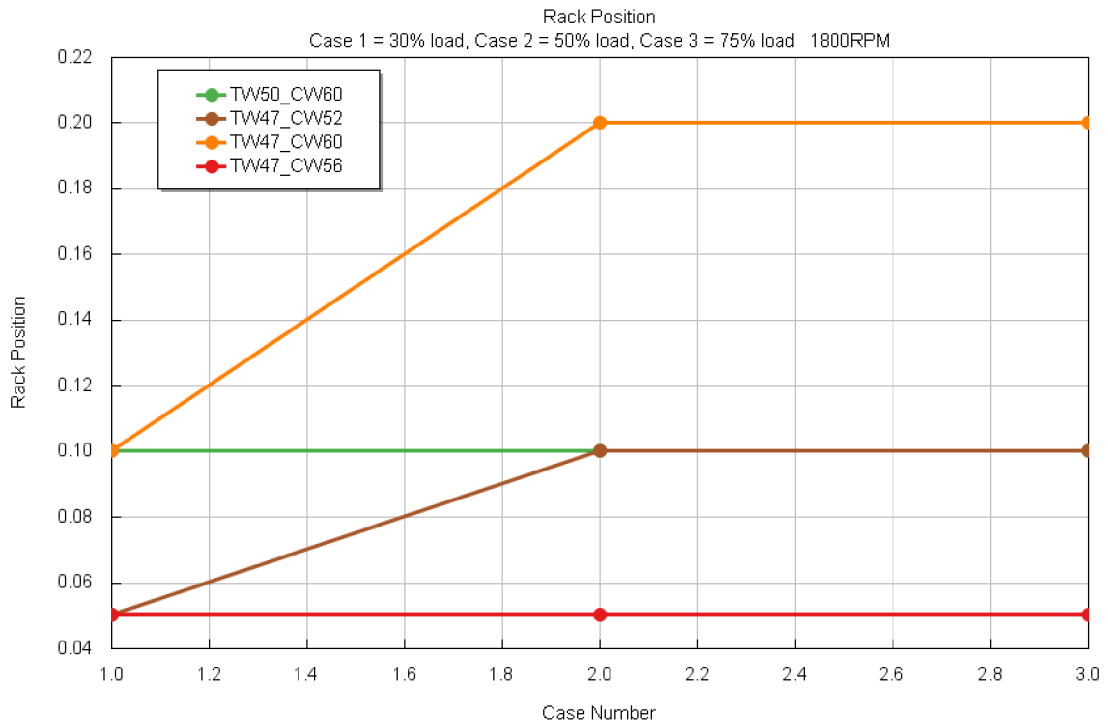
Figure 79 Rack position comparison

Turbine inlet pressure is based on rack position as it was for full load. Pressure for combination 1 gradually increases (same rack position) while for combination 2 pressure is changed due to the different rack postion.
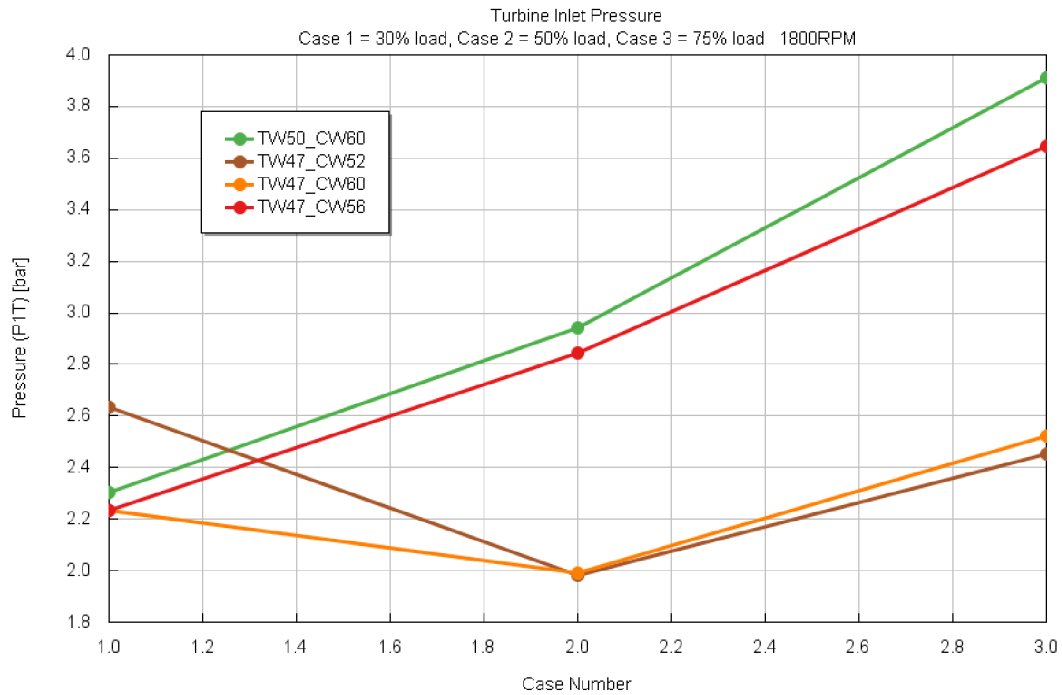
Figure 80 Turbine inlet pressure comparison

Turbocharger speed increases lineary for combination 1 and 4 because of the same rack position for all loads. But for combination 2 and 4 there is small change due to the change of the rack position at 50 % load.
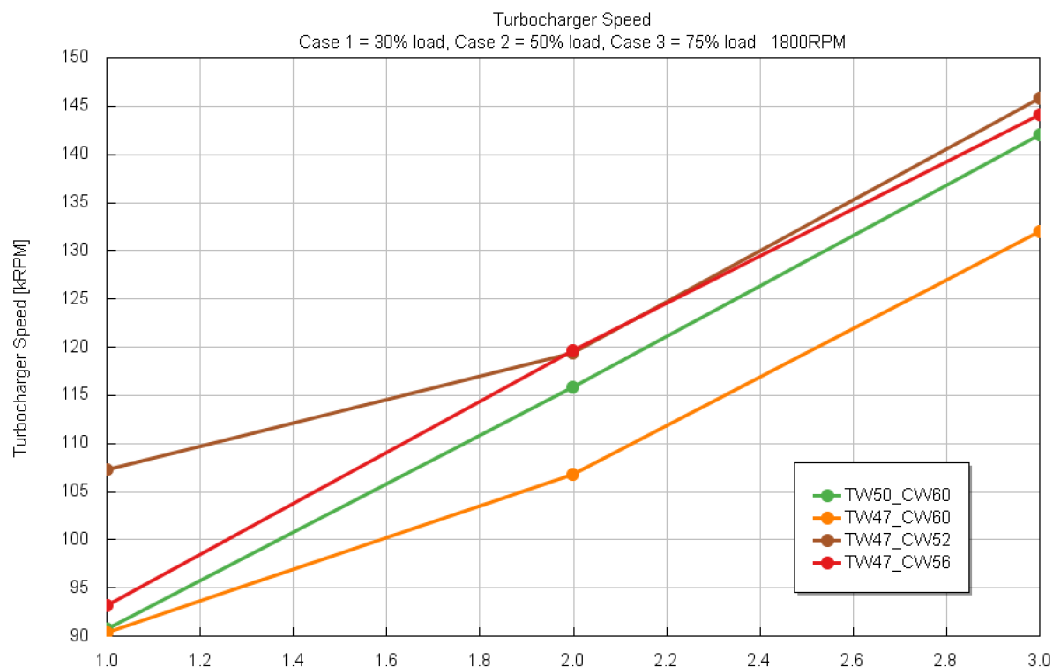
Figure 81 Turbocharger speed comparison

From fuel consumption comparison (Figure 82), the combination reached expected values. It is obvious from the graph that only combination 1 and 2 are usefull for this engine type application where both combinations are capable of recover energy (Figure 78).
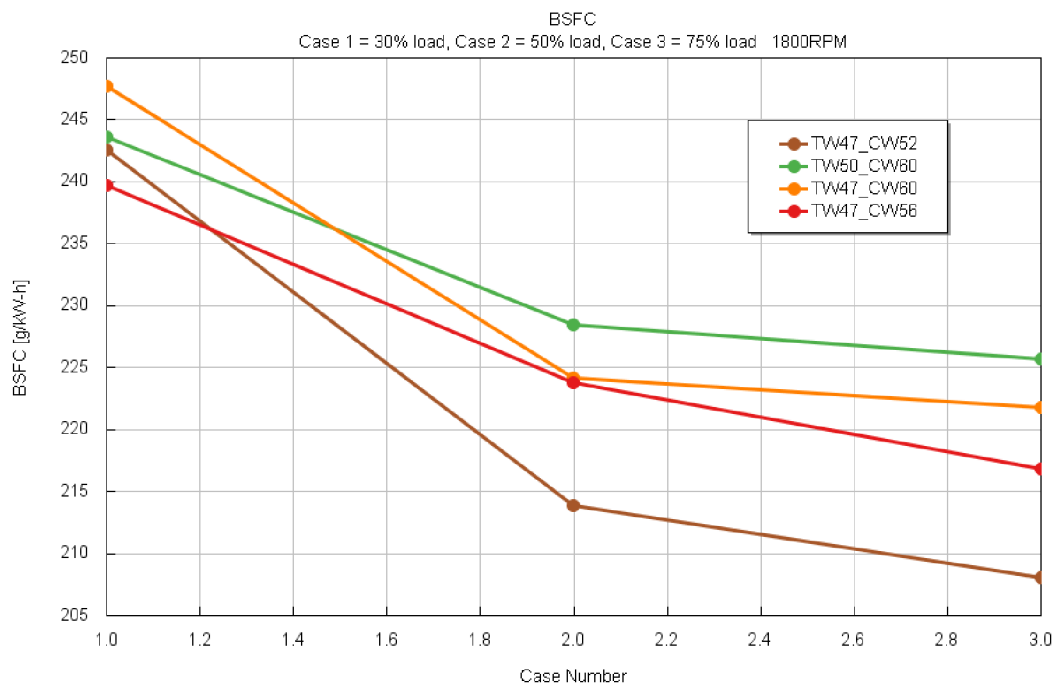
Figure 82 BSFC comparison

From all the data mentioned and shown above it is clear that only two combinations make sence in terms of energy recovery for Iveco Daily application but with given limits to prevent e.g. turbocharger overspeeding or too high pressure at the turbine inlet.

Table 7 – Suitability of compressor and turbine wheels for Iveco Daily application

	Suitability for Iveco Daily engine application
Combination 1	YES
Combination 2	YES
Combination 3	NO
Combination 4	NO

9 SPECIFIC FUEL CONSUMPTION STUDY

For this study were chosen two operating points of full engine load and their possible BSFC reduction. This was done for original combination 1 of turbine and compressor wheel diameters (Table 2). As it was mentioned the BSFC value depends on electric load of motor-generator and energy recovery or supply. BSFC values for this consumption study were calculated according to the equation 26 (Page 74).

9.1 FULL LOAD 1200 RPM

This consumption study is done by gradually loading of E-Turbo with no other modification done and convergence criteria remain the same. E-Turbo was loaded from -10 % to 10 % (mulplier -0.1 to 0.1) as could be seen in Figure 83. Withnout any load of E-Turbo (0 %), the target value of air-fuel ratio is reached but the BSFC value is higher. With supplied energy from the battery to the E-Turbo, it is possible to find an operating point where the target air-fuel ratio will be reached (meet convergence criteria) and also BSFC value will be lower. In this case it could be probably point of load -4 % where the BSFC value is on the lower limit and energy is supplied from the battery but the target air-fuel ratio is reached.
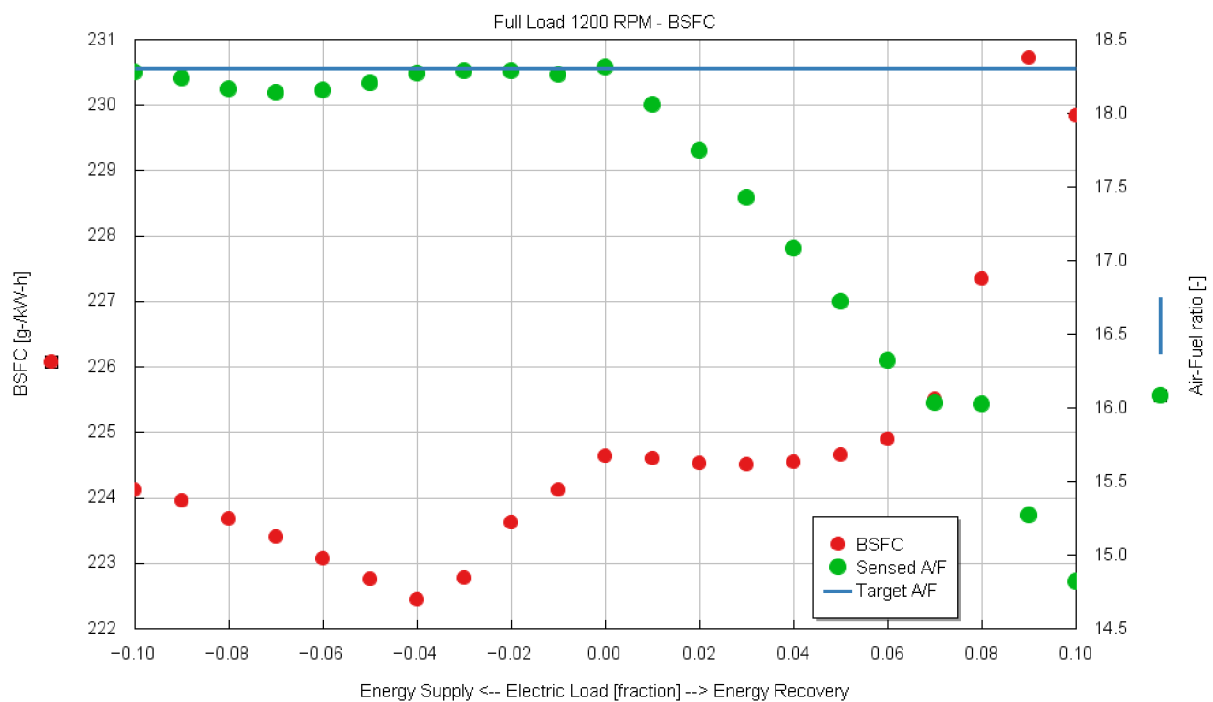
Figure 83 Electric load of E-Turbo affects BSFC

Figure 84 describes the electric load dependence on rack position and supplied energy from the battery. For best value of BSFC corresponds approximately 0.5 kW power supplied from the battery (steady state simulation) and not completely closed rack position. With closing the rack postion and recovering more energy.
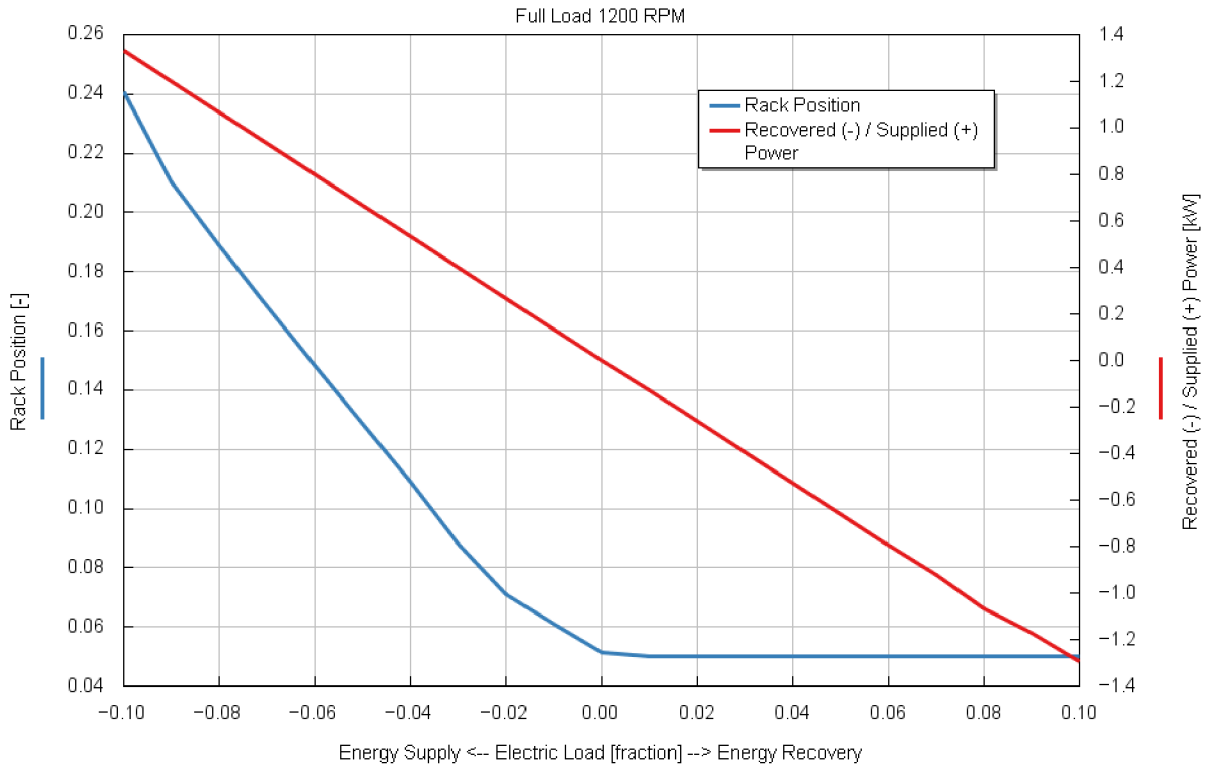
Figure 84 Energy and rack position comparison for specific electric load

In Figure 85 is shown battery state of charger and its running before the simulation reaches steady state and meet convergence criteria. In this case battery is discharging and power is supplied to the E-Turbo.
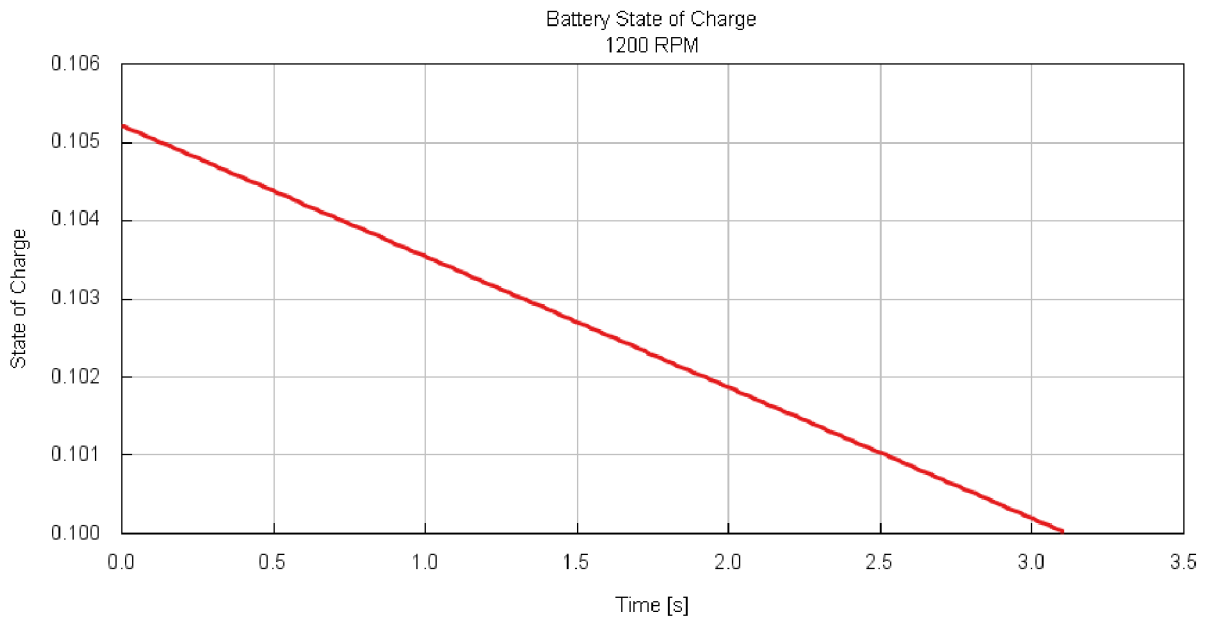
Figure 85 Battery state of charge and supplying E-Turbo (discharging battery)

9.2 Full load 1800 RPM

For this fuel consumption study is used operatin point 1800 RPM and E-Turbo is loaded just for one side of load and that is where E-Turbo recovers energy. E-turbo was loaded from 0 % to 20 % where recovers energy. As it is illustrated in the Figure 86 if the E-Turbo was loaded at 4 % the BSFC value is the same or little bit lower but at the same time is possible to recover some amount of energy which could be than used for battery charging.
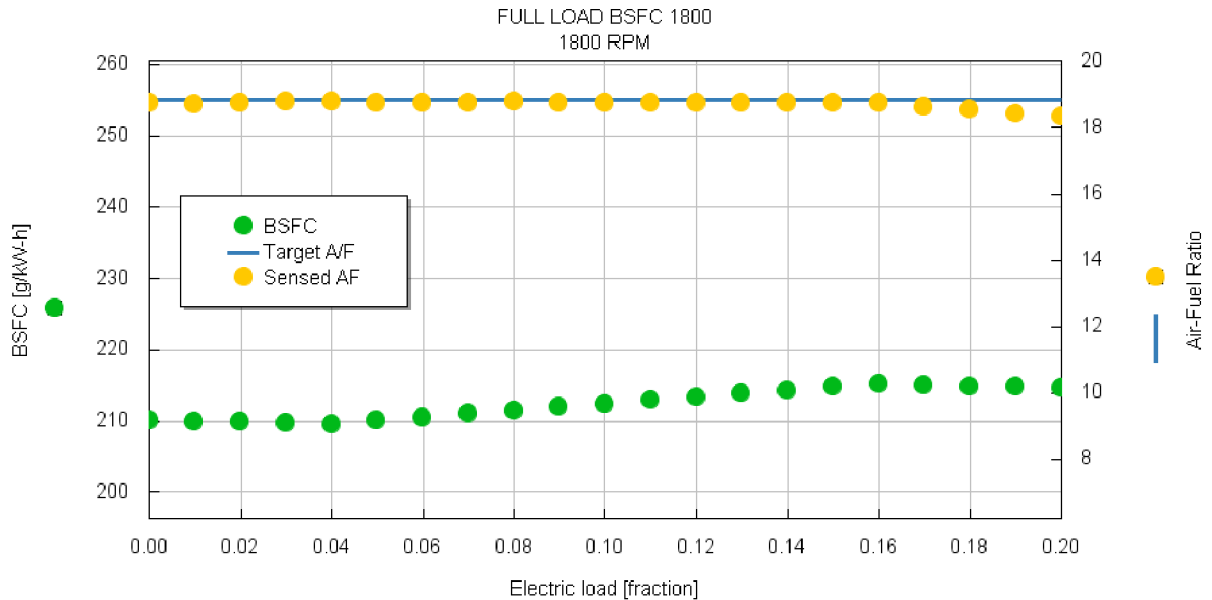
Figure 86 Electric load of E-Turbo affects BSFC

Figure 87 describes amout of power recovered for specific load. For best BSFC value where E-Turbo was loaded, the amout of electric power recovered is about 0.6 kW for steady state and the rack position is not fully closed.
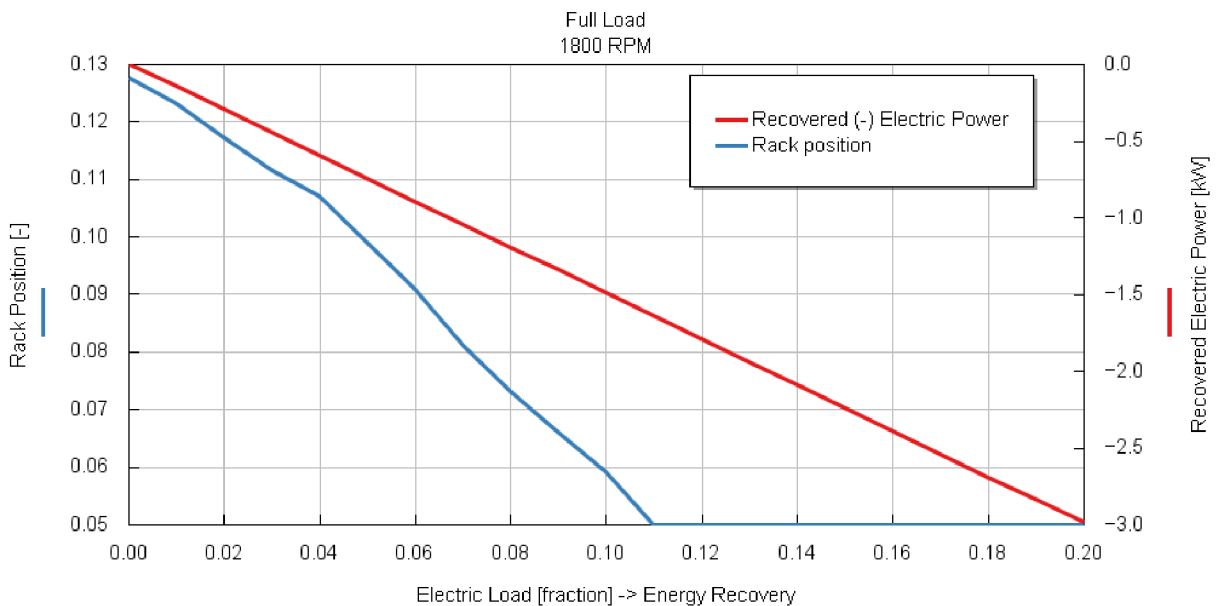
Figure 87 Energy and rack position comparison for specific electric load

With closing vanes and higher load of E-Turbo, the recovered energy will be higher but the BSFC value will rise as well. In Figure 88 is also illustrated battery state of charger till turbocharger meet convergence criteria for steady state.
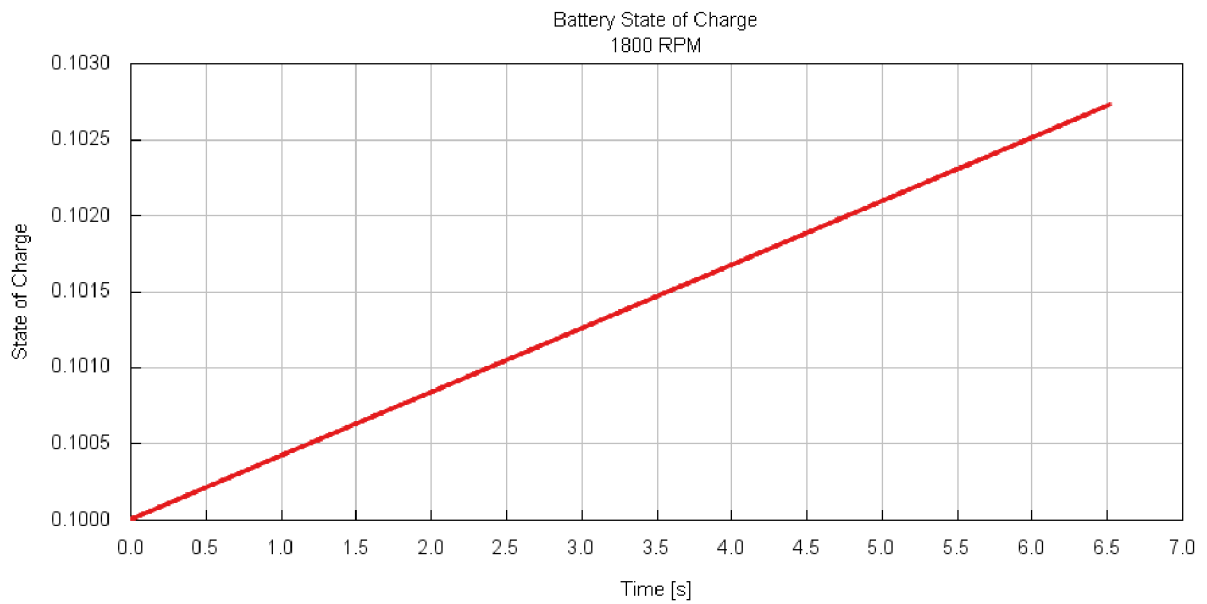
Figure 88 Battery state of charge (charging battery)

CONCLUSION

This master's thesis was focused on adaptation of electrically assisted turbocharger and its utilization in hybrid powertrain especially in terms of possible energy recovery. Turbocharger was firstly studied in terms of its functionality and other factor or criteria.

Electrically assisted turbocharger was introduced about its possible functionalities which include energy recovery, electric boosting etc. Possible utilization of electrically assisted turbocharger in terms of energy recovery for hybrid powertrain is defined and recommended for specific types of hybrid vehicles. Utilization of electrically assisted turbocharger in hybrid powertrain represents another degree of freedom with regenerative braking system to gain the energy which could be than trasferred into the battery especially in case of plug-in hybrid vehicles, which can lead to lower fuel consumption and thus emission production.

Computational model in GT-SUITE was firstly adjusted and compared to the original tested model for validation. After that were added motor-generator and battery to find out the amount of energy which could be recovered in specific engine loads. Controlling the power of the turbine was selected to target steady state of the engine and thus future validated results.

Comparison of different combinations of turbine and compressor wheels was done with expected results from which emerged that diameters of wheels larger than for current application have no utilization because their utilization is in higher engine speed and for engines providing higher brake power. Combination with smaller diameters and given limits could have potencional for further studies and have to be considered in engine application with E-turbo because of faster turbocharger response and possible energy recovery at low engine speed. Another study results that with utilization of electrically assisted tubocharger with battery it is possible to find out a better value of BSFC in specific operating point of engine load or operating point with same BSFC value but possible energy recovery in this operating point of engine. That could lead to a reduction in total consumption in all engine loads and thus total emission reduction.

The simplified engine model and thus lesser compressor and especially turbine efficiency could influenced the amount of recovered power which would be probably greater for original tested engine.

For futher study, with accurate (original) engine model it is possible to compare the best two combinations of compressor and turbine wheels in specific driving cycle and find out the amount of energy which could be recovered during the whole cycle and also with target to lower total BSFC during whole cycle.

REFERENCES

[1] NGUYEN-SCHÄFER, Hung. *Rotordynamics of automotive turbochargers*. Second edition. Cham: Springer, [2015]. Springer tracts in mechanical engineering. ISBN 978-3-319-17643-7.

[2] HIERETH, Hermann a Peter PRENNINGER. *Charging the internal combustion engine*. Wien: Springer, c2007. Powertrain. ISBN 978-3-211-33033-3.

[3] Chu, S., Majumdar, A. Opportunities and challenges for a sustainable energy future. *Nature* 488, 294–303 (2012). https://doi.org/10.1038/nature11475

[4] Worldwide Emission Standards and Related Regulations. In: *Continental-Automotive* [online]. 2019 [cit. 2021-03-01]. Dostupné z: https://www.continental-automotive.com/getattachment/8f2dedad-b510-4672-a005-3156f77d1f85/EMISSIONBOOKLET_2019.pdf

[5] Prof. Rolf D. Reitz,. *Reciprocating Internal Combustion Engines* [online]. [cit. 2021-03-01]. Dostupné z: https://cefrc.princeton.edu/sites/cefrc/files/Files/2012%20Lecture%20Notes/Reitz/Princeton-CEFRC2.pdf. University of Wisconsin-Madison.

[6] BARTONÍČEK, Ladislav. *Přeplňování pístových spalovacích motorů*. Liberec: Technická univerzita v Liberci, 2004. ISBN 80-708-3800-0.

[7] EHSANI, Mehrdad, Yimin GAO, Stefano LONGO a Kambiz M. EBRAHIMI. *Modern electric, hybrid electric, and fuel cell vehicles*. Third edition. Boca Raton, [2018]. ISBN 978-1-4987-6177-2.

[8] Turbocharger section view. In: *Its My Machine* [online]. 2011 [cit. 2021-03-01]. Dostupné z: https://itsmymachine.wordpress.com/2011/01/08/a-turbocharger/

[9] GOVARDHAN, Ojas M. Fundamentals and Classification of Hybrid Electric Vehicles. International Journal of Engineering and Techniques (IJET) [online]. 2017, 3(5), 194-198 [cit. 2020-02-09]. ISSN 2395 - 1303. Dostupné z: http://oaji.net/articles/2017/1992-1515159589.pdf

[10] JÄÄSKELÄINEN, Hannu. *Turbocharger Bearings* [online]. 2016 [cit. 2021-03-01]. Dostupné z: https://dieselnet.com/tech/air_turbo_bearings.php

[11] Garrett Installer Connect. *Garrett Motion* [online]. [cit. 2021-03-01]. Dostupné z: https://www.garrettmotion.com/turbo-replacement/installer-connect/

[12] Turbo Tech 101 | Basic: Understanding the Parts of the Turbocharger. In: *Garrett Motion* [online]. 2019 [cit. 2021-03-03]. Dostupné z: https://www.garrettmotion.com/wp-content/uploads/2019/10/GAM_Turbo-Tech-101_BASIC.pdf

[13] JÄÄSKELÄINEN, Hannu a Magdi K. KHAIR. Turbocharger Fundamentals. *DieselNet Technology* [online]. 2017 [cit. 2021-03-03]. Dostupné z: https://dieselnet.com/tech/air_turbocharger.php

[14] WANG, Tie, Cheng PENG a Jing WU. Back swept angle performance analysis of centrifugal compressor. Mechanics [online]. 2014, 20(4), 382-389 [cit. 2021-03-04]. ISSN 2029-6983. Dostupné z: doi:10.5755/j01.mech.20.4.4615

[15] SHAABAN ABDALLAH, Rachel Schwind, Cheng PENG a Jing WU. A Look at Compressor Impeller Technologies for Turbochargers Focusing on Surge Mitigation. Global Journal of Technology and Optimization [online]. 2015, 06(03), 382-389 [cit. 2021-03-04]. ISSN 22298711. Dostupné z: doi:10.4172/2229-8711.1000185

[16] LUKIC, S.M., A. EMADI a Jing WU. Effects of Drivetrain Hybridization on Fuel Economy and Dynamic Performance of Parallel Hybrid Electric Vehicles. IEEE Transactions on Vehicular Technology [online]. 2004, 53(2), 385-389 [cit. 2021-03-04]. ISSN 0018-9545. Dostupné z: doi:10.1109/TVT.2004.823525

[17] Turbo Tech 102 | Advanced: Understanding Air Flow. In: *Garrett Motion* [online]. 2019 [cit. 2021-03-03]. Dostupné z: https://www.garrettmotion.com/wp-content/uploads/2019/10/GAM_Turbo-Systems-102_Advanced.pdf

[18] ALSHAMMARI, Mamdouh, Fuhaid ALSHAMMARI a Apostolos PESYRIDIS. Electric Boosting and Energy Recovery Systems for Engine Downsizing. Energies [online]. 2019, 12(24), 385-389 [cit. 2021-03-04]. ISSN 1996-1073. Dostupné z: doi:10.3390/en12244636

[19] CANOVA, Marcello, Massimo NADDEO, Yuxing LIU, Junqiang ZHOU a Yue-Yun WANG. A Scalable Modeling Approach for the Simulation and Design Optimization of Automotive Turbochargers. SAE International Journal of Engines [online]. 2015, 8(4), 1616-1628 [cit. 2021-03-04]. ISSN 1946-3944. Dostupné z: doi:10.4271/2015-01-1288

[20] MAMO, Samuel, Miao Zhang ZHANG a Mario Farrugia FARRUGIA. Automotive turbocharger hot-gas test-stand data acquisition and control. 2016 17th International Conference on Mechatronics - Mechatronika (ME) [online]. 2016 [cit. 2021-03-03]. Dostupné z: https://ieeexplore.ieee.org/document/7827844

[21] LÉONARD, Olivier, Olivier ADAM, Yuxing LIU, Junqiang ZHOU a Yue-Yun WANG. A quasi-one-dimensional CFD model for multistage turbomachines. Journal of Thermal Science [online]. 2008, 17(1), 7-20 [cit. 2021-03-04]. ISSN 1003-2169. Dostupné z: doi:10.1007/s11630-008-0007-z

[22] ŠTĚTINA, Josef. *Turbocharging: Přeplňování [přednáška]*. VUT v Brně, 2019.

[23] SUBRAMANI, D. A., R. DHINAGARAN, V. R. PRASANTH, Junqiang ZHOU a Yue-Yun WANG. Introduction to Turbocharging—A Perspective on Air Management System. Design and Development of Heavy Duty Diesel Engines [online]. Singapore: Springer Singapore, 2020, 2020-11-06, 17(1), 85-193 [cit. 2021-03-04]. Energy, Environment, and Sustainability. ISBN 978-981-15-0969-8. ISSN 1003-2169. Dostupné z: doi:10.1007/978-981-15-0970-4_4

[24] SID ALI, Litim, Hamel MOHAMMED a Hamidou MOHAMED KAMEL. THE NUMBER OF BLADE EFFECTS ON THE PERFORMANCE OF A MIXED TURBINE ROTOR. Engineering Review [online]. 2017, , 349-360 [cit. 2021-03-03]. Dostupné z: http://161.53.40.220/index.php/ER/article/viewFile/847/475

[25] MOHAMMAD, Mohand Mosa, Ahmed ESMAEL MOHAN, Hiyam ADIL HABEEB, Junqiang ZHOU a Yue-Yun WANG. IMPROVING AND ANALYSIS TURBINE WHEEL OF TURBOCHARGER FOR HIGH-PERFORMANCE ENGINES. Journal of Mechanical Engineering Research and Developments [online]. Singapore: Springer Singapore, 2018, 2020-11-06, 41(3), 91-96 [cit. 2021-03-04]. Energy, Environment, and Sustainability. ISBN 978-981-15-0969-8. ISSN 10241752. Dostupné z: doi:10.26480/jmerd.03.2018.91.96

[26] What's the big deal about twin scroll turbochargers? In: AudiBoost [online]. 2016 [cit. 2021-03-03]. Dostupné z: https://www.audiboost.com/content.php?7391-What-s-the-big-deal-about-twin-scroll-turbochargers

[27] JÄÄSKELÄINEN, Hannu. Fixed Geometry Turbochargers. DieselNet Technology Guide [online]. 2014 [cit. 2021-03-03]. Dostupné z: https://dieselnet.com/tech/air_turbo_fixed.php

[28] JÄÄSKELÄINEN, Hannu. Variable Geometry Turbochargers. DieselNet Technology Guide [online]. 2016 [cit. 2021-03-03]. Dostupné z: https://dieselnet.com/tech/air_turbo_vgt.php

[29] COLIN, G, Y CHAMAILLARD, B BELLICAUD, Junqiang ZHOU a Yue-Yun WANG. Robust control for the air path of a downsized engine. Proceedings of the Institution of Mechanical Engineers, Part D: Journal of Automobile Engineering [online]. Singapore: Springer Singapore, 2011, 2020-11-06, 225(7), 930-943 [cit. 2021-03-04]. Energy, Environment, and Sustainability. ISBN 978-981-15-0969-8. ISSN 0954-4070. Dostupné z: doi:10.1177/0954407011401503

[30] WIBMER, Michael, Timo SCHMIDT, Oliver GRABHERR, Bodo DURST a Yue-Yun WANG. Simulation of Turbocharger Wastegate Dynamics. MTZ worldwide [online]. Singapore: Springer Singapore, 2015, 2020-11-06, 76(2), 28-31 [cit. 2021-03-04]. Energy, Environment, and Sustainability. ISBN 978-981-15-0969-8. ISSN 2192-9114. Dostupné z: doi:10.1007/s38313-014-1009-8

[31] OLIVÍK, Pavel. Volkswagen 1.5 TSI (EA211 evo) – Další krok. In: Automobil [online]. 2016 [cit. 2021-03-04]. Dostupné z: https://www.automobilrevue.cz/rubriky/clanky/technika/volkswagen-1-5-tsi-ea211-evo-dalsi-krok_45095.html

[32] TANG, Huayin, Andrew PENNYCOTT, Sam AKEHURST, Chris J BRACE a Yue-Yun WANG. A review of the application of variable geometry turbines to the downsized gasoline engine. International Journal of Engine Research [online]. Singapore: Springer Singapore, 2014, 2020-11-06, 16(6), 810-825 [cit. 2021-03-04]. Energy, Environment, and Sustainability. ISBN 978-981-15-0969-8. ISSN 1468-0874. Dostupné z: doi:10.1177/1468087414552289

[33] BAUER, Karl-Heinz, Craig BALIS, David PAJA, Peter DAVIES a Damien MARSAL. High Volume Series Production of Ball Bearing Turbochargers. MTZ worldwide [online]. Singapore: Springer Singapore, 2011, 2020-11-06, 72(4), 48-51 [cit. 2021-03-04]. Energy, Environment, and Sustainability. ISBN 978-981-15-0969-8. ISSN 2192-9114. Dostupné z: doi:10.1365/s38313-011-0041-1

[34] ZEPPEI, Dieter, Silvio KOCH, Amir ROHI, Peter DAVIES a Damien MARSAL. Ball Bearing Technology for Passenger Car Turbochargers. MTZ worldwide [online]. Singapore: Springer Singapore, 2016, 2020-11-06, 77(11), 26-31 [cit. 2021-03-04]. Energy, Environment, and Sustainability. ISBN 978-981-15-0969-8. ISSN 2192-9114. Dostupné z: doi:10.1007/s38313-016-0109-z

[35] CHOI, Bok-Lok, Seong-Ki HONG, Byoung-Ho CHOI, Peter DAVIES a Damien MARSAL. Prediction of Sealing Performance of V-Coupling of Turbocharger Housing Using Analytical and Finite Element Analysis. International Journal of Automotive Technology [online]. Singapore: Springer Singapore, 2020, 2020-11-06, 21(6), 1587-1595 [cit. 2021-03-04]. Energy, Environment, and Sustainability. ISBN 978-981-15-0969-8. ISSN 1229-9138. Dostupné z: doi:10.1007/s12239-020-0149-x

[36] WEI, Jiangshan, Yingxian XUE, Kangyao DENG, Mingyang YANG a Ying LIU. A direct comparison of unsteady influence of turbine with twin-entry and single-entry scroll on performance of internal combustion engine. Energy [online]. Singapore: Springer Singapore, 2020, 2020-11-06, 212(6), 1587-1595 [cit. 2021-03-04]. Energy, Environment, and Sustainability. ISBN 978-981-15-0969-8. ISSN 03605442. Dostupné z: doi:10.1016/j.energy.2020.118638

[37] DENG, Jian, Dong Su ZHANG, Shao Ming WANG, Lian Tao HU a Hua KONG. Experimental study on controlled pulse turbocharging system for a six-cylinder diesel engine. Journal of Marine Science and Technology [online]. Singapore: Springer Singapore, 2014, 2020-11-06, 19(4), 503-509 [cit. 2021-03-04]. Energy, Environment, and Sustainability. ISBN 978-981-15-0969-8. ISSN 0948-4280. Dostupné z: doi:10.1007/s00773-014-0264-3

[38] FENELEY, Adam J., Apostolos PESIRIDIS, Amin Mahmoudzadeh ANDWARI, Lian Tao HU a Hua KONG. Variable Geometry Turbocharger Technologies for Exhaust Energy Recovery and Boosting-A Review. Renewable and Sustainable Energy Reviews [online]. Singapore: Springer Singapore, 2017, 2020-11-06, 71(4), 959-975 [cit. 2021-03-04]. Energy, Environment, and Sustainability. ISBN 978-981-15-0969-8. ISSN 13640321. Dostupné z: doi:10.1016/j.rser.2016.12.125

[39] RODE, Martin, Tetsu SUZUKI, Georgios IOSIFIDIS, Tobias SCHEUERMANN a Hua KONG. Electric Turbocharger Concept for Highly Efficient Internal Combustion Engines. MTZ worldwide [online]. Singapore: Springer Singapore, 2019, 2020-11-06, 80(7-8), 120-125 [cit. 2021-03-04]. Energy, Environment, and Sustainability. ISBN 978-981-15-0969-8. ISSN 2192-9114. Dostupné z: doi:10.1007/s38313-019-0056-6

[40] GÖDEKE, Holger, Tetsu PREVEDEL, Georgios IOSIFIDIS, Tobias SCHEUERMANN a Hua KONG. Hybrid Turbocharger with Innovative Electric Motor. MTZ worldwide [online]. Singapore: Springer Singapore, 2014, 2020-11-06, 75(3), 120-125 [cit. 2021-03-04]. Energy, Environment, and Sustainability. ISBN 978-981-15-0969-8. ISSN 2192-9114. Dostupné z: doi:10.1007/s38313-014-0030-2

[41] DAVIES, Peter, Nathaniel BONTEMPS, Torsten TIETZE, Eike Tim FAULSEIT a Hua KONG. Electric Turbocharging - Key Technology for Hybridized Powertrains. MTZ worldwide [online]. Singapore: Springer Singapore, 2019, 2020-11-06, 80(10), 30-37 [cit. 2021-03-04]. Energy, Environment, and Sustainability. ISBN 978-981-15-0969-8. ISSN 2192-9114. Dostupné z: doi:10.1007/s38313-019-0096-y

[42] Mercedes-AMG´s new turbo engine will recover exhaust heat energy, just like in f1. In: Motor Authority [online]. 2020 [cit. 2021-03-04]. Dostupné z: https://www.motorauthority.com/news/1128524_mercedes-amg-s-new-turbo-engine-will-recover-exhaust-heat-energy-just-like-in-f1?fbclid=IwAR2i3fWGe-bgN5UxFgiSTPXm4sOYklMgbRgZ_kqRJIXsM_REdKgrGIAmxHk

[43] PETRÁNY, Máté. How Formula One's Amazing New Hybrid Turbo Engine Works. Jalopnik [online]. 2014 [cit. 2021-03-04]. Dostupné z: https://jalopnik.com/how-formula-ones-amazing-new-hybrid-turbo-engine-works-1506450399

[44] LEE, Woongkul, Erik SCHUBERT, Yingjie LI, Eike Tim SILONG LI, Dheeraj BOBBA a Bulent SARLIOGLU. Electrification of turbocharger and supercharger for downsized internal combustion engines and hybrid electric vehicles-benefits and challenges. 2016 IEEE Transportation Electrification Conference and Expo (ITEC) [online]. Singapore: IEEE, 2016, 2016, 80(10), 1-6 [cit. 2021-03-04]. Energy, Environment, and Sustainability. ISBN 978-1-5090-0403-4. ISSN 2192-9114. Dostupné z: doi:10.1109/ITEC.2016.7520254

[45] DIMITRIOU, Pavlos, Richard BURKE, Qingning ZHANG, Colin COPELAND, Harald STOFFELS a Bulent SARLIOGLU. Electric Turbocharging for Energy Regeneration and Increased Efficiency at Real Driving Conditions. Applied Sciences [online]. Singapore: IEEE, 2017, 2016, 7(4), 1-6 [cit. 2021-03-04]. Energy, Environment, and Sustainability. ISBN 978-1-5090-0403-4. ISSN 2076-3417. Dostupné z: doi:10.3390/app7040350

[46] BONTEMPS, N., A. BAS, M. LADONNET, D. ZECCHETTI, S. HEINTZ a Peter DAVIES. Electric turbo, a key technology to achieve Eu7 hybridized powertrain (lambda 1, performance and energy efficiency). Internationaler Motorenkongress 2019 [online]. Wiesbaden: Springer Fachmedien Wiesbaden, 2019, 2019-05-31, 7(4), 103-113 [cit. 2021-03-04]. Proceedings. ISBN 978-3-658-26527-4. ISSN 2076-3417. Dostupné z: doi:10.1007/978-3-658-26528-1_6

[47] JÄÄSKELÄINEN, Hannu. Assisted Turbocharging [online]. 2016 [cit. 2021-03-04]. Dostupné z: https://dieselnet.com/tech/air_turbo_assist.php

[48] ALSHAMMARI, Mamdouh, Nikolaos XYPOLITAS, Apostolos PESYRIDIS, D. ZECCHETTI, S. HEINTZ a Peter DAVIES. Modelling of Electrically-Assisted

Turbocharger Compressor Performance. Energies [online]. Wiesbaden: Springer Fachmedien Wiesbaden, 2019, 2019-05-31, 12(6), 103-113 [cit. 2021-03-04]. Proceedings. ISBN 978-3-658-26527-4. ISSN 1996-1073. Dostupné z: doi:10.3390/en12060975

[49] SZYMKO, Shinri, Owen CREESE-SMITH, Gael DE CREVOISIER, Michela MASCHERIN, Richard GOODYEAR a Henry CARR. Design of electrified turbomachinery for use in modern industrial hybrid powertrains. Internationaler Motorenkongress 2020 [online]. Wiesbaden: Springer Fachmedien Wiesbaden, 2020, 2020-08-29, 12(6), 225-238 [cit. 2021-03-04]. Proceedings. ISBN 978-3-658-30499-7. ISSN 1996-1073. Dostupné z: doi:10.1007/978-3-658-30500-0_15

[50] CHAN, C.C., A. BOUSCAYROL, K. CHEN, Michela MASCHERIN, Richard GOODYEAR a Henry CARR. Electric, Hybrid, and Fuel-Cell Vehicles: Architectures and Modeling. IEEE Transactions on Vehicular Technology [online]. Wiesbaden: Springer Fachmedien Wiesbaden, 2010, 2020-08-29, 59(2), 589-598 [cit. 2021-03-04]. Proceedings. ISBN 978-3-658-30499-7. ISSN 0018-9545. Dostupné z: doi:10.1109/TVT.2009.2033605

[51] EMADI, Ali, ed. Advanced electric drive vehicles. First issued in paperback. Boca Raton: CRC Press, Taylor & Francis Group, 2017. Energy, power electronics, and machines. ISBN 978-1-138-07285-5.

[52] JAIN, Shailendra a Lalit KUMAR. Fundamentals of Power Electronics Controlled Electric Propulsion. Power Electronics Handbook [online]. Elsevier, 2018, 2018, , 1023-1065 [cit. 2021-03-04]. ISBN 9780128114070. Dostupné z: doi:10.1016/B978-0-12-811407-0.00035-0

[53] JAIN, Achin, Tobias NUEESCH, Christian NAEGELE, Pedro Macri LASSUS a Christopher H. ONDER. Modeling and Control of a Hybrid Electric Vehicle With an Electrically Assisted Turbocharger. IEEE Transactions on Vehicular Technology [online]. Elsevier, 2016, 2018, 65(6), 4344-4358 [cit. 2021-03-04]. ISBN 9780128114070. ISSN 0018-9545. Dostupné z: doi:10.1109/TVT.2016.2533585

[54] SELLERS, Roscoe, Pascal REVEREAULT, Tobias STALFORS, Marie STENFELDT a Christopher H. ONDER. Optimizing the Architecture of 48-V Mild Hybrids. MTZ worldwide [online]. Elsevier, 2018, 2018, 79(2), 26-31 [cit. 2021-03-04]. ISBN 9780128114070. ISSN 2192-9114. Dostupné z: doi:10.1007/s38313-017-0166-y

[55] Mild Hybrid Electric Vehicle (MHEV) – architectures. X-engineer.org [online]. [cit. 2020-03-04]. Dostupné z: https://x-engineer.org/automotiveengineering/vehicle/hybrid/mild-hybrid-electric-vehicle-mhev-architectures/

[56] GAO, Yimin. Regenerative Braking. Transportation Technologies for Sustainability [online]. [cit. 2021-03-04]. ISBN 978-1-4614-5844-9. Dostupné z: https://doi.org/10.1007/978-1-4614-5844-9

[57] Reduce consumption. Protect the environment. Regenerative braking systems. In: Bosch Mobility Solutions [online]. Germany [cit. 2021-03-04]. Dostupné z: https://www.bosch-mobility-solutions.us/media/global/products-and-services/passenger-cars-and-light-commercial-vehicles/driving-safety-systems/regenerative-braking-system/brochure_regenerative_braking_systems_reduce_consumption_protect_the_environment.pdf

[58] GORE, Ajinkya, S.B. SANAP a R. V. MULIK. Design of Regenerative Braking Control Strategy for Parallel Hybrid Vehicle. International Engineering Research Journal [online]. , 140-143 [cit. 2021-03-04]. Dostupné z: http://www.ierjournal.org/pupload/mitpgcon/MD1-39.pdf

[59] ZHOU, Shilei, Paul WALKER, Nong ZHANG, Marie STENFELDT a Christopher H. ONDER. Parametric design and regenerative braking control of a parallel hydraulic hybrid vehicle. Mechanism and Machine Theory [online]. Elsevier, 2020, 2018, 146(2), 26-31 [cit. 2021-03-04]. ISBN 9780128114070. ISSN 0094114X. Dostupné z: doi:10.1016/j.mechmachtheory.2019.103714

[60] ZHAO, Wanzhong, Gang WU, Chunyan WANG, Leiyan YU a Yufang LI. Energy transfer and utilization efficiency of regenerative braking with hybrid energy storage system. Journal of Power Sources [online]. Elsevier, 2019, 2018, 427(2), 174-183 [cit. 2021-03-04]. ISBN 9780128114070. ISSN 03787753. Dostupné z: doi:10.1016/j.jpowsour.2019.04.083

[61] LV, Ming, Zeyu CHEN, Ying YANG, Jiangman BI a Yufang LI. Regenerative braking control strategy for a hybrid electric vehicle with rear axle electric drive. 2017 Chinese Automation Congress (CAC) [online]. IEEE, 2017, 2017, 427(2), 521-525 [cit. 2021-03-04]. ISBN 978-1-5386-3524-7. ISSN 03787753. Dostupné z: doi:10.1109/CAC.2017.8242823

[62] GEYER, Roland, Donald E. MALEN, Ying YANG, Jiangman BI a Yufang LI. Parsimonious powertrain modeling for environmental vehicle assessments: part 2—electric vehicles. The International Journal of Life Cycle Assessment [online]. IEEE, 2020, 2017, 25(8), 1576-1585 [cit. 2021-03-04]. ISBN 978-1-5386-3524-7. ISSN 0948-3349. Dostupné z: doi:10.1007/s11367-020-01775-z

[63] BO ZHU, JIAGENG RUAN a P. WALKER. Experimental Verification of regenerative braking energy recovery system based on electric vehicle equipped with 2-speed DCT. 7th IET International Conference on Power Electronics, Machines and Drives (PEMD 2014) [online]. Institution of Engineering and Technology, 2014, 2014, , 0240-0240 [cit. 2021-03-04]. ISBN 978-1-84919-815-8. Dostupné z: doi:10.1049/cp.2014.0356

[64] ZHANG, Liang, Xue CAI, P. WALKER, Jiangman BI a Yufang LI. Control strategy of regenerative braking system in electric vehicles: part 2—electric vehicles. Energy Procedia [online]. Institution of Engineering and Technology, 2018, 2014, 152(8), 496-501 [cit. 2021-03-04]. ISBN 978-1-84919-815-8. ISSN 18766102. Dostupné z: doi:10.1016/j.egypro.2018.09.200

[65]   IVECO. *IVECO* [online].   [cit.   2021-5-17].   Dostupné   z: https://www.iveco.com/czech/produkty/pages/nova-daily-van.aspx#overview

ABBREVIATIONS AND SYMBOLS

A/F	[-]	Air-Fuel ratio
BMEP	[bar]	Break Mean Effective Pressure
BSFC	[g/kW·h]	Break Specific Fuel Consumption
BSR		Blade Speed Ratio
CFD		Computational Fluid Dynamics
CHRA		Centre Housing Rotating Assembly
CO_2		Carbon Dioxide
C_0		Ideal stator exit velocity
c	[m/s]	Gas velocity
c_p	[J/kg·K]	Heat capacity at constant pressure
DOH	[-]	Degree of hybridization
D_s	[-]	Specific diameter
d_1	[m]	Inducer diameter
d_2	[m]	Exducer diameter
d_{tip}	[m]	Tip diameter
EAT		Electric-Assisted Turbocharger
EGR		Exhaust Gas Recirculation
E_{ext}	[J/kg]	Energy extracted (Euler´s Equation)
HEV		Hybrid Electric Vehicle
HF	[-]	Hybridization Factor
Δh_{ideal}	[J/kg]	Ideal enthalpy change across the turbine
Δh_{sC}	[J/kg]	Increase of isentropic enthalpy
h_s	[J/kg]	Gas specific enthalpy
h_t	[J/kg]	Total specific enthalpy
h_{1t}	[J/kg]	Total specific enthalpy at the compressor inlet
h_{2st}	[J/kg]	Total specific isentropic enthalpy at the compressor outlet
h_{2t}	[J/kg]	Total specific polytropic enthalpy at compressor outlet
ICE		Internal Combustion Engine
MGU-H		Motor-Generator Unit on Turbocharger
MGU-K		Motor-Generator Unit on Crankshaft
MHEV		Mild-Hybrid Electric Vehicle
$\dot{m}_a$	[kg/s]	Air mass flow

$\dot{m}_C$	[kg/s]	Mass flow rate through compressor
$\dot{m}_{ccor}$	[(kg/s)·($\sqrt{K/bar}$)]	Corrected mass flow rate
$\dot{m}_{fuel}$	[kg/s]	Fuel mass flow
$\dot{m}_T$	[kg/s]	Mass flow rate through turbine
NEDC		New European Driving Cycle
NO$_x$		Nitrogen Oxides
N_c	[1/min]	Rotational speed of compressor
N_{ccor}	[1/min]	Corrected rotational speed of compressor
N_s	[-]	Specific speed
n	[-]	Polytropic coefficient
PID		Proportional Integral Derivate (controller)
PHEV		Plug-in Hybrid Electric Vehicle
P$_{amb}$	[Pa]	Ambient pressure
P_C	[W]	Power input of the compressor
$P_{C,ideal}$	[W]	Ideal compressor power at the isentropic compression
P$_{intake}$	[Pa]	Intake pressure
P_{ICE}	[W]	Power of internal combustion engine
P_{EM}	[W]	Power of electric motor-generator
P$_{exhst}$	[Pa]	Exhaust pressure
P_{recu}	[W]	Amount of recuperated power
P_T	[W]	Turbine power output
ΔP_T	[W]	Turbine power change
ΔP_{pump}	[W]	Scavenging power change
p_{in}	[Pa]	Pressure at the compressor inlet
p_{ref}	[Pa]	Reference pressure
p_{1t}	[Pa]	Total pressure at the compressor inlet
p_{2t}	[Pa]	Total pressure at the compressor outlet
p_3	[Pa]	Pressure at the turbine inlet
$p_3{}'$	[Pa]	Incread pressure at the turbine inlet
p_{3t}	[Pa]	Total pressure at the turbine inlet
p_{4s}	[Pa]	Static pressure at the turbine outlet
Q_2	[m^3/s]	Volumetric flow rate through the turbine
r	[J/kg·K]	Specific gas constant

RPM	[1/s]	Revolutions Per Minute
TSI		Turbo Stratified Engine
T_{dyn}	[K]	Dynamic temperature
T_{in}	[K]	Turbine inlet temperature
T_{ref}	[K]	Reference temperature
T_s	[K]	Static temperature
T_t	[K]	Total temperature
T_{1t}	[K]	Compressor inlet temperature
T_{2st}	[K]	Temperature after isentropic compression in compressor
T_{2t}	[K]	Temperature after polytropic compression in compressor
T_{3t}	[K]	Temperature before turbine inlet
T_{4s}	[K]	Temperature after isentropic expansion
T_{4t}	[K]	Temperature after the polytropic expansion
U	[m/s]	Blade speed of turbine wheel
u	[J/kg]	Specific internal energy of gas
US06		United States driving cycle
V	[m/s]	Absolute Flow velocity of turbine wheel
VGT		Variable Geometry Turbine
VNT		Variable Nozzle Turbine
WLTP		Worldwide Harmonised Light Vehicles Test Procedure
η_C	[-]	Total-total compressor isentropic efficiency
η_m	[-]	Mechanical efficiency
η_T	[-]	Total-static turbine isentropic efficiency
η_{TC}	[-]	Turbocharger efficiency
η_{trans}	[-]	Efficiency of conversion to electrical power
η_{vol}	[-]	Volumetric efficiency
κ_a	[-]	Isentropic exponent of the charged air
κ_g	[-]	Isentropic exponent of the exhaust gas
ρ	[kg/m^3]	Gas density
ω	[rad/s]	Rotor angular velocity